FINAL REPORT
FOR THE
HIGH DATA RATE STORAGE SYSTEM
(ENGINEERING MODELS EM-1 & EM-2)

Contract No. NAS5-3772

Prepared by

RCA Astro Electronics
Princeton, New Jersey

for

National Aeronautics and Space Administration
Goddard Space Flight Center
Greenbelt, Maryland

FINAL REPORT
FOR THE
HIGH DATA RATE STORAGE SYSTEM
(ENGINEERING MODELS EM-1 & EM-2)

Contract No. NAS5-3772

Prepared by

RCA Astro Electronics
Princeton, New Jersey

for

National Aeronautics and Space Administration
Goddard Space Flight Center
Greenbelt, Maryland

PREFACE

This report summarizes the work performed by the Astro-Electronics Division (AED) of RCA for the Goddard Space Flight Center of the National Aeronautics and Space Administration under contract NAS5-3772. The work was performed during the period starting March 5, 1964 and ending May 31, 1967. Effective September 3, 1965, the contract name was changed from "APT Camera/ Tape Recorder Study" to "High Data Rate Storage System," (HDRSS).

Contract NAS5-3772 consisted of three phases: Phase I - Preliminary Design Study; Phase II - Study Tasks; and Phase III, parts A and B. Part A was called Breadboard Model and Demonstration; Part B was called Engineering models and Feasibility Demonstration. The results of Phase I, Phase II, and Phase IIIA are contained in separate reports referenced in Section 1, Paragraph C-1. The result of Phase IIIB, obtained from work performed from September 1965 to May 1967, are contained in this report.

SUMMARY AND CONCLUSIONS

Tests performed on the HDRSS EM-1 and EM-2 have demonstrated compliance with the performance requirements listed in Section 2. In particular, the data shows that for the BCU test conditions, the amplitude responses of ID and HRIR are within 0 and -12 db, and 0 and -8 db, respectively.

In the early phases of the Engineering Model program there was some question as to what amplitude response specification could be met by the ID and HRIR channels. Based on the data presented in Section 7 and the calculations of Section 8, there is ample evidence that the ID and HRIR channels can meet the amplitude response specifications given in Section 2. It is recommended that those specifications be adopted for the HDRSS-B flight models.

The SNR of the analog channels, without intentional noise added, exceeded the Nimbus A (30 db p-p/rms) criterion in all cases. The SNR of the Nimbus A AVCS system (camera, tape recorder and demodulator) was specified as 30 db p-p/rms at ambient without link noise or other intentional noise sources. The HDRSS SNR was approximately 30 db B-W/rms with all noise sources included. Refer to Appendix IV for the RF Link SNR analysis.

System test indicated that the BER of the biphase data channels under all operating conditions was less than 1×10^{-5}. System testing also indicated that the biphase repeater was not required to meet the BER specification. Therefore, it was recommended that the biphase repeater be deleted from the system.

The timing error due to intersymbol interference in the IRIS channel is quite large (about 18 percent of a bit for one selected word; 25 percent of a bit for another word). This is primarily due to the sharp band limiting in the channel. It is recommended that future biphase systems employ a wider bandwidth, for example, 1.3 to 1.5 times the bit rate if steep filters are used. If gradual (Bessel) filters are used the -3 db bandwidth may be equal to the bit rate.

Finally, as shown in Appendix III, the loss due to intersymbol interference with a sample type signal conditioner is 10 db; this loss would be less for an integrate-dump signal conditioner, and it is recommended that an integrate-dump signal conditioner be used for the HDRSS flight model programs.

TABLE OF CONTENTS

TABLE OF CONTENTS (Continued)

TABLE OF CONTENTS (Continued)

TABLE OF CONTENTS (Continued)

TABLE OF CONTENTS (Continued)

LIST OF ILLUSTRATIONS

LIST OF ILLUSTRATIONS (Continued)

LIST OF TABLES

LIST OF TABLES (Continued)

LIST OF TABLES (Continued)

SECTION 1
INTRODUCTION

A. PURPOSE OF REPORT

The purpose of this report is to present technical discussions on the fabrication and test of two spacecraft subsystems (Engineering Models 1 and 2); the associated test equipment (Bench Check Units 1 and 2); and the design, manufacture, and test of ground station equipment required to modify existing Nimbus ground stations No. 1 and No. 2 for the High Data Rate Storage System (HDRSS). This effort is defined as Phase IIIB of the contract.

B. CONTRACT OBJECTIVES

The original objective of Contract NAS5-3772 was to design, fabricate, and test a tape-recorder system that would record the APT Camera video signal, and produce video data of AVCS subsystem quality on existing TIROS or Nimbus ground stations. Modifications to the contract provided for the addition of High Resolution Infra-red data (HRIR), the NASA Minitrack time code, Medium Resolution Infra-red data (MRIR), and Interferometer Spectrometer data (IRIS).

C. HDRSS HISTORICAL DATA

Tasks specified by Contract NAS5-3772, dated March 4, 1964, were divided into four categories: Phase I, Phase II, Phase IIIA, and Phase IIIB.

1. Phase I and II.

The effort specified by Phase I (Preliminary Design Study) and Phase II (Study Tasks) was performed during the period starting March 4, 1964, to July 1964. The objectives of the study phases were to determine 1) the performance specifications for a magnetic tape-recorder subsystem to be used in conjunction with an APT Camera Subsystem, and 2) the performance specifications for additional transmitting, receiving and video processing equipment required for existing TIROS or Nimbus Ground Stations.

The Phase I study considered two modes of operation. The first of these (Mode A) accepts the amplitude modulated subcarrier output of the APT Camera Subsystem and frequency modulates a second subcarrier which is recorded on the tape at slow speed. The signal is reproduced at a high speed to approximate AVCS picture rates and then transmitted to a ground station. The second mode

(Mode B) uses the analog video signal of the APT Camera Subsystem and a suitable timing signal. The video signal frequency modulates a subcarrier which is recorded on one channel of the tape recorder; a timing signal is recorded on a second channel of the tape recorder. The signals are recorded at a slow speed, are reproduced at a high speed, and are frequency multiplexed for transmission to a ground station.

Mode B was selected for the Phase II study as it required less magnetic tape, 1045 feet as compared to 2026 for Mode A; and a reduced playback speed, 42.9 ips as compared to 83.2 ips for Mode A. Other considerations that contributed to the selection of Mode B are outlined in a report issued in August 1964.[1]

The Phase II study evaluated three tape recorder systems against the criteria established by Mode B. The primary difference of each system was the format of the data recorded on the tape recorder. The formats are as follows:

- System 1. - Composite video (analog video and horizontal sync) are recorded on one track; the clock signal is recorded on the second track. The data on the second track is used to generate vertical sync and provides for flutter and wow correction.

- System 2. - Analog video is recorded on one track; a clock signal is recorded on a second track. The data on the second track is used to generate vertical and horizontal sync, and provides for flutter and wow correction.

- System 3. - Analog video is recorded on one track; horizontal sync data is recorded on a second track; and a clock signal is recorded on a third track. The data of the third track is used to generate vertical sync and provides for flutter and wow correction.

The relative merits of the three systems were evaluated, and system 1 was selected for use in Phase III. A System Design Review of the proposed configuration was conducted in November 1964. Conclusions reached at this review indicated that the proposed configuration conformed to the basic system design principles and that the configuration would meet contract objectives.

Thus, at the conclusion of the Phases I and II, the HDRSS consisted of a two channel tape recorder with its associated electronics and a multiplexer. The system was capable of the following:

- Accepting two inputs (composite video and clock),
- Processing and recording the signals on magnetic tape at 1.34 ips,
- Reproducing the signals at 32 times the record speed (42.9 ips), and
- Frequency multiplexing the two signals to provide a signal for application to an S-band transmitter.

Significant parameters of the HDRSS tape recorder for the record and playback modes are listed in Table 1.

TABLE 1. HDRSS TAPE RECORDER PARAMETERS

Parameters	Record Mode	Playback Mode
Tape Recorder		
Tape Speed	1.34 ips	42.9 ips
Length of Tape	1045 feet	1045 feet
Operating Time	156 minutes	4.9 minutes
Motor Drive	400 cps - 2 phase with 90° displacement	400 cps - 2 phase with 90° displacement
Power (Operating)	4.0 watts	7.25 watts
Power (Start)	7.4 watts	37.00 watts
Video Signal		
Analog Signal	0 - 1.600 kHz	0 - 51.2 kHz
Subcarrier	3.0 kHz	96.0 kHz
Deviation	2.255 - 3.750 kHz	72 - 120 kHz
Upper Sideband	5.35 kHz	171.2 kHz
Lower Sideband	0.65 kHz	20.8 kHz
Baseband	----	32.8 - 120 kHz
Clock		
Frequency	1.200 kHz	38.4 kHz
Signal (1/2 of basic frequency)	----	19.2 kHz

2. Phase III

The effort specified by Phase III was divided into two parts, A and B. Phase III A (Breadboard Models and Demonstration) was defined by modifications 1 through 5 to the original contract. Phase III B (Engineering Models and Feasibility Demonstration) was defined by modifications 6 through 30 to the original contract. Phase III directives provided for one breadboard model, three engineering models, test equipment, and ground station modifications.

The objectives of Phase III A, performed during the period starting in June 1964, to September 1965, were to construct and experimentally evaluate the performance of a breadboard HDRSS which encompassed the conclusions and recommendations which evolved during Phases I and II of the contract. The results of the breadboard tests proved the feasibility of transforming APT video information into a compatible format for transmission to modified TIROS or Nimbus ground stations. The picture quality obtained during breadboard testing did not meet the signal-to-noise ratio or picture-element displacement of AVCS Camera Systems. These deficiencies were related to the flutter spectrum of the tape recorder which was traced to a mechanical gear train. A belt driven system tested during breadboard tests, reduced tape-recorder flutter and improved picture quality. Frequency response of the tape recorder was equivalent to the AVCS Camera System Resolution (700 and 750 TV elements) and there was no evidence of peppering, white bounce or interference in the reproduced RETMA patterns. Vertical shading which existed in the APT camera system was visible in the reproduced pictures. The overall results of the breadboard tests are outlined in a report issued May 5, 1966.[2]

Shortly after Phase III A was authorized, NASA requested that RCA investigate the feasibility of adding a High Resolution Infrared (HRIR) data channel and substitution of the NASA Minitrack time code. A further objective was to determine performance specifications for the additions and modifications required to process HRIR data on existing Nimbus ground stations. The results of this study indicated that it would be feasible to record the HRIR data and to substitute the NASA Minitrack time code for the 2400 Hz signal on the tape recorder specified by the Phase II study. It was recommended that the Time Code and HRIR Data channels be frequency multiplexed along with the video data to provide an output signal for application to the S-band transmitter. The overall results of this study are contained in a report issued November 30, 1965.[3]

The objectives of Phase IIIB were to fabricate and test two engineering models (EM-1 and EM-2) to Nimbus specifications, and one engineering model (EM-3) to TIROS Operational Satellite (TOS) specifications; update the test equipment used during the Phase IIIA effort; and to design and fabricate the equipment required to modify existing TOS and Nimbus ground stations for HDRSS use.

a. Engineering Models

The Phase IIIB effort included two major changes to the engineering models; the addition of the HRIR channel and the substitution of the NASA Minitrack time code as specified in the Phase IIIA effort, and the addition of two biphase data channels. The contract directed that the tape recorder for EM-1 and EM-2 would process and record 5 separate signals which are as follows:

- An analog video signal containing Image Dissector (ID) data with an APT format.
- An analog video signal containing High Resolution Infrared (HRIR) data.[4]
- An amplitude-modulated subcarrier containing the NASA Minitrack time code (TC).[5]
- A biphase digital signal containing Medium Resolution Infrared (MRIR) data.
- A biphase digital signal containing Interferometer Spectrometer Infrared (IRIS) data.

On command, the signal would be reproduced and applied to a multiplexer where the signal frequencies would be shifted to produce a 10- to 695-kHz baseband for application to an S-band transmitter. The reproduced time code would be frequency modulated with flutter and wow data caused by speed variations of the magnetic tape during the record or playback mode.

The requirements for EM-3 were identical to those specified for EM-1 and EM-2 except as follows: only three signals would be processed and recorded. The signals specified were as follows:

- An analog video signal from an APT camera system
- An analog video signal from a redundant APT camera system
- A 2400 kHz clock signal from the spacecraft clock.

Except for the redundant video signal and the availability of two additional channels, EM-3 meets the basic concepts described in the Phase I study report.[6] The Phase IIIB effort also specified that EM-3 would contain the circuits required for the Nimbus mission. However, these circuits (doublers in the viceo channels, and biphase circuits) would be bypassed for the TOS mission. This requirement made all the engineering models readily interchangeable. Later in the program, work on EM-3 was deleted except for the fabrication of the tape transport assembly which was operated during vibration tests that simulated launch conditions. The results of the vibration tests are summarized in Appendix I.

b. Test Equipment

Concurrent with the engineering model effort, RCA was directed to update the test equipment (Bench Check Unit) used during the Phase IIIA effort for testing the engineering models, and perform a study to determine what modifications were required to convert the AVCS BCU at the Integration Contractors site* and two TOS-BCU's at RCA for HDRSS use. As a result of the study, NASA directed RCA to fabricate an additional BCU for use at RCA and to fabricate the necessary circuits required to modify the AVCS-BCU for HDRSS operation. Maximum use of existing equipment was utilized in the design of modifications for the AVCS-BCU. The requirements for the TOS-BCU's were eliminated when the EM-3 requirement was deleted.

RCA also modified an AVCS/HRIR Demultiplexer Test Set for the test of HDRSS Demultiplexers at RCA. Maximum use of existing equipment was utilized in the design of modifications for the test set.

c. Ground Station Equipment

Concurrent with the engineering model effort, RCA was directed to perform a study to determine what modifications were required to convert the following ground stations for HDRSS operation.

---

* General Electric Company, Valley Forge, Pennsylvania.

- Nimbus Ground Station 1 (GS-1) located at the Integration Contractor's site
- Nimbus GS-2 located at the Pacific Missile Range
- TOS receiving station (Van) Gilmore Creek, Alaska
- TOS receiving station, Wallops Island, Virginia
- TOS receiving station, United States Weather Bureau, Suitland, Maryland
- TOS receiving station, Goddard Space Flight Center, Greenbelt, Maryland

As a result of the study, NASA directed RCA to fabricate the necessary circuits required to modify Nimbus GS-1 and GS-2. The requirements for the TOS receiving stations were eliminated when the EM-3 requirement was deleted.

In addition to the tasks specified by the study, RCA was directed to supply an additional demultiplexer and two signal conditioners for GS-1. These additions increased the station capability of receiving and processing signals from one S-band channel to two S-band channels.

D. HDRSS OPERATIONAL DESCRIPTION

The Spacecraft Subsystem of the HDRSS was designed for use on the Nimbus B Meteorological Satellite, an earth-stabilized spacecraft designed to circle the earth in a 600-nmi, near-polar, sun-synchronous orbit with an orbital period of approximately 107 minutes. The television and infrared sensors provide complete coverage of every point on the earth's surface once in daylight and once in darkness every 24 hours. During each orbital revolution, continuous infrared mappings and 31 single-frame television photographs are made. To provide the capability both for real-time transmission to the local stations and complete orbital readout at the CDA station, a tape recorder speed-up concept was adopted. The Spacecraft Subsystem shown on Figure 1 was specifically designed for use on Nimbus B (Nimbus III).

Two command and data-acquisition (CDA) stations provide for transmission of data obtained from 93 percent of the Nimbus orbital passes at an altitude of 600 nmi. The Alaska station (GS-3) is located at Gilmore Creek near Fairbanks, Alaska; the other, Rosman, is located at Rosman, North Carolina. The Alaska station acquires the spacecraft on an average of 10 out of 14 orbital passes each day. Two of the passes missed by the Alaska station are acquired by the Rosman station. The remaining passes are stored on the redundant HDRSS subsystem.

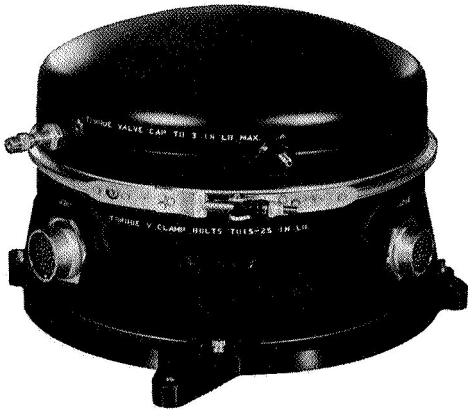

Tape Transport

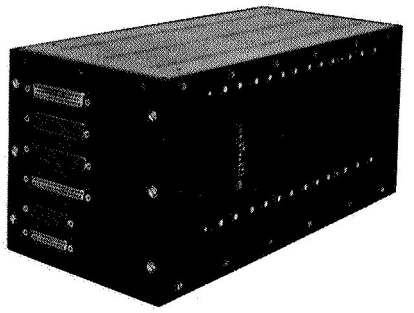

Electronics Module

TAPE RECORDER

BIPHASE REPEATER

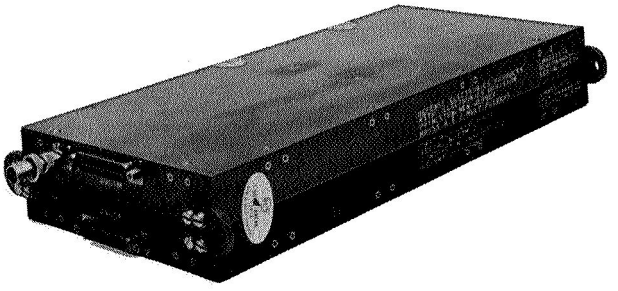

MULTIPLEXER

Figure 1. Spacecraft Subsystem of the High Data Rate Storage System

S-band data received at the Alaska station is detected, demultiplexed and transmitted as VHF data via long lines to the data processing center at the Goddard Space Flight Center (GS-7) in Greenbelt, Maryland. S-band data received at the Rosman station is transmitted to the data processing center via a wideband microwave link. Additional ground stations are located at the integration contractor's site (GS-1) and the Pacific Missile Range (GS-2). The ground stations were originally designed for the Nimbus I and II programs, and modified for HDRSS operation on the Nimbus B program (GS-1 and GS-2 on contract NAS5-3772, GS-3 and GS-7 on contract NAS5-10205).

1. Spacecraft Subsystem

The Spacecraft Subsystem contains a 5-channel tape recorder (electronics module and tape transport), a multiplexer, and a biphase repeater as shown on Figure 1. The tape recorder records and reproduces digital data and analog video signals for transmission as the spacecraft passes over a Nimbus ground station. All the data is played back at 32 times the record rate frequency multiplexed, and transmitted to earth via an S-band F-M communications link (See Figure 2). During orbital revolution, the signals from the ID and HRIR sensors are also transmitted to local weather stations in real time, and are analyzed for local weather conditions.

2. Ground Stations

S-band data received at the GSFC ground station is detected, demultiplexed, and passed to the respective processing circuits for further processing and to a tape recorder for storage (See Figure 2). VHF data received at the GSFC ground station is applied directly to the processing circuits and to the tape recorder.

The ID subcarrier is demodulated and applied to the horizontal sync detector and the kine complex for display. Horizontal sync and vertical sync is detected from the analog video and applied to the deflection generator in conjunction with a flutter and wow signal. Thus, the video signal is displayed on a kinescope and projected onto the 70-mm film in the film processor with unity magnification. The picture size is approximately 2 by 2 inches with a vertical sweep period of 6.5 seconds and a horizontal sweep rate of 128 lines per second, 800 lines per picture. At the end of the picture, a decimal readout from the ID index computer is illuminated and focused onto the film below the video display. At the end of each decimal readout, the film is automatically advanced, developed, fixed, dryed in approximately one minute, and displayed on a viewer.

The HRIR signal received from the demultiplexer cannot be processed until the frequency is reduced by a factor of 4. Therefore, the HRIR signal, along with

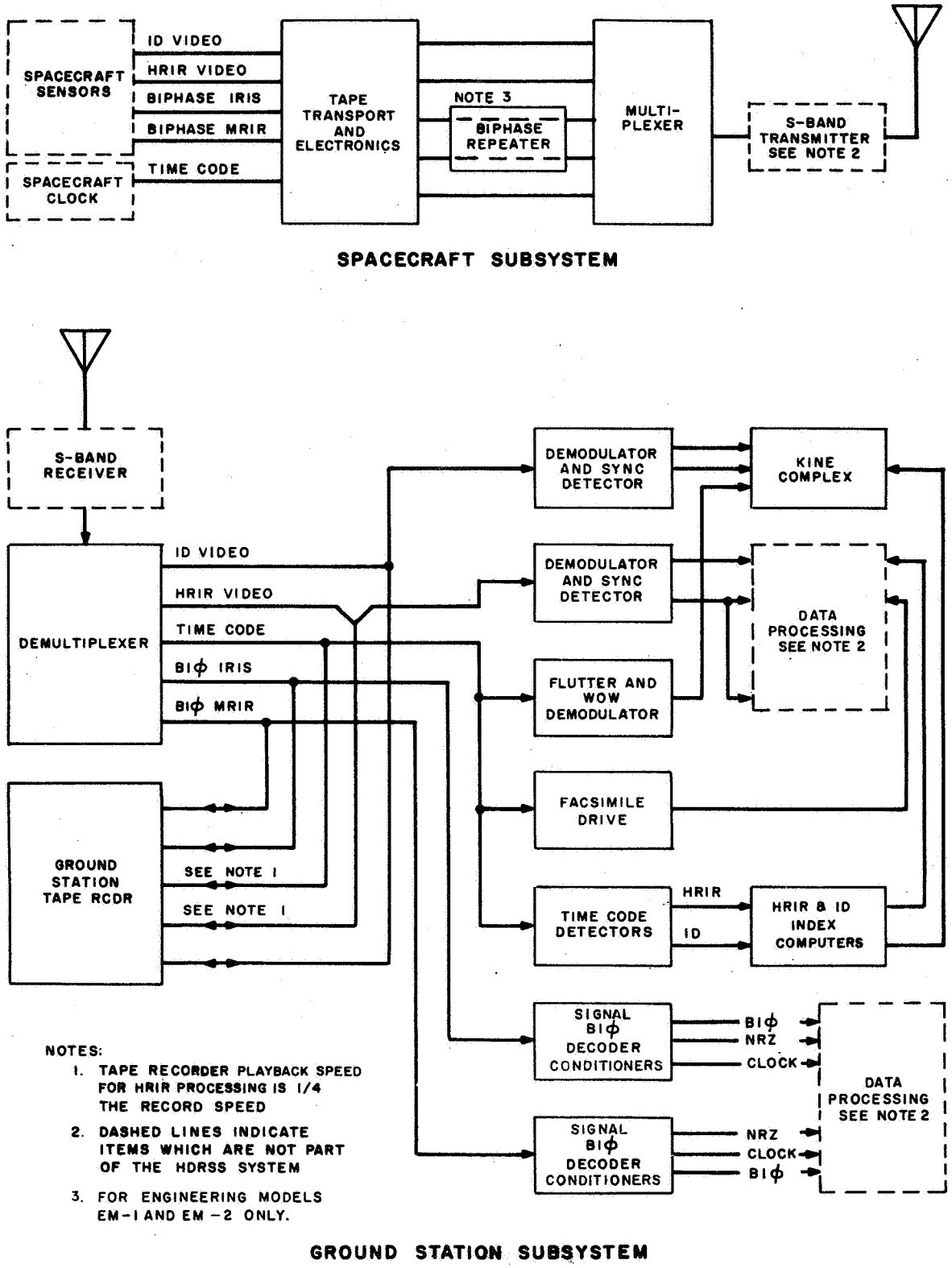

Figure 2. High Data Rate Storage System (HDRSS), Block Diagram

the timing signal, is recorded on a ground station tape recorder, and played back at one fourth the record speed. The slow-rate HRIR is demodulated and then displayed on a Westrex facsimile recorder. The slow-rate timing signal is envelope detected, and used to drive the facsimile recorder motor. At the beginning of each picture, a decimal readout from the HRIR index computer is illuminated and focused onto the picture.

The time code signal is applied to envelope detectors that recover the 100-bit Minitrack time code and supplies a PWM time code to the index computers that drive the decimal displays for the HRIR or ID video pictures. The PWM time codes are also applied to gridding computers (not shown in Figure 2) that supply latitude and longitude data for superimposition on the ID and HRIR video subcarrier by means of grid mixers. The time code is also supplied to a flutter and wow demodulator to provide a correction signal that modifies the sweep rate to coincide with speed variations introduced by the spacecraft subsystem tape recorder.

The two biphase digital signals (IRIS and MRIR) are applied to signal conditioners where they are converted to a non-return-to-zero (NRZ) by a sampling detector. A clock signal, a biphase signal, and the NRZ signal are detected and applied to data processing circuits for analysis and display.

Two additional stations (one at the Pacific Missile Range, the other at the Integration Contractor's site) provide for spacecraft subsystem verification.

3. Test Equipment

Spacecraft subsystem performance is verified with a bench check unit at the system level. This unit simulates all spacecraft interfaces, including signal inputs, commands, power, and telemetry, and provides quantitative measurement of all specified parameters. All subsystem interfaces are routed to breakout boxes to facilitate fault isolation to the subsystem level. The bench check unit includes a link simulator in which shaped noise is added to simulate the noise of the FM communication link. In addition, noise is added to each of the signal inputs and the power supply to verify spacecraft subsystem operation under realistic noise conditions.

Spacecraft subsystem operation is demonstrated by recording simulated analog and digital signals on the tape recorder and processing the signals on equipment similar to that contained in the ground stations. Photographic copies of all signal outputs are made for reference purposes. Quantitative measurements of the ID and HRIR signals are made to determine system linearity, drift, frequency response, transient response, and signal-to-noise ratio. The time code is checked for an acceptable bit-error rate and for a flutter correction capability which is observed on the ID pictures. The IRIS and MRIR signals are compared with a reference signal to determine the bit-error rate.

SECTION 2
SYSTEM PERFORMANCE OBJECTIVES

Each HDRSS engineering model consists of a five-track tape recorder and a five-channel, frequency-division multiplexer. Two tape recorder tracks record biphase digital data; two tracks record FM subcarriers containing analog video data, and one track records an amplitude-modulated signal containing a minitrack time code and is also used for flutter correction.

The digital portions of the system are designed for a maximum bit-error-rate (BER) of 1×10^{-5}. The analog and flutter channels of the HDRSS system were designed to duplicate the performance of the Nimbus AVCS and HRIR systems.

Nimbus AVCS and HRIR performance data, summarized at the conceptual design review, are as follows:

(AVCS)

Signal-to-Noise Ratio	30 db p-p/rms
Frequency Response	-10 db @ 800 TV lines
Linearity (% Black-to-White)	±2.7% (black), 5.4% (white)
Drift	±2.7% (black), 5.4% (white)
Flutter Correction	±½ TV element

HRIR

Signal-to-Noise	30 db (p-p/rms)
Linearity	2.7% (black), 5.4% (white)
Drift	2.7% (black), 5.4% (white)
Frequency Response	-12 db @ 360 cps

In certain cases, actual Nimbus A designs were used; in addition, certain design constraints changed during the course of the program and these objectives evolved into a firm set of performance specifications. These specifications are tabulated in Paragraphs A, B, C, and D.

For the ID channel the performance is specified exclusive of the Mincom recorders. For the HRIR channel, the Mincom recorder amplitude response and amplitude linearity are included in the overall system specification.

The performance of the biphase data channels is specified in terms of a bit error rate and a bit rate stability, observed at the output of the ground station bit synchronizer.

A. ID CHANNEL

The performance on the ID channel, measured between the tape recorder input and the ID demodulator output is:

Amplitude Response:	Within -12 db at 1600 Hz (relative to the low frequency response).
Signal-to-Noise:	30 db B-W/rms (including link noise but excluding sensor noise).
Linearity:	(deviation from best straight line) At Black, ±2.6% of B-W range At White, ±5.2% of B-W range
Drift:	At Black, ±5.0% of B-W range At White, ±6.6% of B-W range
Flutter Correction:	Displacement of two vertically aligned elements on adjacent horizontal lines shall be less than $\pm\frac{1}{2}$ TV element.

B. HRIR CHANNEL

The performance of the HRIR channel, measured from the HDRSS recorder input to the HRIR demodulator output is given below:

Amplitude Response:	Within -8 db at 360 cps relative to the low frequency response.
Signal-to-Noise Ratio:	30 db B-W/rms including link noise but excluding sensor noise.
Linearity:	At Black, 3.1% of B-W range At White, 5.1% of B-W range
Drift:	At Black, 6% of B-W range At White, 7.9% of B-W range
Sync Jitter:	±0.8 milliseconds

C. TIME CODE CHANNEL

The signal to noise ratio at the output of the wow and flutter demodulator will be 20 db rms/rms minimum, including simulated link noise.

D. IRIS AND MRIR

The performance on the biphase digital channels measured between the tape recorder input and the bit synchronizer (decoder) output will be:

(1) Data Bit Error Rate: 10^{-5} maximum, excluding bits lost during acquisition

(2) Data Bit Stability: within ±6.0 percent of nominal bit rate

(3) The output clock waveform delay variation relative to the data output will be within ±25 percent of the bit period.

The output data format is NRZ level and the clock waveform is a squarewave at the instantaneous bit rate of the NRZ output.

SECTION 3
SPACECRAFT EQUIPMENT

A. GENERAL

The Spacecraft Subsystem of the HDRSS consists of a tape recorder, a biphase repeater, and a multiplexer (See Figure 1). As shown, the Spacecraft Subsystem weighs 32 lbs. and requires a power of 23 watts. Detailed descriptions are contained in the spacecraft instruction manual.[7]

B. TAPE RECORDER ASSEMBLY

The tape recorder (See Figure 3) consists of an electronics module and a tape transport assembly. The tape recorder electronics module contains twelve 5.75 by 4.6-inch circuit-boards which plug into respective receptacles on a harness-board. A thirteenth circuit-board, containing the inverter bridge amplifiers, is rigidly mounted at the end of the assembly and connects electrically to the harness-board, by means of a plug and cable arrangement. The latter circuit-board provides a heat sink for the inverter bridge amplifier transistors and a mounting surface for the thermal transducer of the assembly. The fourteenth board provides the cabling which connects the 13 circuit-boards to the six receptacles at the end of the assembly.

The tape transport assembly consists of an enclosure assembly, the tape transport mechanism, and a baseplate. The enclosure assembly consists of a spun magnesium cover which is sealed to a base pan by means of a V-band coupling and is pressurized to 17 psia with an inert gas mixture consisting of 90 percent nitrogen and 10 percent helium. The tape transport mechanism contains two coaxial reels (that contain 1100 feet of mylar-base tape), a five-track record head, a five-track playback head, a permanent-magnet erase-head, eight circuit boards and planetary drive mechanism. The planetary drive mechanism contains two 8,000 rpm motors which employ mylar-belt drives and pulleys to move the tape. The record motor and planetary drive provides a tape speed of 1.34 inches-per-second: the playback motor and planetary drive move the tape in a reverse direction at 42.88 inches-per-second. The tape passes over both the record and playback head in each mode of operation, however, only one is active. The erase head provides erasure after playback and again before record to ensure complete data removal. Power and control signals for the tape transport are supplied by the tape recorder electronics. Five output signals are applied to the multiplexer via the tape recorder electronics.

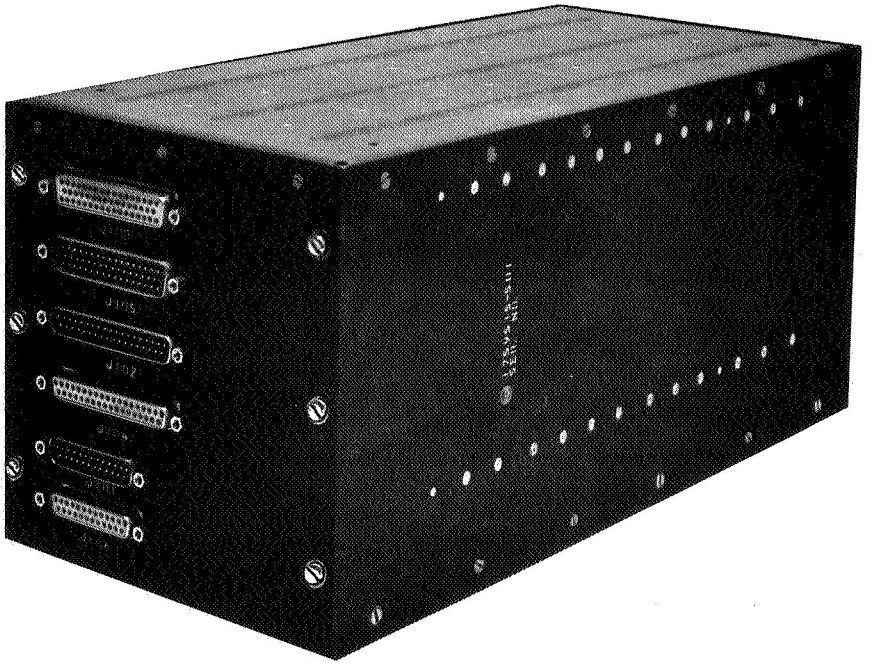

A. Tape Recorder Electronics

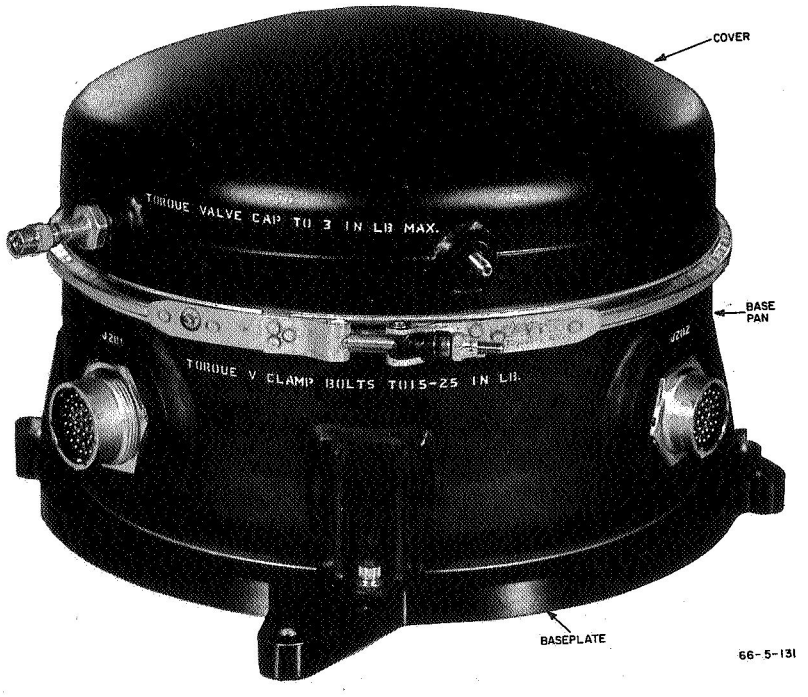

B. Tape Transport Assembly

Figure 3. HDRSS Tape Recorder Assemblies

Tape recorder operation consists of two modes (record and playback) which are controlled by the end of tape switches and ground station commands. Initially, the tape recorder is commanded on (power on) and then commanded to record. Operation continues until the record end-of-tape switch is actuated (recorder reverts to off). Playback is initiated by the playback on command and continues until the playback end-of-tape switch is actuated (reverts to record). This cycle continues until the off command is received.

Five signals are processed and recorded on the tape recorder: the ID video signal (0 to 1,600 Hz); the HRIR signal (0 to 360 Hz); the IRIS signal, a biphase 3,750-bit/s data signal; the MRIR signal, a biphase data signal at a rate of 1,600 bit/s; and the timing signal, a 2,500-Hz carrier, amplitude modulated by the pulse width modulated (PWM) 100 bit Minitrack time code.

The ID video signal is applied to a voltage controlled (See Figure 4) oscillator that converts the analog signal to an FM signal (2.5 to 3.67 kHz) suitable for recording. During playback, the ID signal is reproduced at 32 times the record speed (72 to 117.6 kHz), amplified, limited, and applied to the multiplexer. The HRIR signal is processed in the same manner as the ID signal except for the frequency. The record frequency is 2.3 to 3.16 kHz; the reproduced frequency is 73.6 to 101.12 kHz. The time code signal (2.5 kHz) is amplified and recorded. During playback, the frequency is increased to 80.0 kHz and frequency modulated with a ±800 Hz flutter signal introduced by speed variations of the tape transport during the record and playback modes. The time code is then applied to the multiplexer. The MRIR signal, a 1.666 kb/s biphase digital signal is limited, amplified and recorded. During playback the reproduced signal is increased to 53.3 kb/s. The reproduced signal is then equalized to eliminate phase shift, limited to reduce amplitude variations, and applied to the biphase repeater. The IRIS signal is processed in the same manner as the MRIR signal except for the bit rate. The input signal bit rate is 3.75 kb/s; the reproduced bit rate is 120.0 kb/s.

C. BIPHASE REPEATER ASSEMBLY

The biphase repeater consists of two identical modules that remove the high speed jitter introduced by the flutter of the tape recorder (See Figure 5). Operation of each module is the same except for the input signal data and the bit rate. The incoming signal is amplified, band limited, amplitude limited, and processed simultaneously on two separate paths: a timing extraction path and a data path (See Figure 6). In the timing extractor, the incoming data is differentiated and used to drive a one-shot pulse generator. The standardized pulses from the one-shot are combined with the output of a voltage controlled (saw tooth) oscillator (VCO) in a multiplier. The output of the multiplier is filtered to develop an

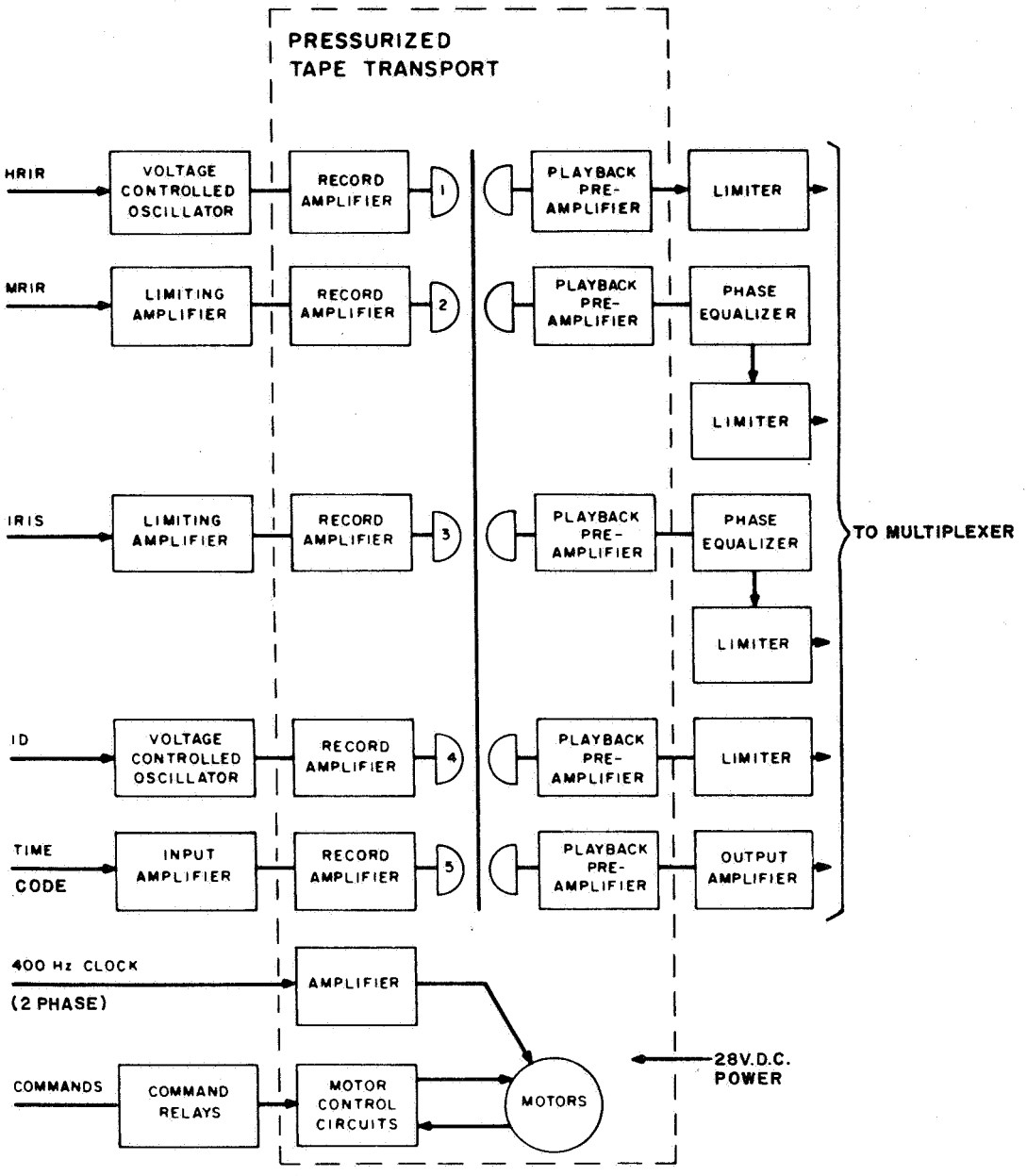

Figure 4. HDRSS Tape Recorder, Block Diagram

Figure 5. Biphase Repeater Assembly

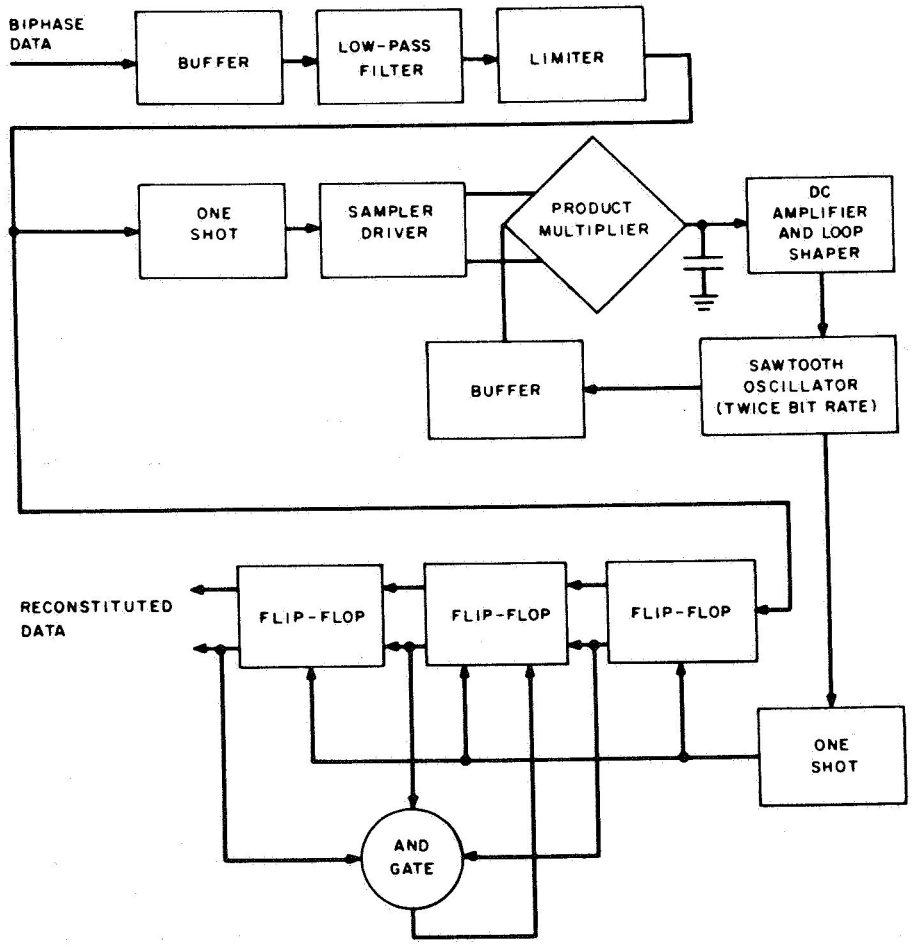

Figure 6. Biphase Repeater, Block Diagram

average bias voltage which controls the frequency of the VCO. The output of the VCO (the extracted timing) is used to sample the incoming signal in the data path. Additional flip-flop stages are used to generate pulses during tape dropouts so that the signal conditioner at the ground station will not lose synchronism. If this feature were not provided, the ground station signal conditioner would lose data during reacquisition of timing in addition to the data lost during the dropout. The output of the IRIS repeater, a square wave digital data signal, still in biphase-level format at 120 kilobits/s (53.33 kilobits/s for MRIR) is passed to the multiplexer.

D. MULTIPLEXER ASSEMBLY

The Multiplexer assembly shown in Figure 7 contains six circuit boards. Power is supplied by the spacecraft via the Tape Recorder Electronics: control signals are supplied by the Tape Recorder Electronics. The IRIS, MRIR, HRIR, timing, and ID signals are fed to the multiplexer where they are heterodyned, filtered, and added to form a composite signal with a frequency spectrum ranging from 12 to 695 kHz (See Figure 8). The input signal amplitudes are approximately 3 volts peak-to-peak, while the composite output signal amplitude is 4.5 volts peak-to-peak.

The IRIS signal is filtered to provide a passband from DC to 132 kHz (within -3 dB). Since heterodyning is not required for the signal, the channel consists simply of a low-pass filter (See Figure 9).

The time code is frequency shifted and passband limited from 171 to 203 kHz. The input signal consists of an 80-kHz carrier, amplitude modulated by a PWM time code which has a pulse repetition frequency of 3.2 kHz and pulse durations of 60 and 180 μs for 0 and 1, respectively. The timing signal is heterodyned with 267-kHz local oscillator; the difference frequencies are selected by the 171-to-203-kHz bandpass filter and applied to the adder amplifier.

The MRIR signal is frequency shifted and passband limited from 235 to 365 kHz. The input from the tape recorder is heterodyned with a 300 kHz oscillator to provide a double-sideband AM signal that is passed through a 235 to 365 kHz filter. The equivalent basebandwidth is $\pm$65 kHz, or approximately $\pm$1.2 times the bit rate.

The ID signal is frequency shifted and passband limited from 400 to 530 kHz. The input signal from the tape recorder is frequency doubled and heterodyned with a 640-kHz local oscillator. The difference frequencies are then passed through a filter having a -3db points of 400 and 530 kHz. The bandwidth is such that the signal received at the ground station is a "single-sideband" FM carrier for

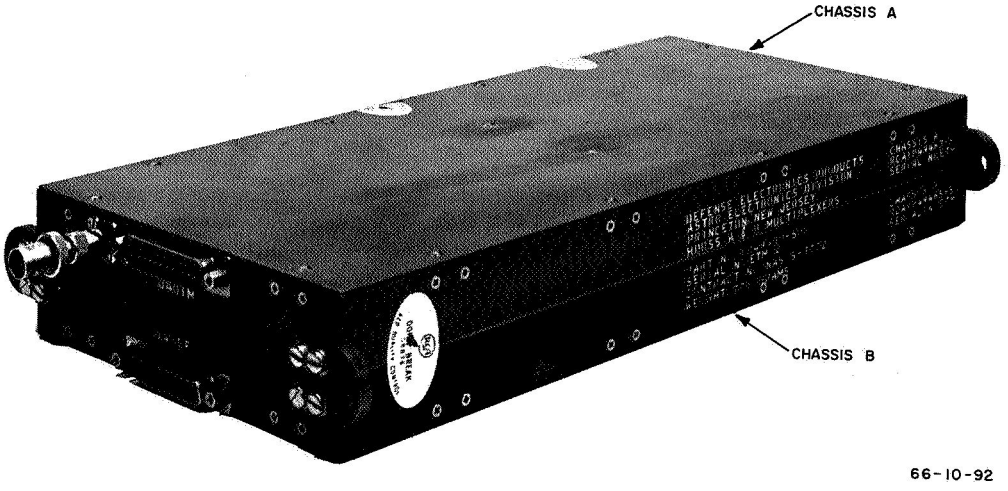

Figure 7. Multiplexer Assembly

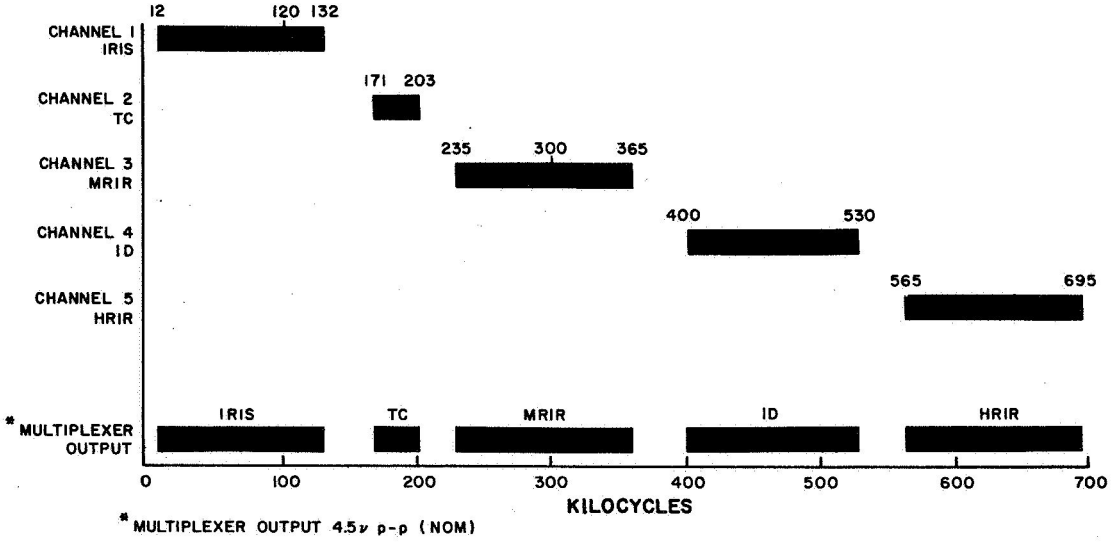

Figure 8. Frequency Spectrum, Multiplexer Output

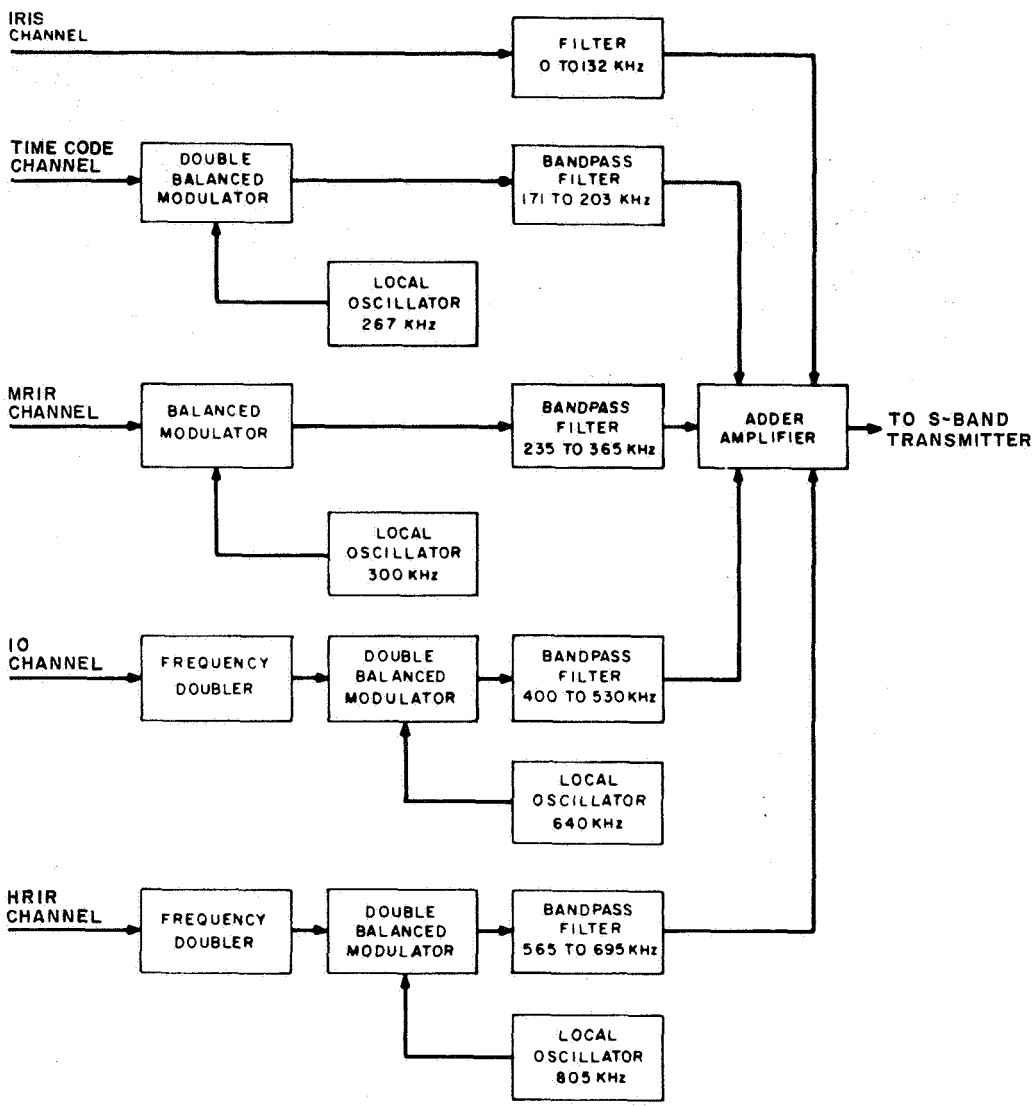

Figure 9. Multiplexer, Block Diagram

certain combinations of peak deviation and modulating frequencies. For example, for video signals superimposed on a white (120 kHz) average field, the signal becomes SSB-FM for any modulating frequency, since all upper sidebands corresponding to the video signal are removed by the multiplexer filter which cuts off at 400 kHz. The resultant signal is applied to the summing amplifier.

The HRIR signal is frequency shifted and passband limited to 565 to 695 kHz. The input signal from the tape recorder is frequency doubled and heterodyned with an 805 kHz local oscillator. The difference frequencies are then passed through a filter having -3db points of 565 and 695 kHz. The bandwidth is such that the signal received at the ground station is a single-sideband FM carrier.

SECTION 4
GROUND STATION MODIFICATIONS

A. GENERAL

The ground station equipment modified for HDRSS operation (GS-1 and GS-2) was orginally designed for the Nimbus I and II programs. HDRSS equipment designs were based on the following:

- Retrofit of existing circuits were possible,
- Removal of obsolete AVCS circuits,
- Instructions for ground station wiring to facilitate HDRSS operation.

Circuit details and interface data are presented in the instruction manual for the ground station modifications.[8]

B. DEMULTIPLEXER

Modification of the demultiplexer for HDRSS operation required the removal of existing AVCS and HRIR circuits, installation of new or modified circuits, and the design of an interface to ensure interchangeability of all HDRSS demultiplexers. The original demultiplexer contained eight channels; the HDRSS demultiplexer contains five channels.

The purpose of the demultiplexer is to separate the five subcarriers and compensate for degradation introduced by the r-f transmission link.

The IRIS channel consists of a low-pass filter and an equalizer (See Figure 10) which corrects the phase response of the cascaded multiplexer-demultiplexer filters to within $\pm 1\,\mu s$. The timing signal is selected by a 171- to 203-kHz filter and supplied directly to the processing circuits. The MRIR signal is selected by a filter with a passband from 235 to 365 kHz and is heterodyned with a 475-kHz local oscillator. The difference frequencies are selected by a low-pass 270-kHz

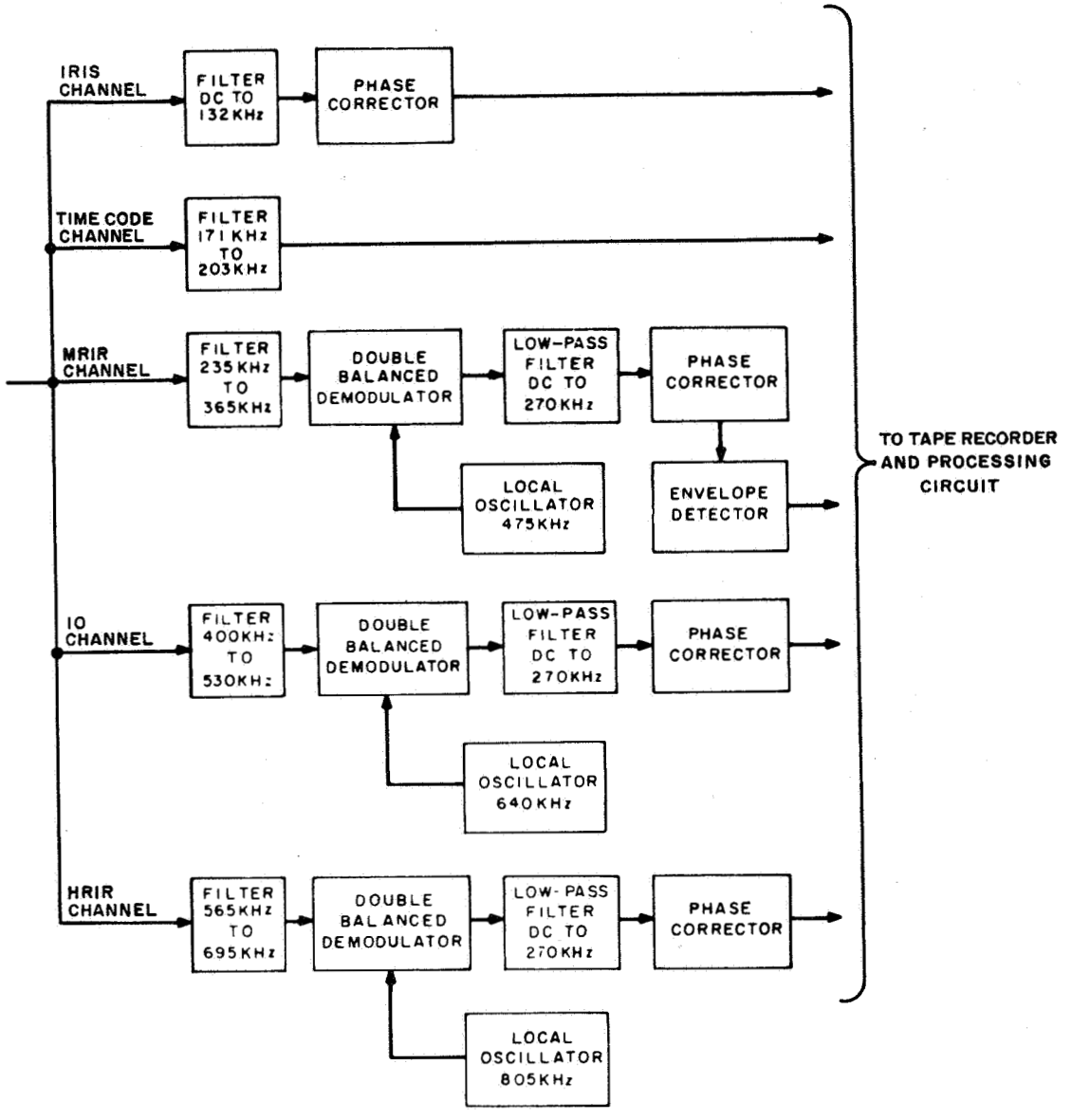

Figure 10. Demultiplexer, Block Diagram

filter and are passed through a phase corrector having a passband from 110 to 240 kHz. This channel, used in Nimbus I for an FM video subcarrier, is phase-equalized to within ±5 μs of constant time delay. At this point, the signal is a double-sideband AM wave with a center frequency of 175 kHz. This signal is envelope detected to recover the biphase MRIR data. The ID signal is selected by a filter with a passband of 400 to 530 kHz and heterodyned with a 640-kHz local oscillator. The difference frequencies are selected by a 270-low-pass filter and are applied to a phase corrector having a passband of 110 to 240-kHz, which corrects the phase response of the cascaded multiplexer-demultiplexer filters to within ±5 μs of constant delay. The HRIR signal is selected by a filter with a passband of 565 to 695 kHz and heterodyned with an 805-kHz local oscillator. The difference frequencies are selected by a 270-kHz low-pass filter and are applied to a phase corrector having a passband of 110 to 240 kHz, which corrects the phase response of the cascaded multiplexer-demultiplexer filters to within ±5 μs of constant delay.

C. AVCS INDEX COMPUTER

AVCS index computer modifications required for HDRSS operation are as follows:

- Adjustment of the film advance circuit to allow for a short interframe time (25 milliseconds).
- Provide for generation of a one storage control pulse after each stop pulse.
- Provide control circuits for redundant operation of the kine complexes.

Modification of the storage register control required the addition of new circuits to inhibit the generation of store pulses until the end of the frame. This change eliminates operation of the storage register relays to once per frame. Modification of the kine control circuits consisted of adding a second control circuit that provides for independent control of each kine complex. This addition provides for operation of redundant HDRSS systems.

D. 70-MM FILM PROCESSOR

Modification of the 70-mm film processor consists of the following:

- Disconnecting the indicator lamps for the legend on the display indicator

- Adjusting the upper positioning mirror to reduce the distance between pictures, and
- Adjusting microswitch MS-2 to provide a 6.2 second lock-out.

Prior to any adjustments, the display lamps (DS-1 through DS-11) that illuminate the legend on the display indicator are disconnected. Then the upper positioning mirror is adjusted until the digital readout is displayed directly beneath the video picture. This action reduces the space required between each 70-mm picture and ensures complete film pull-down between each video picture.

Microswitch MS-2 is adjusted until the film-advance lockout is 6.2 seconds, it was 7 seconds for AVCS operation. This adjustment ensures a film advance at the end of the frame and prevents film advances due to spurious signals during a video readout.

E. ID DEMODULATOR DRAWER

Modification of the ID demodulator drawer consists of the following:

- Installation of a newly designed alternate vertical sync circuit that generates output pulses from detected horizontal sync pulses.
- Rework of the flutter and wow demodulator to obtain operation at a 187-kHz rate.
- Install a doubler circuit for tape recorder checkout.
- Install the limiters, video demodulator, and time code demodulator (existing AVCS circuits).
- Rewire the chassis to provide an interface with the rack wiring.

Vertical sync start and stop pulses are generated at the beginning and end of each frame and are used to drive the deflection generator and the display equipment. Flutter and wow data is generated from the time code signal and used to vary the sweep rate of the kinescope to compensate for speed variations of the spacecraft tape recorder.

In GS No. 1, two identical circuits are used to provide flutter and wow data to each kine complex. A switch controlled relay selects either demodulator for use with either kine complex. In GS No. 2, there is one limiter and two demodulators; the output of the limiter is applied to one of the demodulators by a switch controlled relay. The demodulator outputs are then applied to separate kine complexes for signal processing.

A doubler circuit provides for checkout of the spacecraft tape recorder without the use of a multiplexer. Wiring is completed with patch cords at the jack panel.

The AVCS video demodulator was not changed as the HDRSS ID signal has the same format as the AVCS signal. The time code demodulator was not changed as its operation is independent of frequency, thereby making it suitable for HDRSS or AVCS operation.

The ID demod drawers at GS-1 and GS-2 are interchangeable with the following limitations; the GS-2 unit does not have the doubler or dual flutter and wow capabilities.

F. SCHMITT TRIGGER CIRCUITS

Modification of the Schmitt trigger circuit in the kinescope video chassis of each kine complex consists of installing a new board that provides an additional output signal. This signal is used as an input signal for the alternate vertical sync circuit in the ID demod drawer. The output of each Schmitt Trigger is connected to a switch on the control panel that routes one of the output signals to the alternate vertical sync circuit. This configuration provides for the use of either kine complex. If redundant capabilities are required, a second alternate vertical sync circuit could be installed and two ID video channels could be tested simultaneously.

G. HRIR DEMODULATOR DRAWER

Modification of the HRIR demod drawer consists of the following:

- Installation of a newly designed demodulator and output amplifier (GS-1 and GS-2).
- Installation of a newly designed horizontal sync circuit and time code demodulator (GS-1 only).
- Rework of the fax motor drive circuit for operation with 2000 Hz (GS-1 only).
- Rewire the chassis to provide an interface with the rack wiring.

The HRIR video signal is detected and amplified to provide the proper output level to the processing equipment. In GS-1 the video signal is applied to a facsimile recorder; in GS-2 the video is monitored on an oscilloscope. The horizontal sync circuit drives the sweep circuit in the facsimile recorder and is applied to the facsimile motor drive circuit where the 20 kHz signal is divided by 10, shaped, and supplied to the facsimile recorder as a 2000 Hz signal. The GS-1

chassis does not contain any circuits compatible with the Nimbus I and II HRIR signal. The GS-2 chassis contains an old flutter and wow demodulator, an auxiliary time code demodulator, and a time code demodulator. However, they are not compatible with the HDRSS HRIR time code of 20 kHz. The GS-2 chassis doesn't contain a horizontal sync circuit or a fax-motor drive circuit.

H. SIGNAL CONDITIONERS

Ground station modifications include the addition of signal conditioners for the purpose of converting the biphase format to an NRZ format. The signal conditioners are commercial items that will be mounted adjacent to the jack panels and all coax leads will be held to a minimum. Four units will be installed in GS-1 (two for IRIS signals, and two for MRIR signals) to provide for redundant operation. Two units will be installed in GS-2.

Each biphase signal is passed to timing extraction circuits where bit timing is extracted by a phase-locked loop which is synchronized with the zero crossing of the incoming data (See Figure 11). The extracted timing pulses are then used to sample the polarity of the incoming data and provide a data signal. Both the data signal and the timing signal (clock) are used in the display equipment.

J. JACK PANEL AND SWITCH PANEL OVERLAYS

Jack panel and switch panel overlays were designed to reflect the HDRSS system. The jack panel overlays provide a functional block diagram that depicts signal flow. The switch panel overlays identify the switching functions shown on the jack panel overlays.

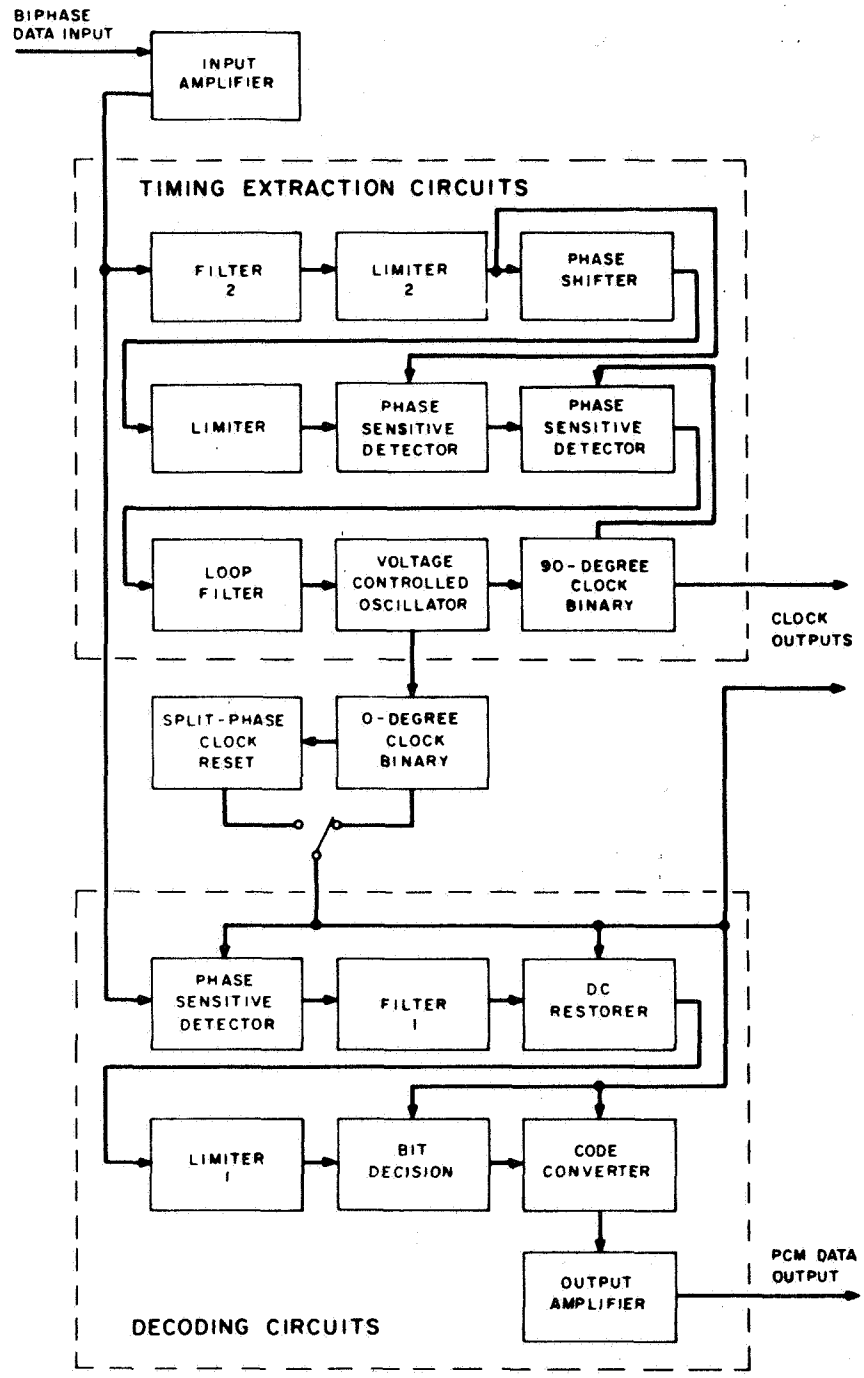

Figure 11. Signal Conditioner, Block Diagram

SECTION 5
BENCH CHECK AND INTEGRATION TEST EQUIPMENT

A. BENCH CHECK UNITS

1. Purpose of Bench Check Units

The BCU shown in Figure 12 is a self-contained test facility that provides all power, timing signals, and command signals for testing and exercising the Spacecraft Subsystem assemblies (as separate entities or as a subsystem) prior to installation in the Spacecraft. The BCU has the capability to do the following:

- Exercise the tape transport assembly, tape recorder electronics module, biphase repeater module, and the multiplexer module under operating conditions that approximate those in the spacecraft/ground station functional loop.
- Obtain quantitative and qualitative data to determine if the HDRSS Spacecraft Subsystem meets established performance criteria.
- Localize malfunctions in the Spacecraft Subsystem under test whenever a performance anomaly is detected.
- Verify the functional integrity of the BCU by self-check features.

Interconnection between the BCU and the Spacecraft Subsystem for six separate conditions are provided by switching circuits. Two of the test conditions provide for complete subsystem tests. They are RECORD-MINCOM PLAYBACK and TAPE RECORDER + MUX PLAYBACK. Switching for module or self test (BCU) are as follows:

- T/R P.B. ONLY - for testing the spacecraft tape recorder without the multiplexer.
- MUX ONLY - for testing the spacecraft multiplexer without the tape recorder.
- TEST MODE - for BCU self-check.
- EXTERNAL - in which all simulator, spacecraft equipment, and processing equipment interfaces are open to permit manual interconnection of equipments for special tests.

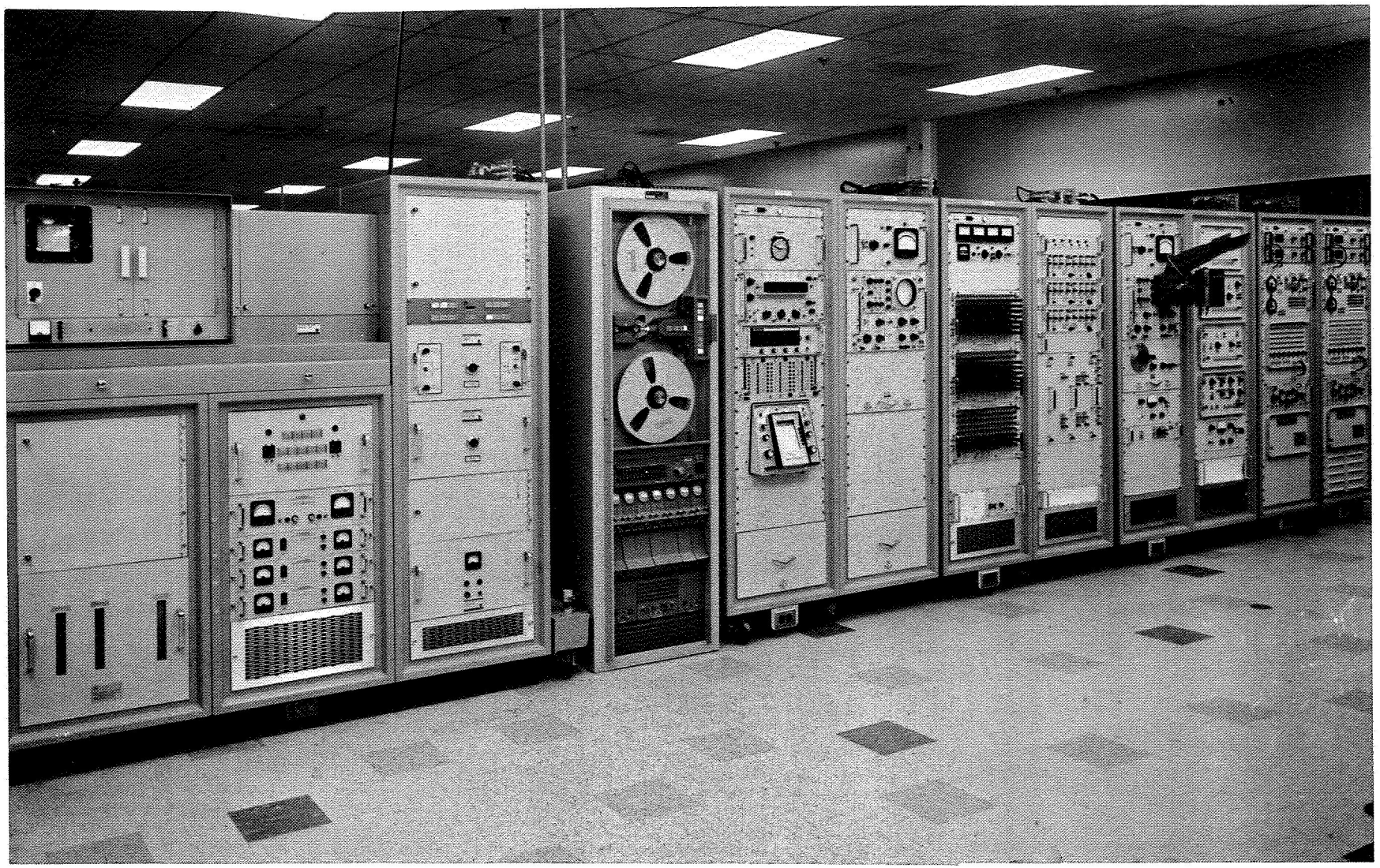

Figure 12. Typical Bench Check Unit

For each of the test conditions except the last item, the BCU provides complete circuit connections and controls the output signal rate of the simulators as required. Detailed descriptions are contained in the BCU instruction manual.[9]

2. Spacecraft Subsystem Test

Test of the Spacecraft Subsystem requires two modes of operation, record and playback. During the playback mode all the data except HRIR can be processed for evaluation. HRIR data must be recorded on the BCU tape recorder and played back at one-fourth the record speed before it can be processed and evaluated. A complete subsystem test requires that the Spacecraft Subsystem be operated in both the record and playback modes. A functional block diagram of the BCU and the Spacecraft Subsystem is shown in Figure 13.

a. Record Mode

When the record mode is selected, the clock simulator is set at record to provide 400 cps sync signals to the Spacecraft tape recorder and timing pulses to the Image Dissector (ID), Time Code (TC), High Resolution Infra-red (HRIR) signal simulators. The timing pulses are also applied to the Bit Error Rate Checkers (BERC) where Infra-red Interferometer Spectrometer (IRIS) and Medium Resolution Infra-red (MRIR) signals are generated. The output of the signal simulators and BERC are then recorded on the Spacecraft tape recorder.

b. Playback Mode

When the playback mode is selected, the clock simulator is set at playback to provide a 400 cps sync signal to the spacecraft recorder, and timing pulses to the ID, TC, and HRIR signal simulators. Timing pulses are also applied to the BERC where IRIS and MRIR signals are generated.

During playback two video and one time code signals are applied directly to the multiplexer; the IRIS and MRIR signals are applied to the biphase repeater and the switching equipment provides open circuits for the simulator and BERC outputs thereby eliminating input signal interference.

In the biphase repeater, timing is derived from the input signal and used to reconstruct biphase data free of high speed jitter. If signal degradation is not a problem, the processing circuits can be bypassed by a command from the command simulator. The outputs from the biphase repeaters are then routed through the biphase repeater to the multiplexer, where the five signals are added together to form a 12- to 695-kHz subcarrier.

The subcarrier is applied to the RF link simulator, where the amplitude of the subcarrier is reduced to a level suitable for processing in the demultiplexer.

Flat or triangular noise that simulates transmitter/receiver loop noise of the Nimbus system may also be added.

c. Signal Processing and Data Evaluation

In the demultiplexer, the 12- to 695-kHz subcarrier is separated and the signals are frequency shifted to the frequencies required for processing and display. The ID signal is displayed on 70-mm film transparencies and analyzed for resolution, linearity, and noise. Processing of the HRIR signal requires playback of the BCU tape recorder at a speed reduction of four to one. When played back, the HRIR signal is demodulated and applied to the horizontal sync detector and video outputs. All the control signals developed from the HRIR video and time code signal are applied to test equipment for display, measurement and analysis. The IRIS and MRIR signals are decoded and applied to the comparators where the input signal is compared with a signal from the pattern generator to provide a bit error count and a word frame count. The bit-error count is used to determine the quality of Spacecraft Subsystem operation.

B. DEMULTIPLEXER TEST SET

The demultiplexer test set is a self-contained unit designed to simulate a multiplexer output signal. The electrical configuration is identical to that used in the Spacecraft multiplexer. The test set is used to obtain the following quantitative information concerning electrical performance of a demultiplexer:

- MRIR amplitude frequency response.
- IRIS channel phase delay.
- MRIR channel phase delay.
- Time Code and flutter and wow channel transmission delay.
- ID channel envelope delay.
- HRIR channel envelope delay.

FOLDOUT FRAME 1

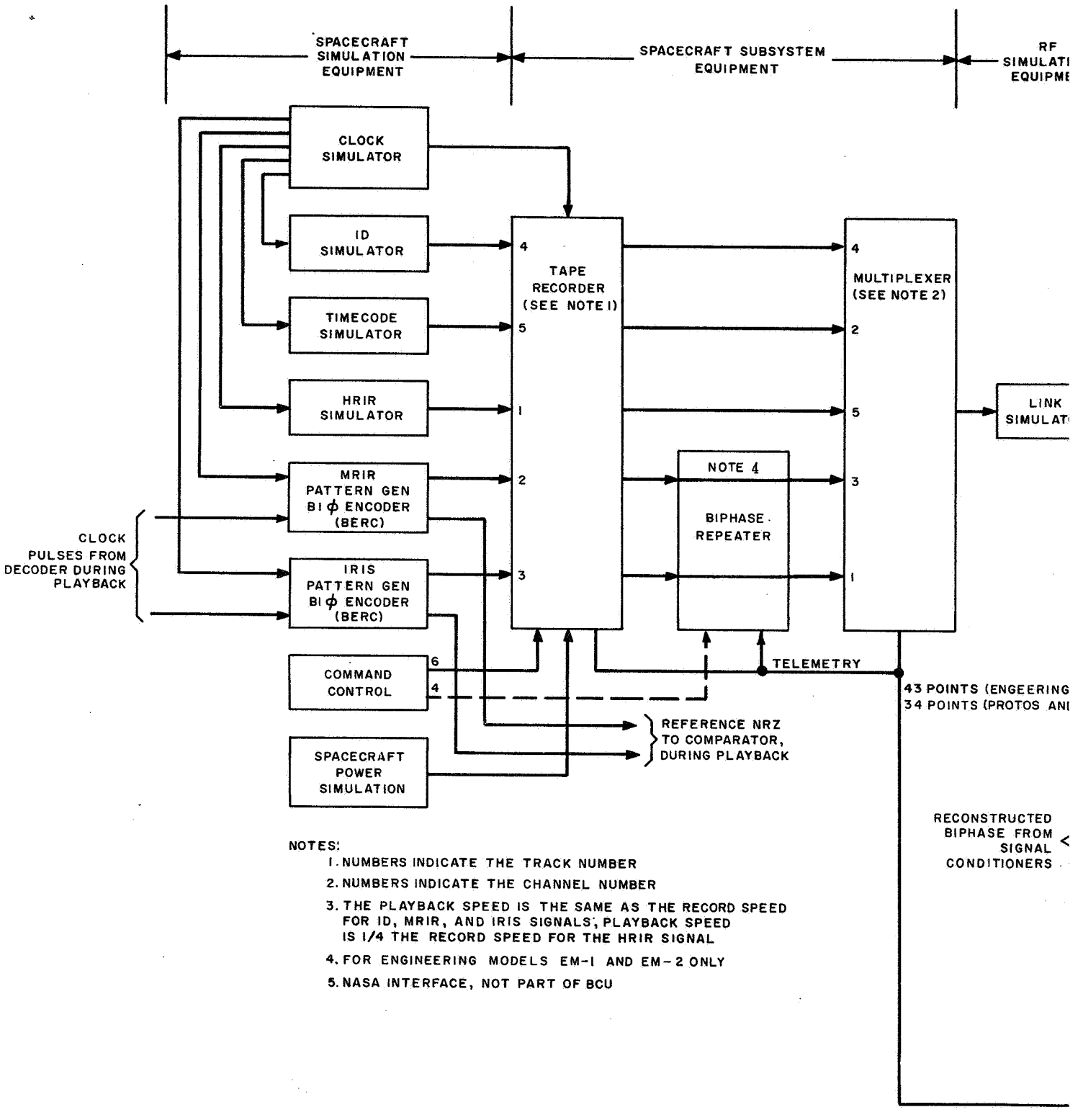

NOTES:

1. NUMBERS INDICATE THE TRACK NUMBER
2. NUMBERS INDICATE THE CHANNEL NUMBER
3. THE PLAYBACK SPEED IS THE SAME AS THE RECORD SPEED FOR ID, MRIR, AND IRIS SIGNALS; PLAYBACK SPEED IS 1/4 THE RECORD SPEED FOR THE HRIR SIGNAL
4. FOR ENGINEERING MODELS EM-1 AND EM-2 ONLY
5. NASA INTERFACE, NOT PART OF BCU

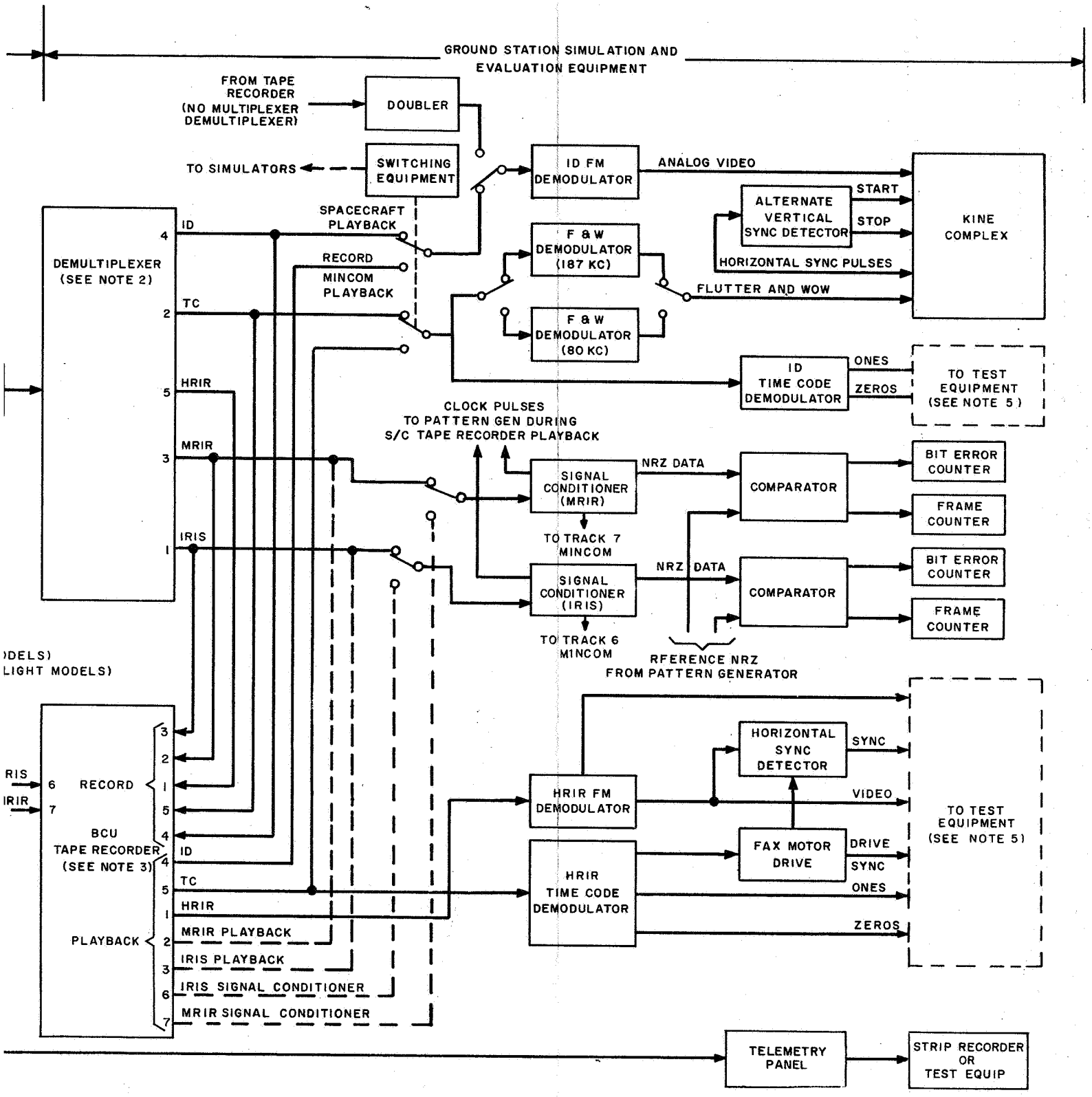

Figure 13. HDRSS BCU, Functional Block Diagram

SECTION 6
SYSTEM MODULE TESTS

A. INTRODUCTION

Descriptions of performance tests conducted prior to system integration and the amplitude frequency response are presented for the following equipment:

- Tape Recorder (tape transport and electronics module)
- Multiplexer/Demultiplexer (ID and HRIR amplitude response)
- HRIR Demodulator
- Signal Conditioners (Bit-Error-Rate vs SNR)

Individual test procedures and performance specifications are referenced when applicable. The detailed data presented in this section was extracted from the equipment log books.

B. TAPE RECORDER

The HDRSS tape recorder consists of a tape transport and the associated electronics module that were tested as a complete entity to ensure satisfactory performance. Performance specifications are contained in RCA Dwg. PS-1849826.

1. Test Descriptions

Module tests of the tape transport for EM-1 and EM-2 consisted of operational tests at -5° C, +25° C, and 55° C. The scope of the tests was to verify proper operation of the tape recorder and to measure the parameters listed in Table 2. A block diagram of the test set-up is shown on Figure 14. A block diagram of the test set-up used for the flutter measurements is shown in Figure 15.

2. Test Data Summary

The test data summary was compiled from tests performed during engineering evaluation at ambient and thermal temperatures. Table 2 contains power profile data, acceleration and deacceleration data, noise feedback into power line, record mode telemetry, and playback data for each channel. The 1/10 octave flutter spectrum (See Figures 16 through 18) obtained from EM-2 was measured with an rms voltmeter at temperatures of -5° C, +25° C, and 55° C. This data was obtained with the tape transport mounted in a container pressurized at 2 psig. The record

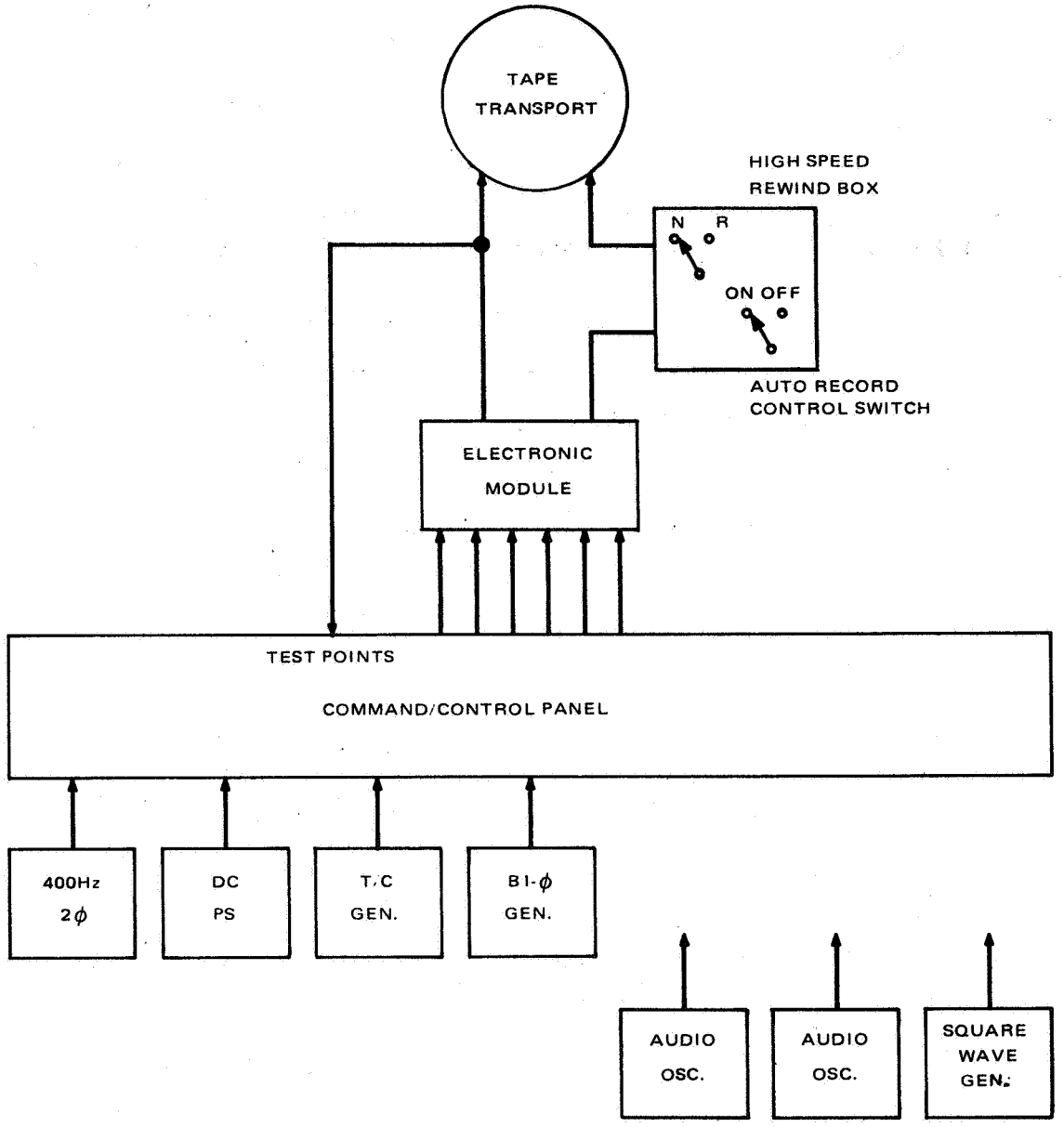

Figure 14. Tape Recorder Test Set-up

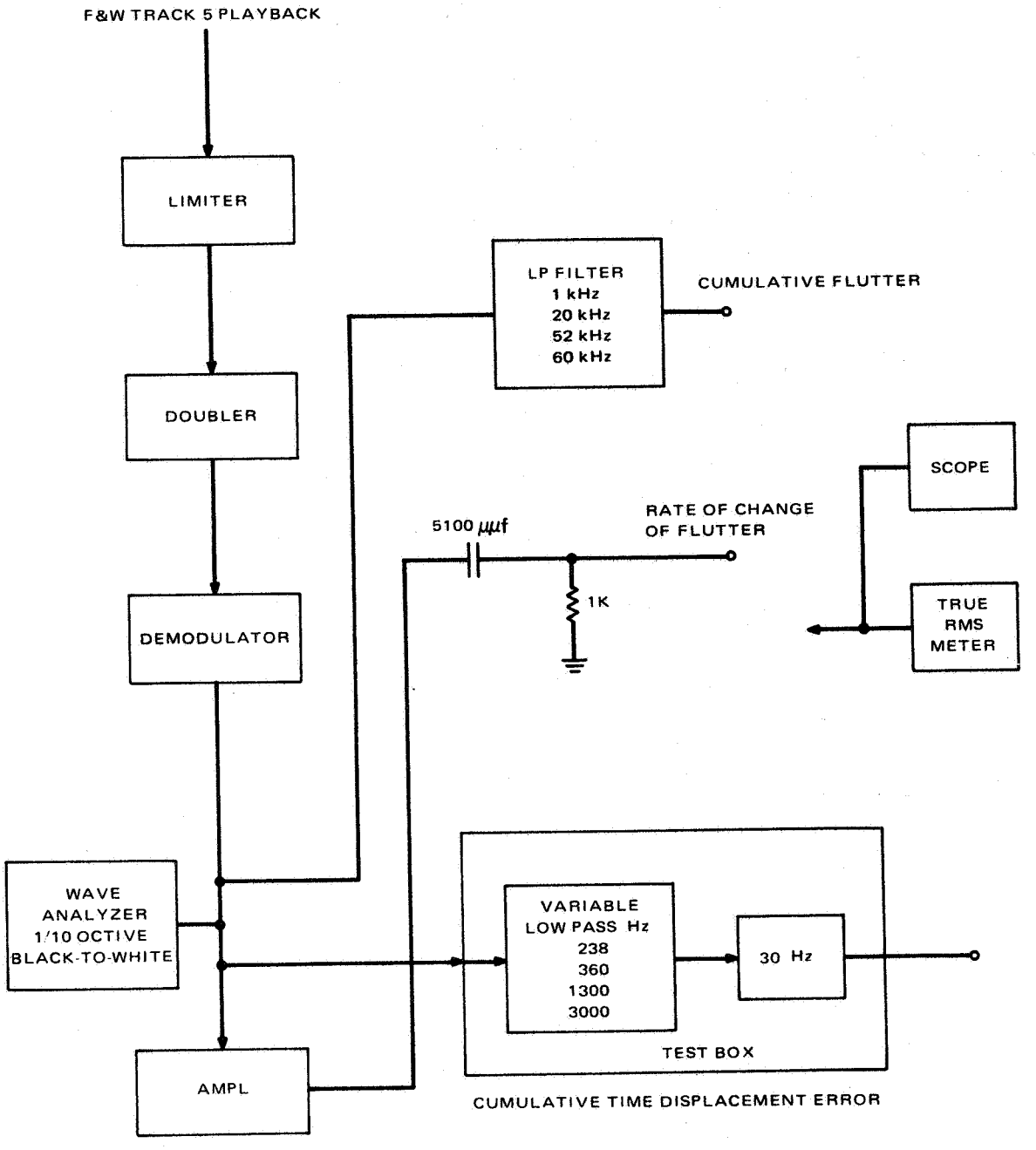

Figure 15. Flutter Measurement Test Set-up

TABLE 2. TEST DATA SUMMARY, TAPE TRANSPORT

Parameter or Mode	Required	Measured			
		EM-1			EM-2
		-5°C	+25°C	+55°C	25°C
POWER PROFILE					
Record Mode					
Start Current	820 ma max	485 ma	480 ma	485 ma	470 ma
Run Current	410 ma max	345 ma	340 ma	340 ma	330 ma
Start to Run Time	210 to 4.0 sec		3.2 sec		2.7 sec
Playback Mode					
Start Current					
Beginning	1.5 A		1.2 A		1.25 A
Middle	1.5 A		1.2 A		1.20 A
End	1.5 A		1.2 A		1.25 A
Run Current					
Beginning	610 ma	530 ma	490 ma	480 ma	500 ma
Middle	610 ma	535 ma	510 ma	510 ma	520 ma
End	610 ma	600 ma	570 ma	620 ma	600 ma
Start to Run Time	2.0 to 4.0 sec				
ACCELERATION AND DEACCELERATION					
Record Motor					
Acceleration	1.0 sec max		0.55 sec		0.52 sec
Deacceleration	0.5 sec max		-		-
Playback Motor					
Acceleration					
Start	1.5 sec max	1.3 sec	0.98 sec	0.98 sec	0.80 sec
Middle	1.5 sec max	1.3 sec	1.1 sec	1.1 sec	0.92 sec
End	1.5 sec max	2.25 sec	1.4 sec	1.55 sec	1.1 sec
Deacceleration	1.5 sec max		-		-
NOISE FEEDBACK INTO POWER LINE					
Record Mode	250 mv p-p		20 mv p-p		5 mv p-p
Playback Mode	max		28 mv p-p		10 mv p-p
RECORD MODE TELEMETRY					
Digital Telemetry					
Motor Rotation	-6.7 to -7.3 V		-6.5 V		-6.4 V
Record EOT	0 ±0.2 V		0.0 V		0.0 V
Playback EOT	0 ±0.2 V		0.0 V		0.0 V
Record On/Off	-6.7 to -7.3 V		-7.0 V		-7.0 V
Record Command	-6.7 to -7.3 V		-7.0 V		-7.0 V
Playback Command	0 ±0.2 V		0.0 V		0.0 V
Full Time Power	-6.7 to -7.3 V		-7.1 V		-7.0 V
Record Motor Start/Run	-6.7 to -7.3 V		-7.0 V		-7.0 V
Playback Motor Start/Run	0 ±0.2 V		0.0 V		0.0 V
HRIR/Alternate	0 ±0.2 V		0.0 V		-
Analog Telemetry					
Recorder Pres	-2.0 to -2.7 V	-3.10 V	-3.10 V	-3.13 V	-2.72 V
Recorder Temp	-2.5 to -3.2 V	-2.12 V	-3.70 V	-4.54 V	-2.80 V
Enclosure Temp	-2.0 to -4.0 V	-0.92 V	-3.0 V	-4.5 V	-2.69 V
ID Record Head	-3.3 to -3.7 V	-3.4 V	-3.5 V	-3.6 V	-3.48 V
HRIR Record Head	-3.4 to -3.9 V	-3.6 V	-3.7 V	-3.8 V	-3.58 V
TC Record Head	-2.5 to -3.5 V	-3.0 V	-3.0 V	-2.9 V	-3.21 V
Inv Power Phase 1-A	-3.5 to -4.0 V	-3.8 V	-3.9 V	-3.85 V	-3.8 V
Inv Power Phase 1-B	-3.5 to -4.0 V	-3.8 V	-3.9 V	-3.85 V	-3.79 V
Inv Power Phase 2-A	-3.5 to -4.0 V	-3.8 V	-3.9 V	-3.84 V	-3.79 V
Inv Power Phase 2-B	-3.5 to -4.0 V	-3.8 V	-3.8 V	-3.80 V	-3.8 V
MRIR Record Head	-2.7 to -3.1 V	-0.79 V	-2.9 V	-2.96 V	-3.08 V
IRIS Record Head	-2.7 to -3.1 V	-2.9 V	-2.98 V	-2.98 V	-3.1 V
ID TRACK PLAYBACK AT 51.2 kHz					
Frequency Response	-10 db max		-10.2 db	-7.4	
Overshoot (black-to-white)	10% max		-		0%
ID Limiter Output	6.5 ±0.64 p-p	5.9 V p-p	6.0 V p-p	6.0 V p-p	6.1 V p-p
HRIR TRACK PLAYBACK AT 11.5 kHz					
Frequency Response	-2.5 db max		-0.4 db		-1.0 db
Overshoot (black-to-white)	10% max		-		0%
HRIR Limiter Output	6.5 ±0.6 V p-p	-	6.2 V p-p	6.4 V p-p	6.1 V p-p
TIME CODE PLAYBACK					
Output Amplifier	6.5 ±0.6 V p-p	6.8 V p-p	6.4 V p-p	8.4 V p-p	6.0 V p-p
Valley-to-Peak Pat	0.3 to 0.65	0.47	0.55	0.48	0.4
MRIR TRACK PLAYBACK					
Frequency Response at 90 kHz	-				-4.2 db
MRIR Limiter Output (60 kHz)	6.5 ±0.6 V p-p	6.2 V p-p	6.2 V p-p	6.3 V p-p	6.1 V p-p
IRIS TRACK PLAYBACK					
Frequency Response					
30 kHz	-				0 db
90 kHz	-				-4.4 db
120 kHz	-				-7.7 db
150 kHz	-18.0 db				-12.2 db
180 kHz	-				-17.3 db
IRIS Limiter Output (60 kHz)	6.5 ±0.6 V p-p	5.9 V p-p	6.0 V p-p	6.2 V p-p	6.0 V p-p

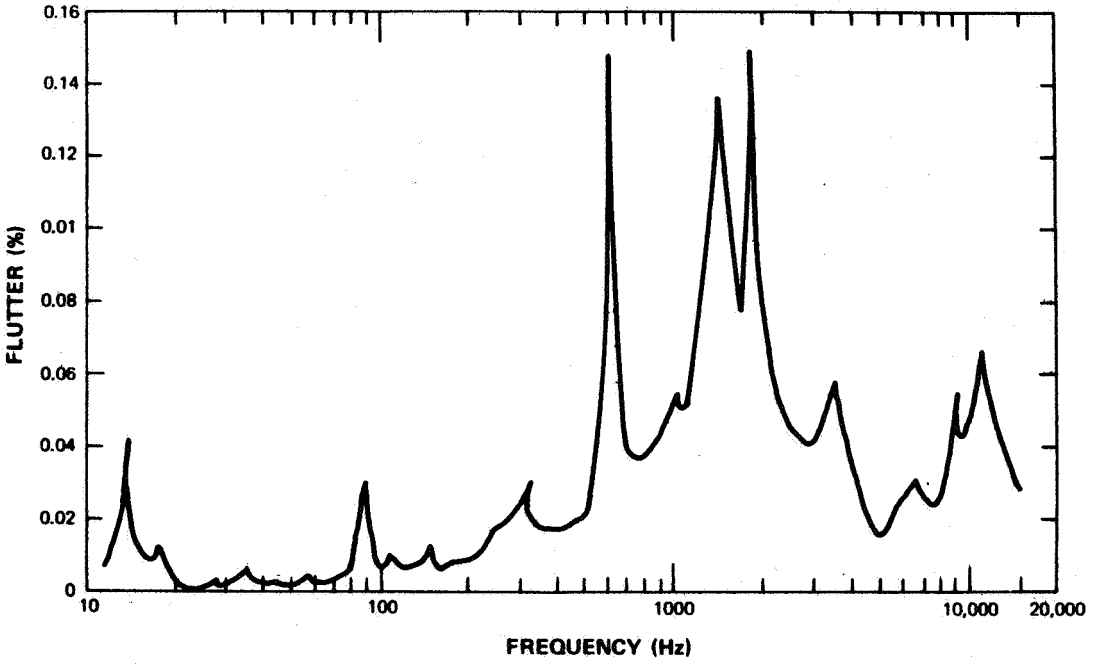

Figure 16. 1/10 Octave Flutter Spectrum, -5°C

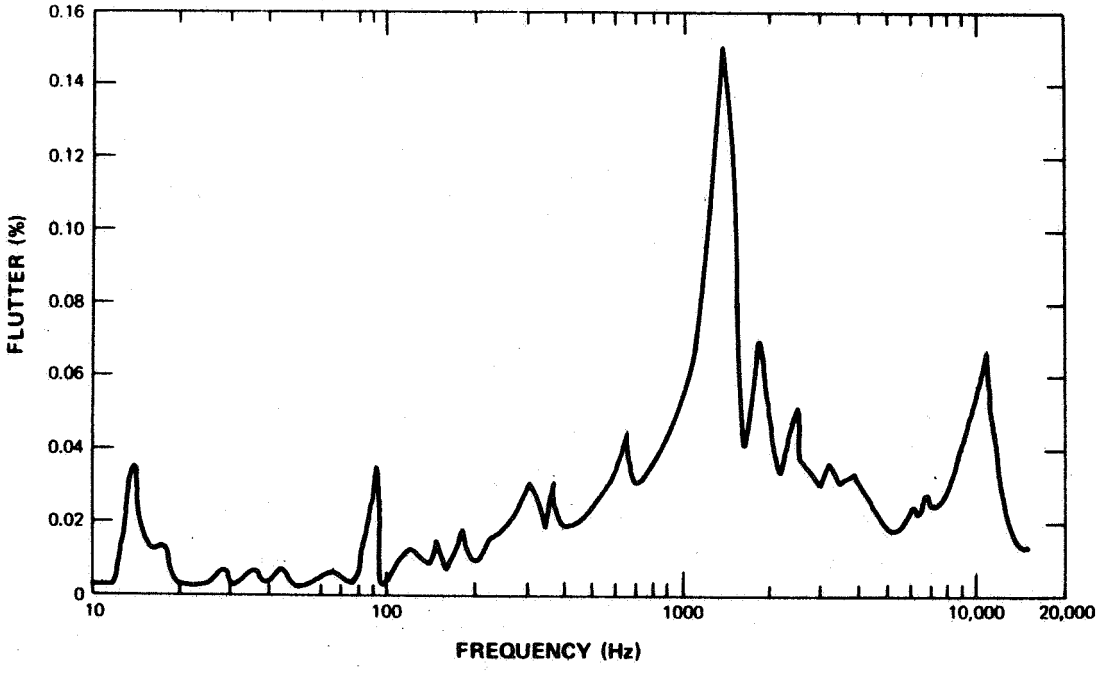

Figure 17. 1/10 Octave Flutter Spectrum, +25°C

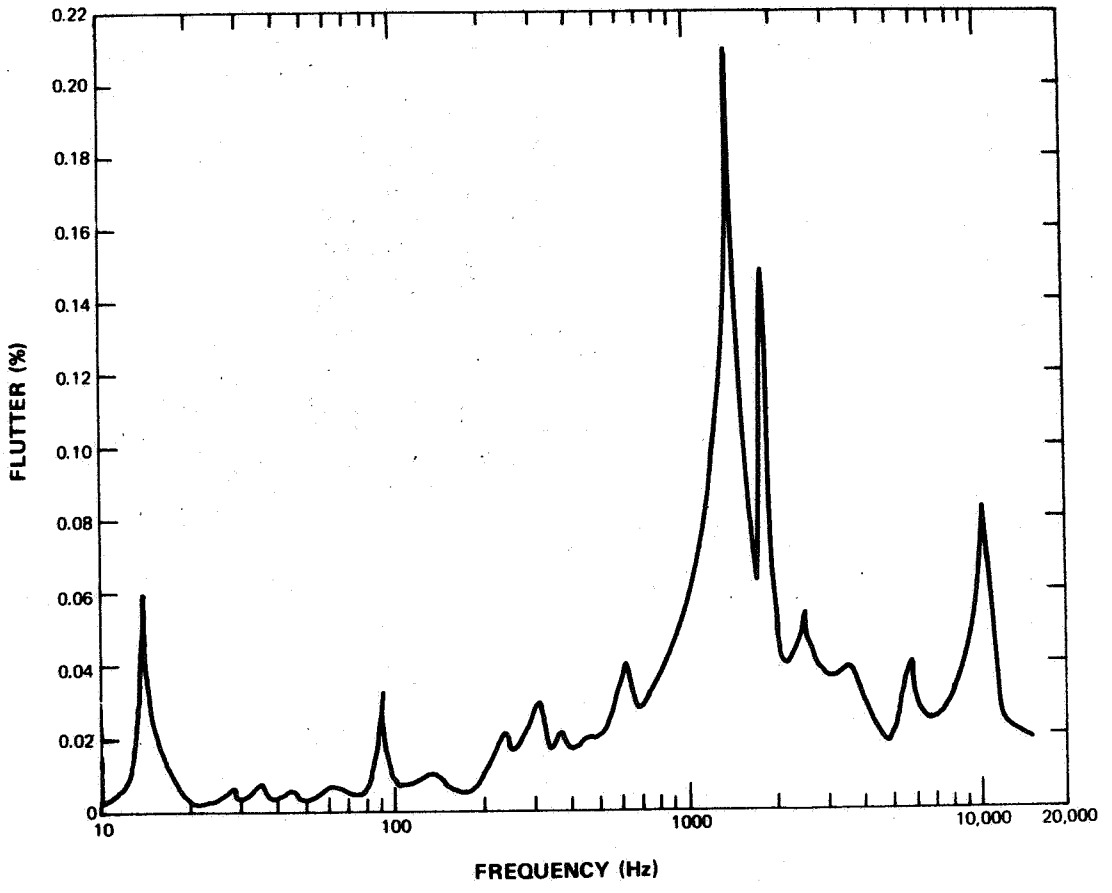

Figure 18. 1/10 Octave Flutter Spectrum, +55° C

motor (No. 66-10-71 as of October 15, 1966) two dampers, and two planetary flywheels provided an inertia of 0.187 lbs-in^2. The total flutter measured (See Figure 19) at each temperature was measured under the same conditions specified for the 1/10 octave flutter spectrum. The total jitter measured (See Figure 20) was also obtained under the same test conditions.

C. MULTIPLEXER/DEMULTIPLEXER

The performance specifications for both the multiplexer and demultiplexer are contained in RCA performance specification PS-1849480. Module tests of the engineering model multiplexers were conducted with a demultiplexer as shown on Figure 21. Some of the parameters considered are amplitude-frequency response, noise immunity, telemetry, channel crosstalk, harmonic distortion, and bit error rate. Detailed test procedures for the multiplexer and demultiplexer are contained in RCA test procedures TP-1849480 and TP-1849418, respectively. The amplitude-frequency response data for the ID and HRIR channels was extracted from the equipment log books.

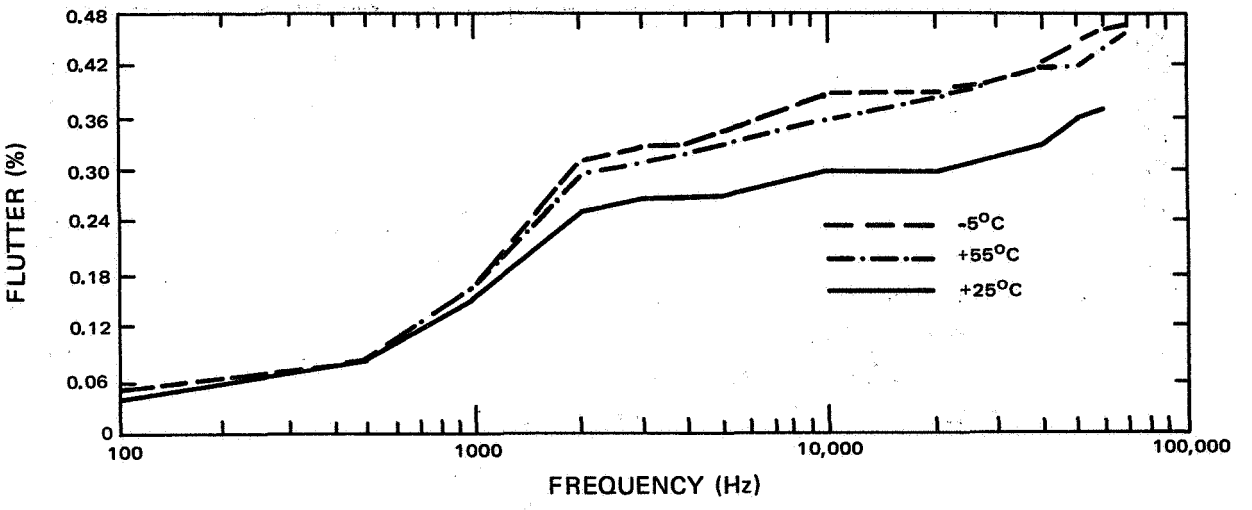

Figure 19. Cumulative Flutter, EM-2 Tape Transport

1. ID Channel Amplitude-Frequency Response

The amplitude-frequency response of the ID channel in the engineering model multiplexers for three different temperatures are presented in Table 3. The amplitude-frequency response of the demultiplexer is presented in Table 4. The amplitude-frequency response of the EM-2 multiplexer-demultiplexer is presented in Table 5. The EM-1 multiplexer-demultiplexer amplitude-frequency response is not presented as the EM-2 data is typical of the system.

2. HRIR Channel Amplitude Frequency Response

The amplitude frequency response of the HRIR channel was obtained in the same manner as the ID channel data and is presented in Tables 6 through 8.

D. HRIR DEMODULATOR

Module tests of the HRIR demodulator consists of SNR, amplitude-frequency response, drift, and linearity. Detailed test procedures for the HRIR demodulators are contained in RCA Test Procedure TP-1769312. The frequency response of the HRIR demodulator is determined by the post-detection filter. The amplitude response of this filter, a fifth order Bessel, is shown on Figure 22. The frequency of interest for the test conditions is 2880 Hz (the max bandwidth frequency times the spacecraft record speed times the ground station playback speed -360 $\times$ 32 $\times$ 1/4). The filter response at this frequency is -1.0 db.

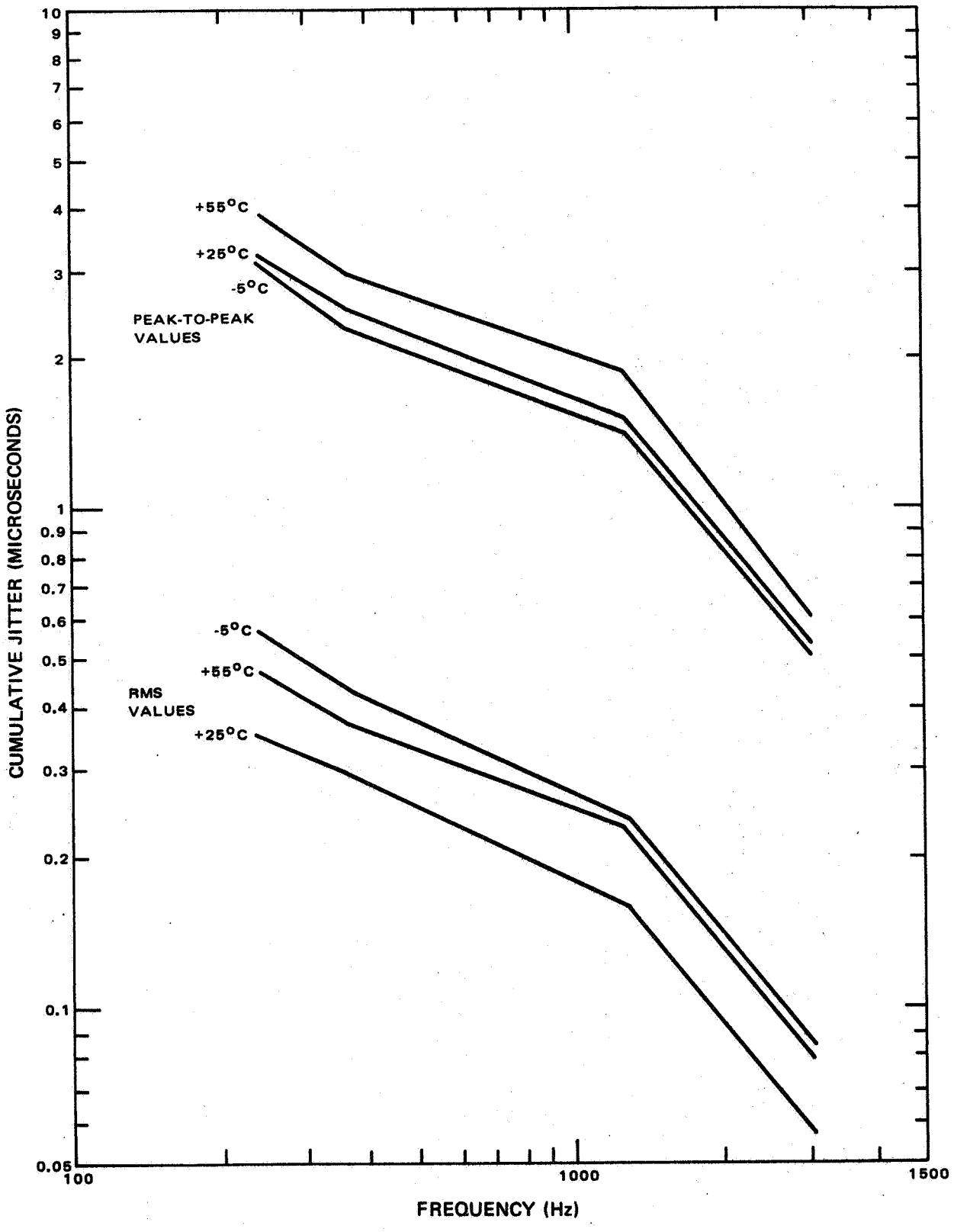

Figure 20. Cumulative Jitter, EM-2 Tape Transport

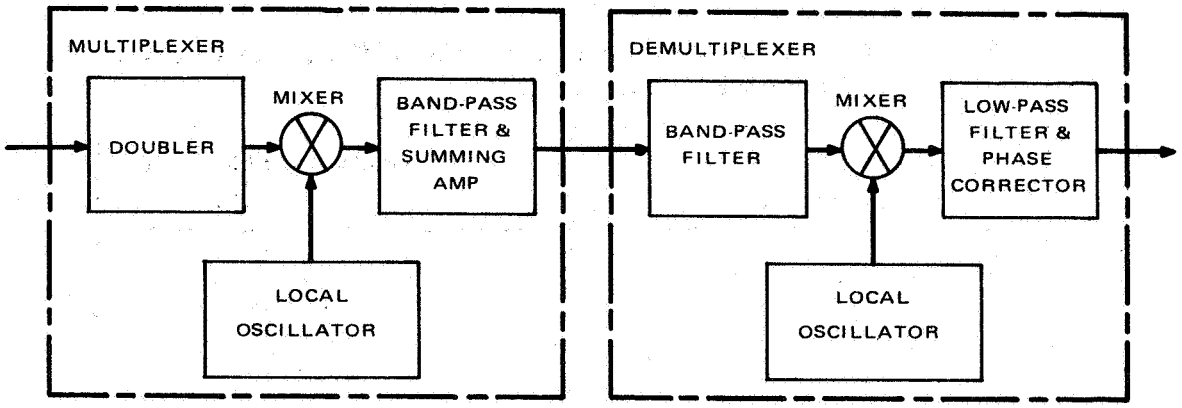

Figure 21. Multiplexer/Demultiplexer, Block Diagram

TABLE 3. MULTIPLEXER AMPLITUDE-FREQUENCY RESPONSE, ID CHANNEL

Multiplexer Frequency (kHz)		Amplitude-Frequency Response (db)					
		EM-1			EM-2		
Input	Output*	25° C	-5° C	+55° C	25° C	-5° C	+55° C
37.5	565.0	-45.8	-41.6	-51.6	-45.3	-44.2	-48.8
46.0	548.0	-18.3	-16.8	-22.4	-16.0	-17.8	-20.2
55.0	530.0	- 2.0	- 1.2	- 2.8	- 1.0	- 0.5	- 2.0
73.9		0.0	0.0	0.0	---	---	---
75.0		---	---	---	0.0	0.0	0.0
120.0	400.0	- 2.0	- 2.2	1.8	- 1.8	- 2.2	- 2.0
128.5	383.0	-30.6	-34.2	29.0	-31.9	-32.5	-30.5
137.5	365.0	-54.0	-54.5	53.4	-55.0	-55.5	-55.5

*Nominal output frequency; the local oscillator frequency is 640 kHz.

TABLE 4. EM-1 DEMULTIPLEXER AMPLITUDE-FREQUENCY RESPONSE, ID CHANNEL

Demultiplexer Input Frequency (kHz)	Amplitude Response (db)
365.0	-45.5
383.0	-30.0
400.0	- 2.2
478.3	0.0
530.0	- 1.7
548.0	-19.3
565.0	-44.8

TABLE 5. EM-2 MULTIPLEXER-DEMULTIPLEXER AMPLITUDE-FREQUENCY RESPONSE, ID CHANNEL

Doubled Input* Frequency (kHz)	Response (db)
100	- 9.5
110	- 1.2
120	- 0.3
130	- 0.1
140	0
150	0.1
160	- 0.5
170	- 1.1
180	- 1.0
190	- 1.2
200	- 1.2
210	- 1.4
220	- 2.0
230	- 1.8
240	- 5.2
250	-37.9
260	-49.1
270	-48.5

*Input to Local Oscillator.

TABLE 6. MULTIPLEXER AMPLITUDE-FREQUENCY RESPONSE, HRIR CHANNEL

Multiplexer Frequency (kHz)		Amplitude-Frequency Response (db)					
		EM-1			EM-2		
Input	Output*	25° C	-5° C	+55° C	25° C	-5° C	+55° C
35.0	735.0	-50.0	-47.0	-54.9	-51.8	-49.1	-56.0
42.5	720.0	-24.0	-24.0	-30.0	-18.5	-24.5	-31.1
55.0	695.0	- 0.4	- 1.2	- 2.7	- 1.9	- 1.2	- 3.4
		0.0	0.0	0.0	0.0	0.0	0.0
		(80 kHz)	(70 kHz)	(90 kHz)	(70 kHz)	(60 kHz)	(78 kHz)
120.0	565.0	- 2.8	- 3.5	- 1.7	- 2.2	- 2.8	- 2.7
128.5	548.0	-28.0	-30.2	-24.8	-27.0	-30.1	-25.2
137.5	530.0	-54.0	-53.5	-54.5	-57.0	-55.8	-58.8

*Nominal output frequency; the local oscillator frequency is 805 kHz.

TABLE 7. EM-1 DEMULTIPLEXER AMPLITUDE-FREQUENCY RESPONSE, HRIR CHANNEL

Demultiplexer Input Frequency (kHz)	Amplitude Response
530.0	-45.0
548.0	-20.0
565.0	- 3.0
604.8	0.0
695.0	- 3.0
720	-20.0
735	-55.0

TABLE 8. EM-2 MULTIPLEXER-DEMULTIPLEXER AMPLITUDE-FREQUENCY RESPONSE, HRIR CHANNEL

Doubled Input* Frequency (kHz)	Response (db)
100	- 9.7
110	- 2.4
120	- 0.2
130	- 0.2
140	0
150	0
160	0
170	- 0.7
180	- 0.4
190	- 0.8
200	- 1.0
210	- 1.6
220	- 2.1
230	- 3.3
240	- 7.7
250	-23.9
260	-23.7
270	-23.2

*Input to Local Oscillator.

E. SIGNAL CONDITIONER

1. Test Descriptions

Tests of the signal conditioners are performed with the Bench Check Unit simulating the spacecraft equipment as shown on Figure 23. The tests consisted of Bit-Error-Rate (BER) vs SNR, and BER vs SNR with flutter and offset. Prior to all the tests, the signal conditioners were calibrated in accordance with their respective instruction manuals. Detailed test requirements are specified in RCA Test Procedure TP-1769312. The Dynatronics signal conditioner, Model No. BSC-7B, Serial No. 046, was used for the tests.

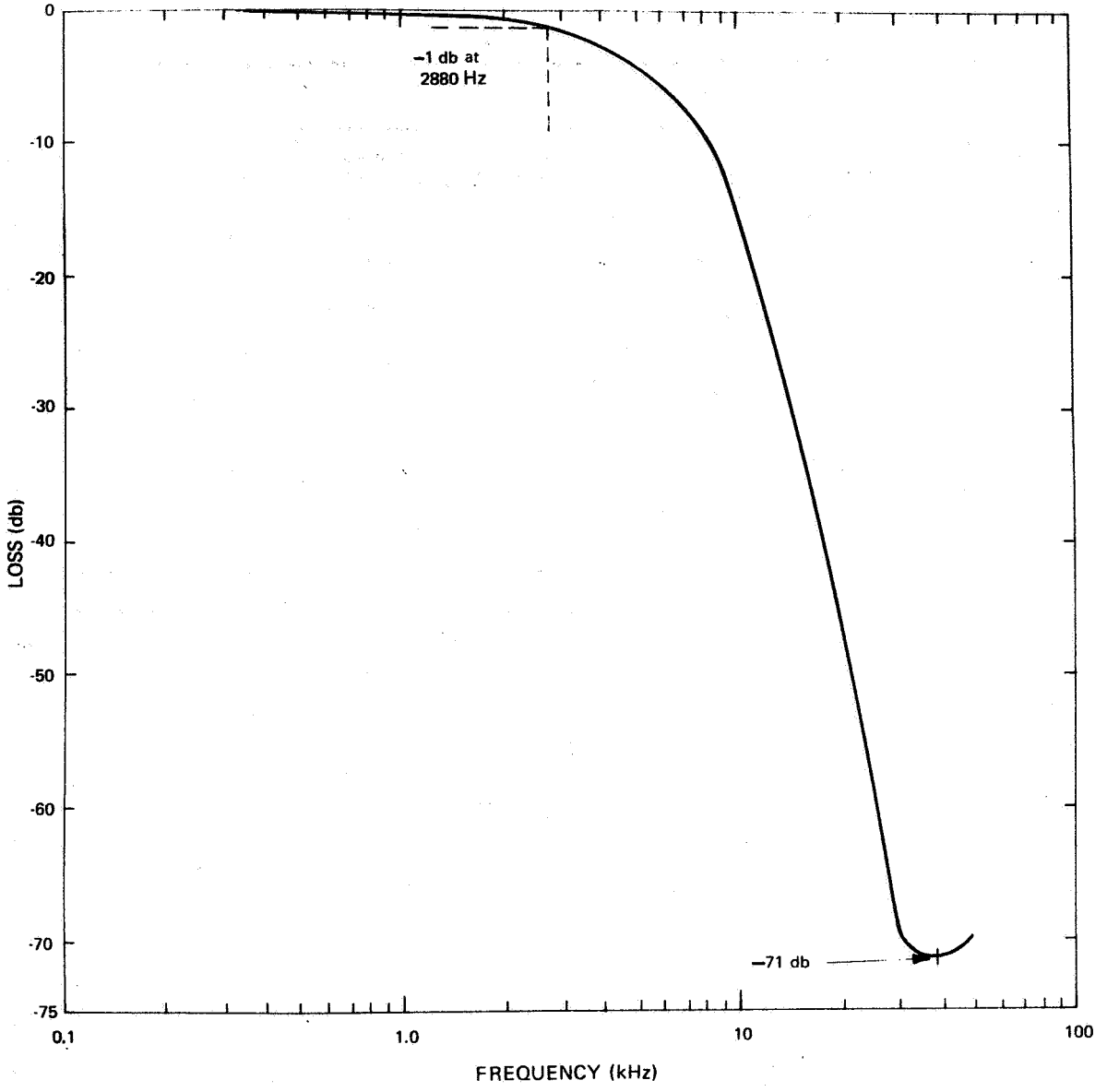

Figure 22. HRIR Demodulator, Filter Amplitude Response

2. Test Summary

The bit synchronizer contains a phase locked loop (PLL) which extracts a clock signal at the bit rate from the incoming data. If the data has been perturbed by flutter, the PLL will extract an average bit rate and will attempt to track the flutter up to certain frequencies. The sinusoidal flutter tracking curve shown on Figure 24 indicates the single frequency range within which the signal conditioner will maintain lock. Since the PLL tracks only the low frequency flutter components, there will be a net phase error between the actual data and

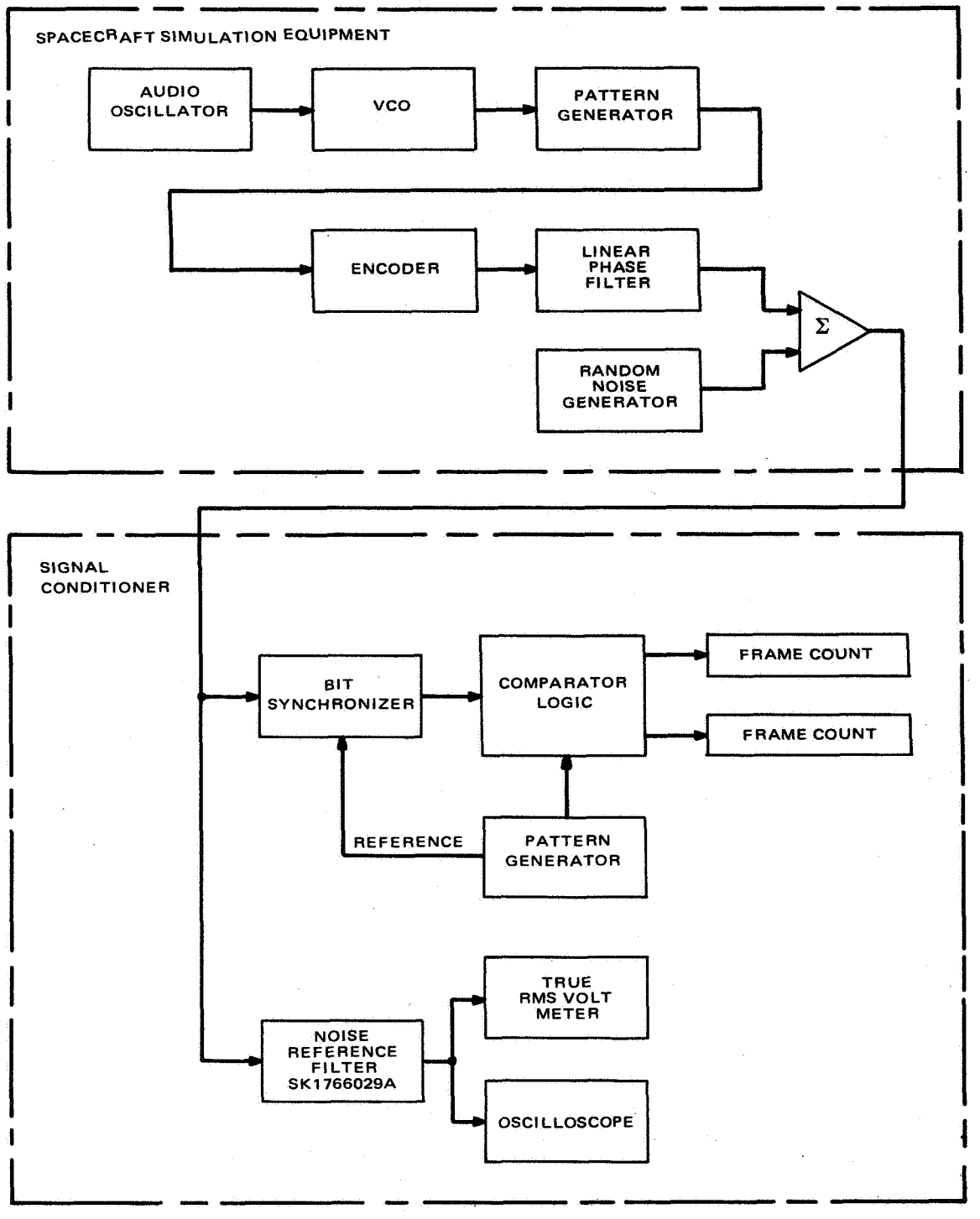

Figure 23. Signal Conditioner Test, Block Diagram

the extracted clock. This error has been calculated for the Dynatronics Signal Conditioner operating on the measured flutter of HDRSS EM-2 tape recorder, and is presented in Table 9.

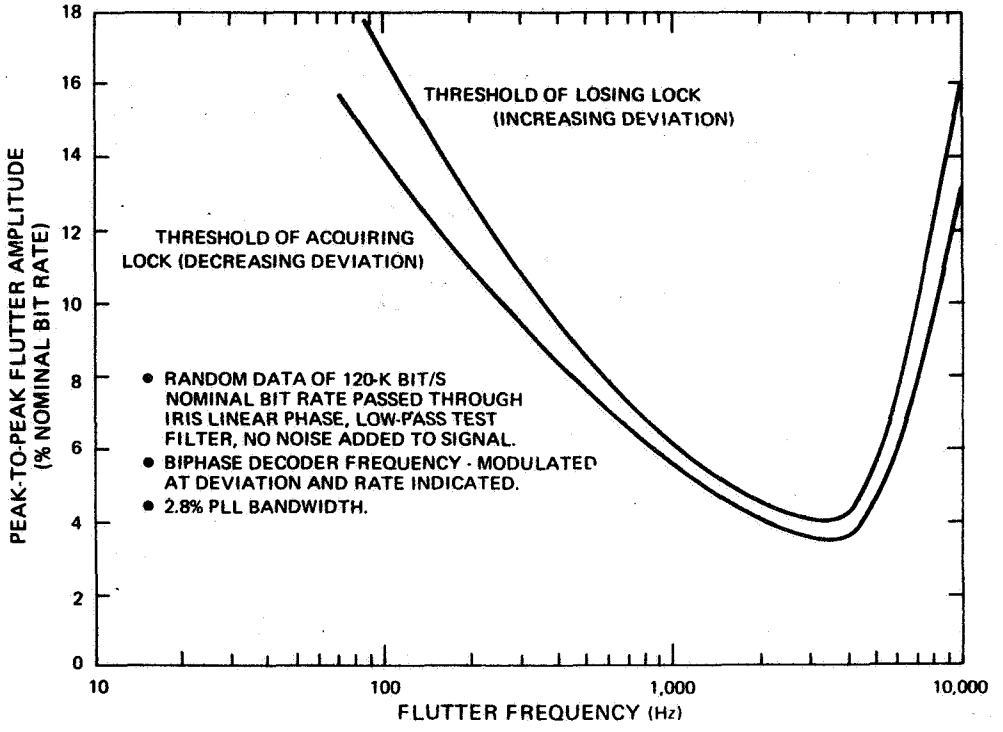

Figure 24. Single Frequency, Sinusoidal Flutter-Following Capability of Bit Synchronizer

TABLE 9. SIGNAL CONDITIONER, EM-2 TAPE RECORDER FLUTTER ERROR

Signal Conditioner Bandwidth Setting*	RMS Error (%Bit)		
	-5° C	+25° C	+50° C
2.8%	0.95	0.76	1.10
5.0%	0.57	0.45	0.65

*The bandwidth setting is the control panel indication on the Dynatronics signal conditioner: it corresponds to the frequency at which the loop gain passes through 0 db.

The errors are very small percentages of a bit, implying that their effect on the system will be minor. This is verified by the curves of BER vs SNR shown on Figure 25. The difference between the curves with and without flutter is in each case less than 0.5 db. Test data obtained from tests of two additional signal conditioners (Dynatronics Serial Nos. 38 and 53) conformed to the data shown.

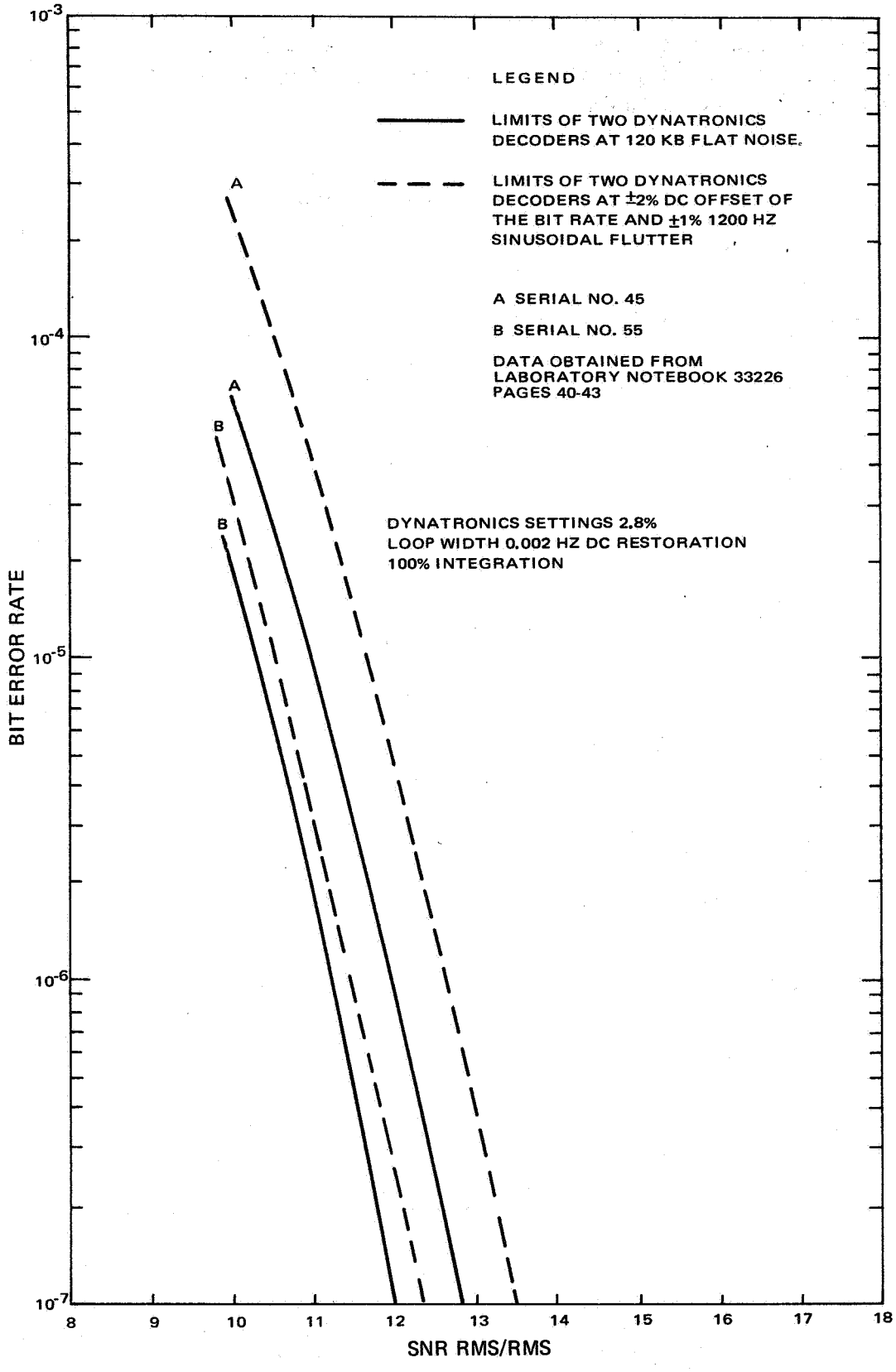

Figure 25. Signal Conditioner BER vs SNR

SYSTEM 7
SYSTEM INTEGRATION TESTS

A. GENERAL

System integration tests for the Engineering Models consisted of operational tests for EM-1 and EM-2, and thermal tests for EM-2. The electrical tests used for system integration are contained in test procedures and complementary data sheets. The test procedures contain step-by-step operating instructions; the data sheets list the parameters and the required values, and provide the space required to record or mount the data. System specifications are contained in Performance Specification PS-1840959; the system test plan is contained in Test Plan PN-1840959.

B. TEST DESCRIPTIONS

1. Operational Test Procedure

Operational tests contained in Test Procedure TP-OT-1849826 provide for a complete check of the HDRSS Tape Recorder subsystem at room ambient temperatures (+25° C). The tests performed consist of the following:

• Total Operating Time	
• Command and Telemetry Tests	Preliminary, Final
• Power Supply Tests	Voltage Variations Dissipation Noise Feedback Switching Transients
• Time Code Channel Tests	Flutter Time Code Detection Signal-to-Noise
• HRIR Channel Tests	Linearity Frequency Response Signal-to-Noise Transient Response Sync Jitter Motor Fax Drive

- ID Channel Tests
  - Linearity
  - Frequency Response
  - Signal-to-Noise
  - Transient Response
  - Sync Jitter
  - 70-mm Pictures
- MRIR and IRIS Channel Tests
  - Acquisition Time
  - Bit Error Rate

2. Thermal Test Procedure

The system Go/No-Go tests outlined in Test Procedure TP-SG 1849826 provide for a comprehensive check of the HDRSS tape recorder subsystem at thermal environments of -5°C and +55° C. The Go/No-Go tests are similar to those specified in Paragraph B1, Operational Test Procedure, and are used to verify system operation.

C. TEST CHRONOLOGY

A chronological summary of major test events that occurred during the integration of EM-1 and EM-2 are contained in Tables 10 and 11, respectively.

NOTE

Detailed test conditions are available in the Equipment Log Book supplied with each unit.

D. TEST DATA SUMMARY

The test data summaries for EM-1 and EM-2 were compiled from the test results obtained during operational and thermal tests. The data for critical parameters are presented in Table 12. The SNR (noise added) data include the specified noise added to the sensor lines, the spacecraft subsystem power lines, and the RF link simulator. A complete set of telemetry data, obtained during operational tests at -5° C, +25° C, and +55° C are contained in Tables 13 through 15.

NOTE

Operational tests of EM-1 were not conducted at temperatures of -5° C and +55° C.

TABLE 10. MAJOR TEST EVENTS FOR EM-1

Date	Event	Comments
3/29/66	Started Integration of EM-1 and BCU-1.	Tape transport mounted in plastic case until a pressure can was available.
4/7/66	Started Operational tests.	Troubleshooting and repair of BCU-1 and EM-1 complete.
4/14/66	Initial bit error rate for Biphase channels not acceptable.	Prepared troubleshooting test plan and completed troubleshooting. Dynatronic signal conditioners were calibrated and tested for flutter-following-capability, and bit error rate versus input signal to noise ratios.
4/21/66	Operational Tests were resumed.	
5/3/66	1600-cps spikes appeared on all channels during playback; bit error rate not acceptable.	Design to eliminate 1600-cps was started.
5/4/66	Resumed operational tests.	1600-cps spikes reduced significantly by a design change.
5/7/66	Installed Tape Transport into pressure container.	
5/8/66	Bit Error Rate acceptable.	Biphase Repeater bypassed.
5/11/66	Operational tests completed.	

TABLE 11. MAJOR TEST EVENTS FOR EM-2

Date	Event	Comments
7/7/66	Started integration of EM-2 and BCU-2.	
7/15/66	Started operational tests.	Troubleshooting of EM-2 and BCU-2 completed.
7/30/66	Initial bit error rate (IRIS) not acceptable.	Tests conducted to find optimum signal conditioner control settings.
8/5/66	Tests resumed, IRIS bit error rate still not acceptable.	Design change incorporated to improve flutter of tape transport.
8/10/66	Operational tests completed, thermal tests at 55° C started.	
8/12/66	Thermal tests at 55° C completed. Biphase bit error rate not acceptable.	
8/15/66	Thermal tests at -5° C started - the tape recorder stopped during the playback mode.	Investigation revealed the presence of an exudate on the magnetic head.
9/19/66	Operational tests at 25° C started after tape transport rework.	Tests were also conducted with noise added to the 400-cps power lines.
9/24/66	Operational tests at 25° C completed.	
9/26/66	Thermal tests at +55° C were started.	Tests were also conducted with noise added to the 400-cps power lines.
9/29/66	Thermal tests at 55° C were completed.	
9/30/66	Thermal tests at -5° C were started.	The MRIR oscillator in the multiplexer failed.

TABLE 11. MAJOR TEST EVENTS FOR EM-2 (Continued)

Date	Event	Comments
10/1/66	The tape transport stopped during the record mode, testing was stopped.	An investigation identified the problem as dry motor bearings.
10/17/66	Operational tests at 25° C were started after rework of tape transport and multiplexer was completed.	
10/19/66	Operational tests at 25° C were completed.	
10/20/66	Thermal tests at +55° C were started.	
10/21/66	Thermal tests at +55° C were completed.	
10/22/66	Thermal tests at -5° C were started.	Tests were also conducted with noise added to the 400-cps power lines.
10/28/66	Thermal tests at -5° C were completed.	
10/31/66	Special tests were started.	Determine performance margin on IRIS channels.

TABLE 12. TEST DATA SUMMARY, ENGINEERING MODELS EM-1 AND EM-2

Parameter or Mode	Required	Measured				Comments
		EM-1	EM-2			
		+25°C	-5°C	+25°C	+55°C	
POWER DISSIPATION						
Off Mode	NA	0.74 watts	0.85 watts	0.735 watts	0.86 watts	
Record Mode	10 watts max	8.95 watts	9.90 watts	9.20 watts	8.95 watts	
Playback Mode with Biphase Repeaters	15 watts max	22.80 watts	26.60 watts	23.10 watts	23.10 watts	See Note 4
Playback Mode without Biphase Repeaters	15 watts max	14.40 watts	16.20 watts	14.80 watts	15.10 watts	
POWER SUPPLY SWITCHING TRANSIENTS						
Off to Record	1.2 amps max		-5.0 amps	3.8 amps	7.5 amps	See Note 3
Off to Playback	1.2 amps max		8.5 amps	5.5 amps	9.5 amps	
Record to Playback	1.2 amps max		8.5 amps	5.5 amps	9.5 amps	
Playback to Record	1.2 amps max		4.1 amps	3.4 amps	7.5 amps	
NOISE FEEDBACK TO POWER SUPPLY						
Record	41.7 mv max	1.79 mv	9.0 mv	7.7 mv	6.0 mv	
Playback	41.7 mv max	4.39 mv	14.0 mv	11.9 mv	15.0 mv	
TIME CODE CHANNEL DATA						
Flutter	2.0% max	0.39%	0.51%	0.54%	0.72%	See Note 1
Speed Change	2.0% max	0.24%	0.19%	0.21%	0.26%	See Note 1
Running Time	5 Minutes min	5 min, 7 sec	5 min, 11 sec	5 min, 8 sec	4 min, 57 sec	See Note 1
Signal-to-Noise Ratio	20 db min	22.7 db	NA	22.0 db	NA	
HRIR CHANNEL DATA						
SNR (Noise Added)	30 db min	34.8 db	29.4 db	31 db	29.8 db	See Note 2
SNR (No Noise Added)	30 db min	40.6 db		39 db		
Linearity	See Figure 26	Passed	Passed	Passed	Passed	See Note 5
Freq response, 360 Hz	-4.3 db max	-1.22 db	NA	-1.3 db	NA	See Figure 28
Sync Jitter	800 μsec max	200.0 μsec	NA	140.0 μsec	NA	
ID CHANNEL DATA						
SNR (Noise Added)	30 db min	33.4 db	27.3 db	30.4 db	28.8 db	See Note 2
SNR (No Noise Added)	30 db min	37.2 db		36.0 db		
Linearity	See Figure 27	Passed	Passed	Passed	Passed	See Note 5
Freq response, 1600 Hz	-17.0 db max	-9.7 db	NA	-8.4 db	NA	See Figure 29
Sync Jitter	8 μsec max	4.0 μsec	NA	9.0 μsec	NA	See Note 2
IRIS CHANNEL DATA						
Acquisition Time	7.0 sec max	1.08 sec	NA	1.30 sec	NA	
Bit Error Rate (BER) Run No. 1	1.0×10^{-5} max	5.85×10^{-7}	7.0×10^{-6}	4.0×10^{-6}	8.8×10^{-6}	
BER Run No. 2	1.0×10^{-5} max	9.00×10^{-7}	9.6×10^{-6}	4.0×10^{-6}	1.0×10^{-5}	
MRIR CHANNEL DATA						
Acquisition Time	7.0 sec max	1.08 sec	NA	1.7 sec	NA	
BER Run No. 1	1.0×10^{-5} max	4.45×10^{-6}	6.9×10^{-6}	4.6×10^{-6}	8.5×10^{-6}	
BER Run No. 2	1.0×10^{-5} max	NA	8.6×10^{-6}	1.0×10^{-5}	1.0×10^{-5}	

NOTE 1: Average of two test runs, at system power supply voltages of -24.0 and -25.0 volts dc.
NOTE 2: Out of specification condition accepted by NASA for EM-2 only.
NOTE 3: Excessive power transients accepted by NASA for EM-2 only.
NOTE 4: Excessive power condition accepted by NASA
NOTE 5: Linearity checked at end-of-record and end-of-playback at -24.0, -24.5, and-25.0 volts dc.

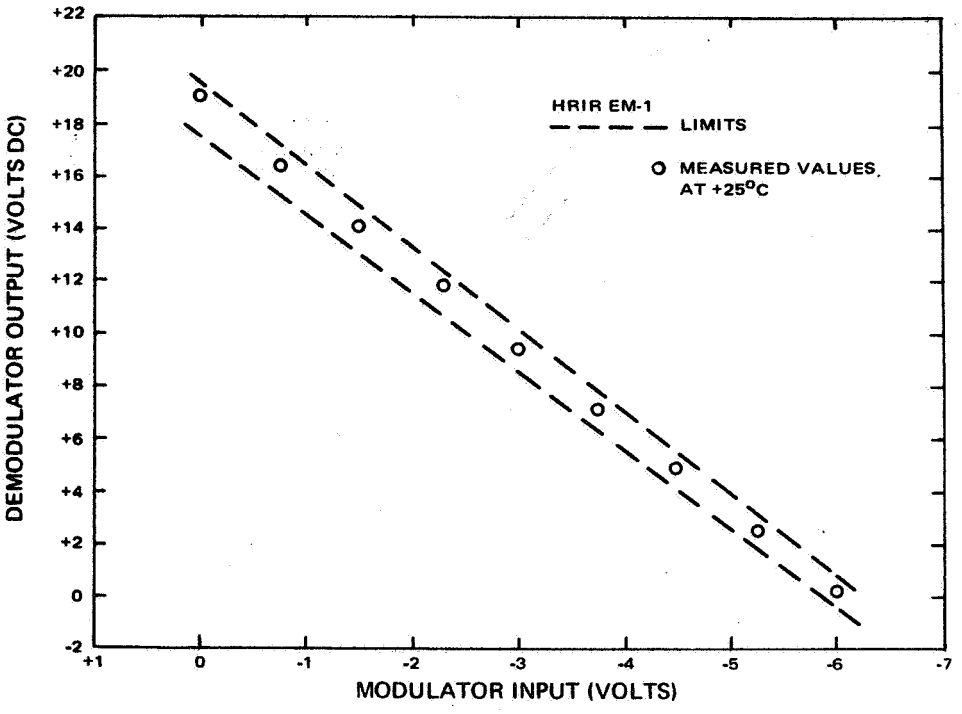

A. Engineering Model EM-1

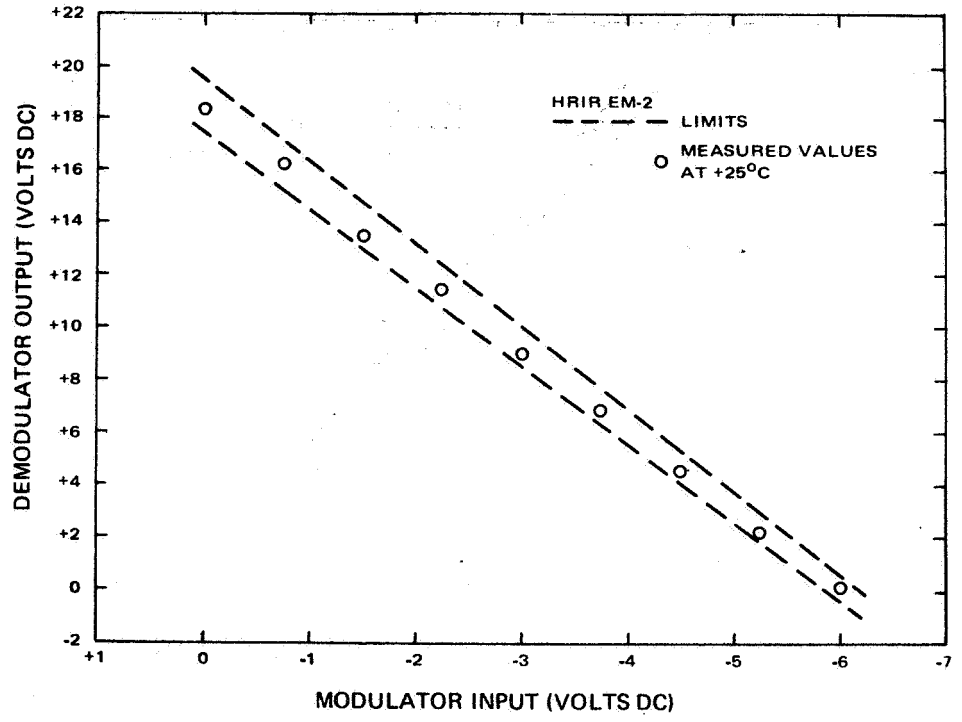

B. Engineering Model EM-2

Figure 26. HRIR Linearity Limits and Typical Test Results

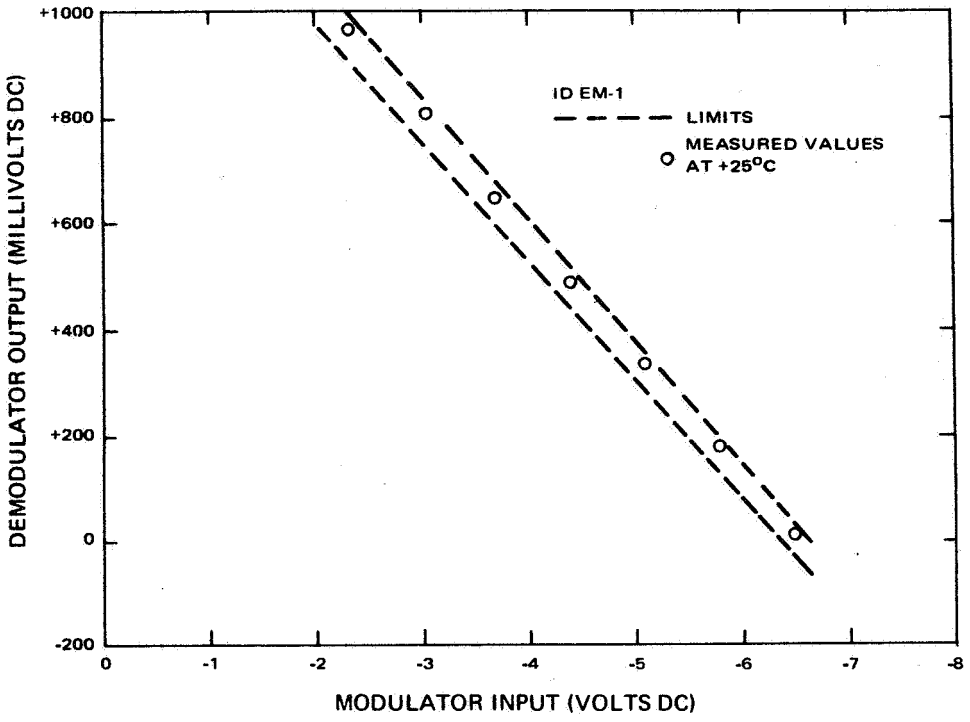

A. Engineering Model EM-1

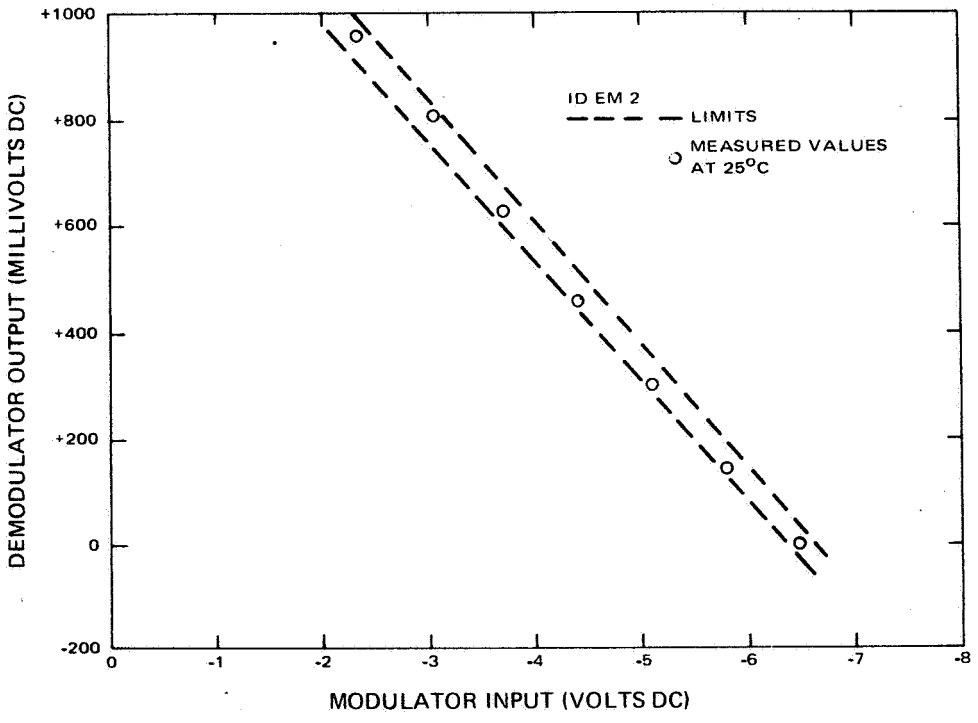

B. Engineering Model EM-2

Figure 27. ID Linearity Limits and Typical Test Results

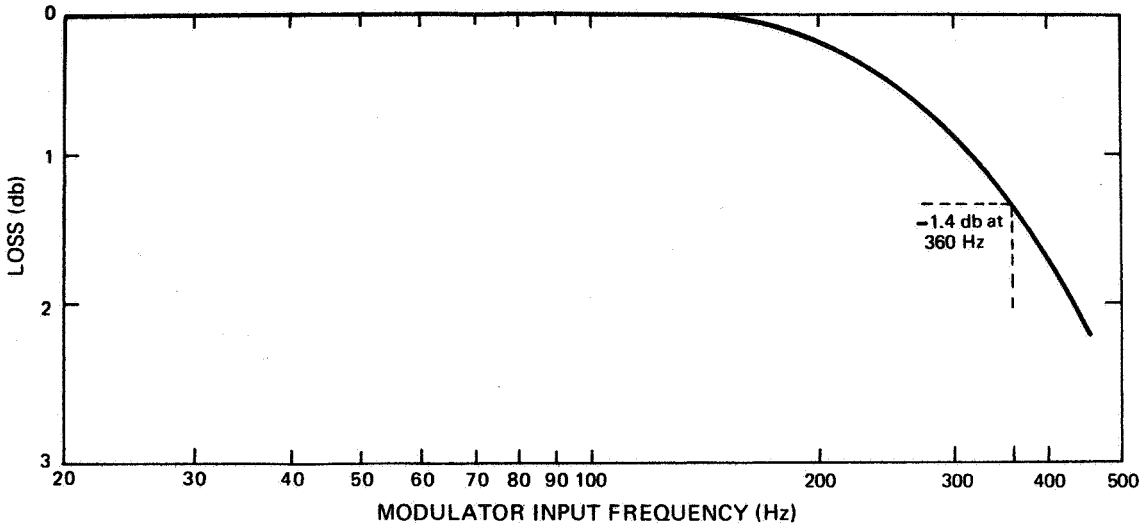

A. Engineering Model EM-1

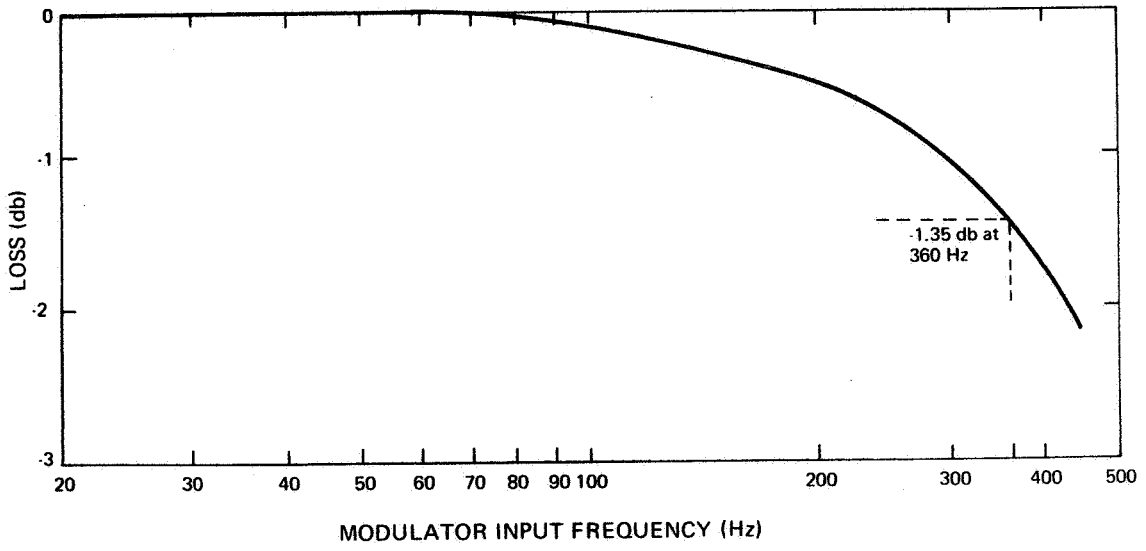

B. Engineering Model EM-2

Figure 28. HRIR Channel Amplitude-Frequency Response

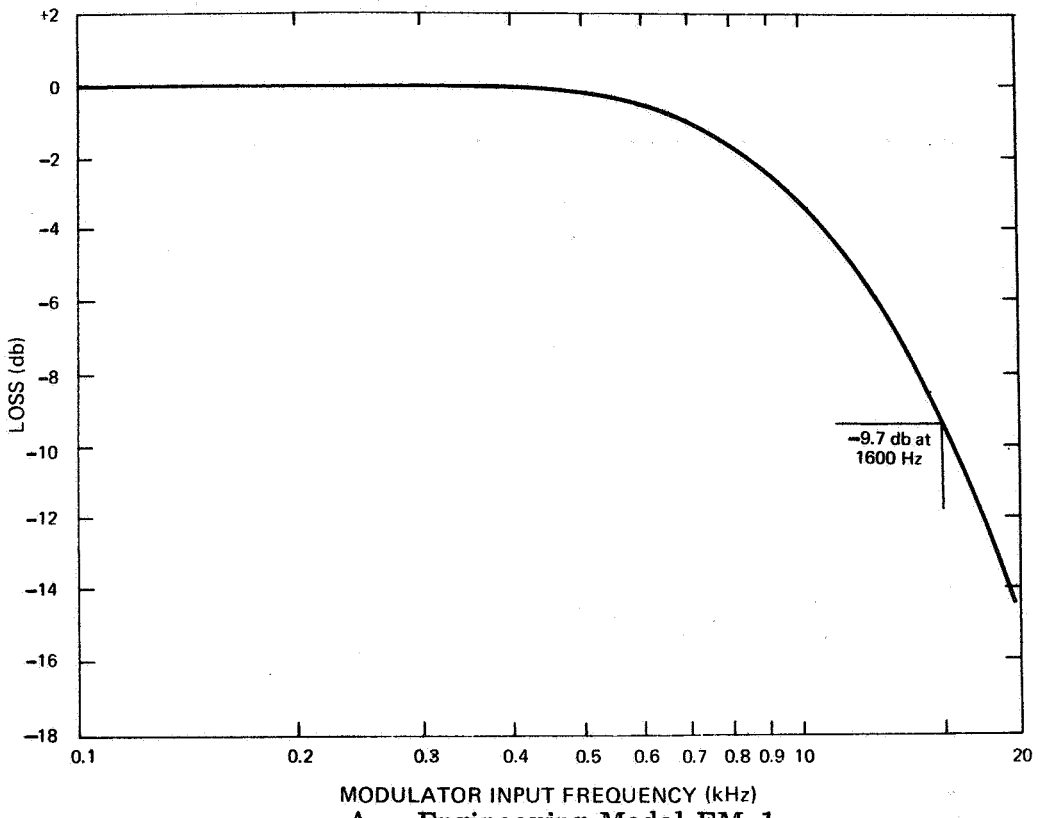

A. Engineering Model EM-1

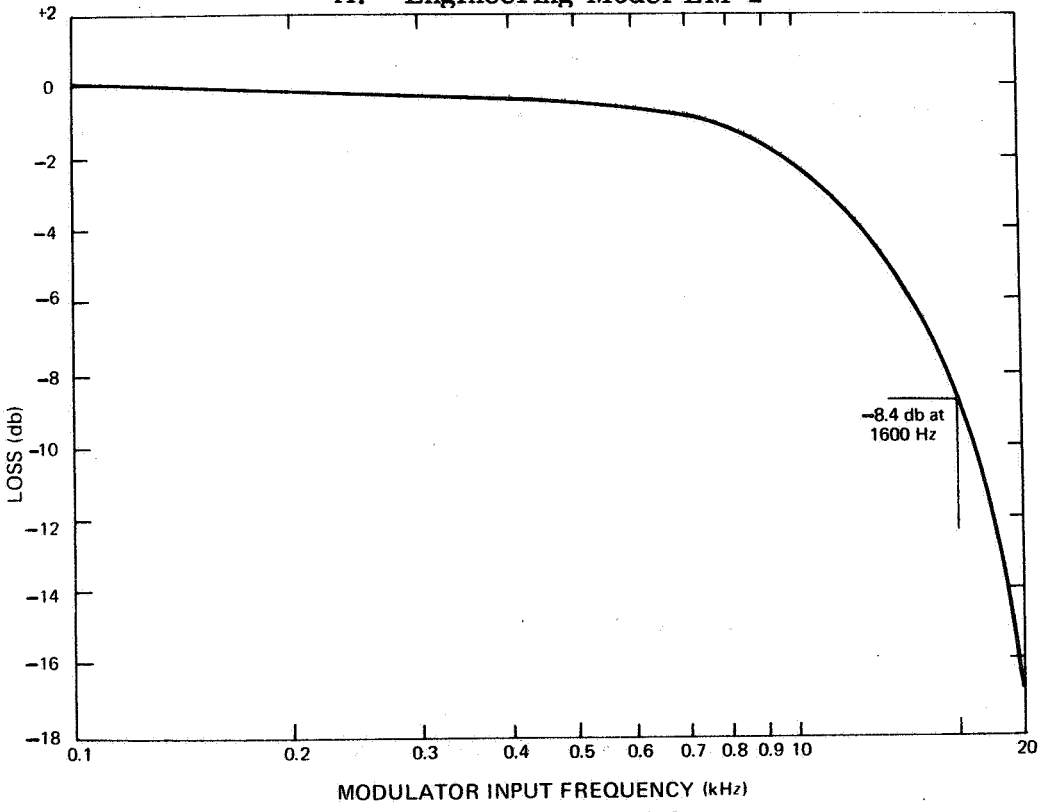

B. Engineering Model EM-2

Figure 29. ID Channel Amplitude-Frequency Response

TABLE 13. RECORD MODE TELEMETRY VOLTAGES

Telemetry Point	Required	Measured			
		EM-1	EM-2		
		+25° C	-5° C	+25° C	+55° C
RECORD ON-OFF	-5.0 to -10.0	-6.7	-6.9	-7.1	-6.9
RECORD COMMAND	-5.0 to -10.0	-6.9	-6.9	-7.1	-6.9
PLAYBACK COMMAND	0.0 to - 1.0	0	0	0	0
MOTOR ROTATION	-5.0 to -10.0	-6.3	-6.3	-6.5	-6.4
RECORD END OF TAPE	0.0 to - 1.0	0	0	0	0
PB END OF TAPE	0.0 to - 1.0	0	0	0	0
INVERTER POWER	-5.0 to -10.0	-7.0	-6.9	-7.1	-7.0
RECORDER PRESSURE	-1.8 to - 3.0	-3.0	-2.0	-2.4	-2.7
RECORDER TEMPERATURE	-1.5 to - 3.6	-3.6	-1.1	-2.6	-4.7
ELECTRONICS TEMPERATURE	-0.9 to - 3.9	-3.1	-0.9	-2.6	-4.4
HRIR REC AMP	-2.8 to - 3.9	-3.5	-3.3	-3.6	-3.7
MRIR REC AMP	-2.7 to - 3.5	-2.8	-3.0	-3.2	-3.1
IRIS REC AMP	-2.7 to - 3.5	-2.8	-2.9	-3.1	-3.1
ID REC AMP	-2.8 to - 3.9	-3.4	-3.2	-3.5	-3.6
TC REC AMP	-2.0 to - 3.3	-2.5	-2.2	-2.2	-2.2
HRIR LIM INPUT	0.0 to - 1.0	0	0	0	0
MRIR LIM INPUT	0.0 to - 1.0	0	0	0	0
IRIS LIM INPUT	0.0 to - 1.0	0	0	0	0
ID LIM INPUT	0.0 to - 1.0	0	0	0	-0.1
TC OUTPUT	0.0 to - 1.0	0	0	0	-0.1
INVERTER ϕ1-A	-3.1 to - 4.0	-3.8	-3.7	-3.8	-3.8
INVERTER ϕ1-B	-3.1 to - 4.0	-3.8	-3.7	-3.8	-3.8
INVERTER ϕ2-A	-3.1 to - 4.0	-3.8	-3.7	-3.8	-3.8
INVERTER ϕ2-B	-3.1 to - 4.0	-3.8	-3.7	-3.8	-3.8
RECORD START/RUN	-5.0 to -10.0	-6.8	-6.9	-7.0	-6.9
PLAYBACK START/RUN	0.0 to - 1.0	0	0	0	0
MRIR POWER	N/A	0	0	0	0
REPEATER TEMPERATURE	N/A	-4.8	-4.2	-4.4	-4.4
MRIR OUTPUT	N/A	0	0	0	0
MRIR INPUT	N/A	0	0	0	0
MRIR PLL ERROR	N/A	0	0	0	0

TABLE 13. RECORD MODE TELEMETRY VOLTAGES (Continued)

Telemetry Point	Required	Measured			
		EM-1	EM-2		
		+25° C	-5° C	+25° C	+55° C
IRIS OUTPUT	N/A	0	0	0	0
IRIS INPUT	N/A	0	0	0	0
IRIS PLL ERROR	N/A	0	0	0	0
MUX POWER	0.0 to - 1.0	0	0	0	0
MUX TEMPERATURE	-2.9 to - 5.5	-3.7	-5.6	-4.3	-2.5
CH2 OSC	0.0 to - 1.0	0	0	0	0
CH3 OSC	0.0 to - 1.0	0	0	0	0
CH4 OSC	0.0 to - 1.0	0	0	0	0
CH5 OSC	0.0 to - 1.0	0	0	0	0
ADDER OUTPUT	0.0 to - 1.0	0	0	0	0
HRIR/ALT SIG	0.0 to - 1.0	0	0	0	0
IRIS POWER	N/A	0	0	0	0

TABLE 14. PLAYBACK MODE TELEMETRY VOLTAGES

Telemetry Points	Required	Measured*			
		EM-1	EM-2		
		+25° C	-5° C	+25° C	+55° C
RECORD ON-OFF	0 to - 1.0	-6.7	-0.1	0	0
RECORD COMMAND	0 to - 1.0	0	-0.1	0	-0.1
PLAYBACK COMMAND	-5.0 to -10.0	-6.7	-6.9	-6.9	-6.9
MOTOR ROTATION	-5.0 to -10.0	-6.2	-6.3	-6.4	-6.3
RECORD END-OF-TAPE	0 to - 1.0	0	0	0	-0.1
PB END-OF-TAPE	0 to - 1.0	0	0	0	-0.1
INVERTER POWER	-5.0 to -10.0	-7.0	-6.9	-7.0	-7.0
RECORDER PRESSURE	-1.8 to - 3.0	-3.1	-2.0	-2.3	-2.7
RECORDER TEMPERATURE	-1.5 to - 3.6	-3.6	-1.1	-2.7	-4.8

TABLE 14. PLAYBACK MODE TELEMETRY VOLTAGES (Continued)

Telemetry Points	Required	Measured*			
		EM-1	EM-2		
		+25°C	-5°C	+25°C	+55°C
ELECTRONICS TEMPERATURE	-0.9 to - 3.9	-2.9	-0.9	-2.7	-4.5
HRIR REC AMP	0 to - 1.0	0	0	0	-0.1
MRIR REC AMP	0 to - 1.0	0	0	0	-0.1
IRIS REC AMP	0 to - 1.0	0	0	0	-0.1
ID REC AMP	0 to - 1.0	0	0	0	-0.1
TC REC AMP	0 to - 1.0	0	0	0	-0.1
HRIR LIM INPUT	-2.0 to - 4.5	-2.7	-3.2	-3.8	-3.8
MRIR LIM INPUT	-3.5 to - 4.9	-3.5	-4.5	-4.6	-4.8
IRIS LIM INPUT	-3.5 to - 4.9	-4.5	-4.3	-4.8	-4.6
ID LIM INPUT	-2.0 to - 4.5	-2.4	-2.7	-3.2	-2.8
TC OUTPUT	-1.9 to - 3.0	-1.6	-2.2	-2.2	-2.1
INVERTER ϕ1-A	-3.1 to - 4.0	-3.8	-3.7	-3.7	-3.8
INVERTER ϕ1-B	-3.1 to - 4.0	-3.8	-3.7	-3.7	-3.8
INVERTER ϕ2-A	-3.1 to - 4.0	-3.8	-3.7	-3.7	-3.8
INVERTER ϕ2-B	-3.1 to - 4.0	-3.8	-3.7	-3.7	-3.8
RECORD START-RUN	0 to - 1.0	0	-0.1	0	0
PLAYBACK START-RUN	-5.0 to -10.0	-6.8	-6.9	-7.0	-6.8
MRIR POWER	N/A	-5.5	0	0	0
REPEATER TEMP	N/A	-4.9	-4.3	-4.4	-4.3
MRIR OUTPUT	N/A	-2.0	0	0	0
MRIR INPUT	N/A	-5.1	0	0	0
MRIR PLL ERROR	N/A	-5.5	0	0	0
IRIS OUTPUT	N/A	-2.0	0	0	0
IRIS INPUT	N/A	-5.1	0	0	0
IRIS PLL ERROR	N/A	-5.3	0	0	0
MUX POWER	-5.0 to -10.0	-4.8	-7.8	-7.7	-7.7
MUX TEMP	-2.9 to - 5.5	-3.6	-5.6	-4.2	-2.4
CH2 OSC	-2.8 to - 5.0	-3.1	-5.3	-5.2	-3.2
CH3 OSC	-2.8 to - 5.0	-2.1	-2.1	-3.4	-3.2
CH4 OSC	-2.8 to - 5.0	-3.3	-4.2	-4.0	-4.0
CH5 OSC	-2.8 to - 5.0	-3.3	-4.3	-4.4	-4.2
ADDER OUTPUT	-1.3 to - 2.5	-1.1	-0.5	-0.8	-0.9
HRIR/ALT SIG	0 to - 1.0	0	0	0	0
IRIS POWER	N/A	-5.7	0	0	0

*Biphase Repeater telemetry was not required for EM-2.

TABLE 15. OFF MODE TELEMETRY VOLTAGES

Telemetry Points	Required	Measured			
		EM-1	EM-2		
		+25°C	-5°C	+25°C	+55°C
RECORD ON-OFF	0 to -1.0	0	0	0	0
RECORD COMMAND	0 to -1.0	0	0	0	-0.1
PLAYBACK COMMAND	0 to -1.0	0	0	0	0
MOTOR ROTATION	0 to -1.0	0	0	0	0
RECORD END OF TAPE	0 to -1.0	0	0	0	0
PB END OF TAPE	0 to -1.0	0	0	0	0
INVERTER POWER	-5.0 to -10.0	-7.0	-7.0	-7.1	-7.0
RECORDER PRESSURE	-1.8 to -3.0	-3.0	-1.9	-2.4	-2.6
RECORDER TEMPERATURE	-1.5 to -3.6	-3.6	-1.0	-2.6	-4.7
ELECTRONICS TEMPERATURE	-0.9 to -3.9	-3.1	-0.8	-2.6	-4.4
HRIR REC AMP	0 to -1.0	0	0	0	0
MRIR REC AMP	0 to -1.0	0	0	0	0
IRIS REC AMP	0 to -1.0	0	0	0	0
ID REC AMP	0 to -1.0	0	0	0	0
TC REC AMP	0 to -1.0	0	0	0	0
HRIR LIM INPUT	0 to -1.0	0	0	0	0
MRIR LIM INPUT	0 to -1.0	0	0	0	0
IRIS LIM INPUT	0 to -1.0	0	0	0	0
ID LIM INPUT	0 to -1.0	0	0	0	0
TC OUTPUT	0 to -1.0	0	0	0	0
INVERTER ϕ1-A	0 to -1.5	-1.2	-1.2	-1.2	-1.2
INVERTER ϕ1-B	0 to -1.5	-1.2	-1.1	-1.2	-1.2
INVERTER ϕ2-A	0 to -1.5	-1.2	-1.2	-1.2	-1.2
INVERTER ϕ2-B	0 to -1.5	-1.2	-1.2	-1.2	-1.2
RECORD START/RUN	0 to -1.0	0	0	0	0
PLAYBACK START/RUN	0 to -1.0	0	0	0	0
MRIR POWER	N/A	0	0	0	0
REPEATER TEMPERATURE	N/A	-4.8	-4.1	-4.4	-4.3
MRIR OUTPUT	N/A	0	0	0	0
MRIR INPUT	N/A	0	0	0	0
MRIR PLL ERROR	N/A	0	0	0	0
IRIS OUTPUT	N/A	0	0	0	0
IRIS INPUT	N/A	0	0	0	0
IRIS PLL ERROR	N/A	0	0	0	0
MUX POWER	0 to -1.0	0	0	0	0

TABLE 15. OFF MODE TELEMETRY VOLTAGES (Continued)

Telemetry Points	Required	Measured			
		EM-1	EM-2		
		+25°C	-5°C	+25°C	+55°C
MUX TEMPERATURE	-2.9 to -5.5	-3.7	-5.6	-4.4	-2.5
CH2 OSC	0 to -1.0	0	0	0	0
CH3 OSC	0 to -1.0	0	0	0	0
CH4 OSC	0 to -1.0	0	0	0	0
CH5 OSC	0 to -1.0	0	0	0	0
ADDER OUTPUT	0 to -1.0	0	0	0	0
HRIR/ALT SIT	0 to -1.0	0	0	0	0
IRIS POWER	N/A	0	0	0	0

SECTION 8
EVALUATION OF ENGINEERING MODEL TEST DATA

A. INTRODUCTION

The parameter of primary interest throughout the module and system tests was the amplitude-frequency response. Therefore, the results of module tests (tape-recorder, multiplexer, and demultiplexer) are correlated with the data from the overall system tests.

B. DATA CORRELATION

In a narrow band FM channel, the net frequency attenuation is given as the arithmetic mean of the channel attenuation of the first upper and lower sidebands. The ID channel playback frequencies are:

	Sync	Black	White
Tape Recorder Output	72 kHz	84 kHz	117.5 kHz
Doubler Output	144 kHz	168 kHz	235.0 kHz

Using the full-scale alternating black-white bar test pattern of the BCU, the average subcarrier ID channel frequency after doubling is 201.5 kHz. At the maximum modulation rate of 51.2 kHz the first lower and upper sidebands around 201.5 kHz are:

LSB	150.3 kHz
USB	252.7 kHz

After subtracting these from the 640-kHz local oscillator frequency the frequencies become:

LSB	489.7 kHz
USB	387.3 kHz

For the HRIR channel, the subcarrier frequencies at the playback rate are:

	Black	White
Tape Recorder Output	73.6 kHz	101.1 kHz
Doubler Output	147.2 kHz	202.2 kHz

Using the full-scale alternating black-white bar test pattern of the BCU, the average HRIR subcarrier frequency at the doubler output is 174.7 kHz. At the maximum modulation rate of 11.5 kHz, the first lower and upper sidebands.

LSB	163.2 kHz
USB	186.2 kHz

After subtracting these from the 805 kHz local oscillator, the frequencies are:

LSB	641.8 kHz
USB	618.8 kHz

From the test data obtained during module tests (Section 6), the response at these frequencies has been inferred as listed in Table 16. The contribution of the Multiplexer/Demultiplexer link (Refer to Table 16) to the demodulated frequency response is found as the average of upper and lower sideband response (Refer to Appendix II),

specifically

$$R_d = \frac{r_u + r_\ell}{2}$$

TABLE 16. SUMMARY OF MULTIPLEXER/DEMULTIPLEXER AMPLITUDE-FREQUENCY RESPONSE

Engineering Model and Channel	Freq (kHz)	Response (db)						
		Multiplexer			Demulti-plexer	Multiplexer/Demultiplexer		
		+25°C	-5°C	+55°C		+25°C	-5°C	+55°C
EM-1 ID	387.3	-30.6	-34.2	-29.0	-30.0	-60.6	-64.2	-59.0
	487.7	0.0*	0.0*	0.0*	-0.5*	0.5	0.5	0.5
HRIR	641.8	0.0*	0.0*	0.0*	-1.0*	-1.0	-1.0	-1.0
	618.8	0.0*	0.0*	0.0*	0.0	0.0	0.0	0.0
EM-2 ID	387.3	-30.0	-30.5	-28.5	-	-	-	-
	489.7	0.0*	0.0*	0.0*	-	-	-	-
HRIR	641.8	0.0*	0.0*	0.0*	0.0*	-	-	-
	618.8	0.0*	0.0*	0.0*	-	-	-	-

* Estimated by interpolating module test data

where

R_d = demodulated amplitude response of the multiplexer/demultiplexer relative to unity of the multiplexer/demultiplexer.

r_u = amplitude response of the multiplexer/demultiplexer at upper sideband frequency.

r_ℓ = amplitude response of the multiplexer/demultiplexer at lower sideband frequency.

for example, for a ID channel response at 51.2 kHz, the contribution of the EM-1 Multiplexer Demultiplexer to demodulated frequency response is

$$R_d = \frac{.001 + .89}{2}$$

$$= -6.6 \text{ db re: unity}$$

Similarly, the response for the EM-2 ID channel, and the response for the HRIR channel of EM-1 and EM-2 are calculated and listed in Table 17.

TABLE 17. DEMODULATED RESPONSE OF THE MULTIPLEXER/DEMULTIPLEXER FOR BCU TEST CONDITIONS

Engineering Model and Channel	Demodulated Response of Multiplexer/Demultiplexer
EM-1	
ID	- 6.6 db
HRIR	- 0.4 db
EM-2	
ID	- 6.0 db
HRIR	- 0.4 db

This multiplexer-demultiplexer response is now combined with the response of the tape recorder and the demodulator to determine the overall channel response. The cumulative response for the ID channels is as follows:

EM-1

Tape Recorder	-2.0 db* (specified)
Multiplexer-Demultiplexer	-6.6 db
FM Demodulator	-1.5 db
TOTAL	10.1 db

EM-2

Tape Recorder	-2.0 db* (specified)
Multiplexer-Demultiplexer	-6.0 db
FM Demodulator	-1.5 db
TOTAL	-9.5 db

The measured system response for the EM-1 and EM-2 ID channels was -9.7 db and -7.4 db, respectively.

The cumulative response for the HRIR channels is as follows:

EM-1

Tape Recorder	-0.4 db
Multiplexer-Demultiplexer	-0.4 db
FM Demodulator	-1.0 db
TOTAL	-1.8 db

EM-2

Tape Recorder	-1.0 db
Multiplexer-Demultiplexer	-0.4 db
FM Demodulator	-1.0 db
TOTAL	-2.4 db

The measured system response for the EM-1 and EM-2 HRIR channels was -1.2 db and -1.3 db, respectively

*The measured response of the tape recorder ID channels is not available as the measured data was obtained with a defective demodulator.

SECTION 9
LIST OF REFERENCES

1. RCA, Astro-Electronics Division, Final Report for APT Camera/Tape Recorder Study, Contract NAS5-3772, Princeton, N.J., March 4, 1964 to July 10, 1964.

2. RCA, Astro-Electronics Division, Final Report on Breadboard Phase of the APT Camera/Tape Recorder Study, Contract NAS5-3772, Princeton, N.J., May 5, 1966.

3. RCA, Astro-Electronics Division, Addendum to Final Report for APT/Tape Recorder Study for Incorporation of HRIR Add-on, Contract NAS5-3772, Princeton, N.J., November 30, 1965.

4. Ibid.

5. Ibid.

6. Ibid Reference 1.

7. RCA, Astro-Electronics Division, Instruction Manual for the Spacecraft Subsystem of the High Data Rate Storage System (HDRSS), Engineering Models EM-1 and EM-2, Contract NAS5-3772, Princeton, N.J., April 14, 1967.

8. RCA, Astro-Electronics Division, High Data Rate Storage System (HDRSS) Modifications for the Nimbus AVCS Ground Stations, Contract NAS5-10205 Princeton, N. J., December 6, 1967.

9. RCA, Astro-Electronics Division, Instruction Manual for the Bench Check Units of the High Data Rate Storage System (HDRSS), Contract NAS5-10205, Princeton, N. J., December 6, 1967.

APPENDIX I
HDRSS TAPE TRANSPORT LIVE-VIBRATION TEST RESULTS

A. INTRODUCTION

The purpose of this test was to subject the HDRSS EM-3 tape recorder to Nimbus B Flight-acceptance vibration levels during the record mode of operation with the objective of obtaining qualitative performance data. The criterion of performance was a bit-error-rate obtained during subsequent readout and decoding. The test results indicated that bit-error-rate degradation was excessive and that information recorded under the specified conditions would be of little value.

B. TEST CONDITIONS

The tape transport was mounted on the vibration fixture as shown on Figure I-1 and was vibrated in each of three planes for 12 minutes with random excitation at the Nimbus B Flight acceptance level: 11.7 g rms with a constant spectral density of 0.07 g^2/Hz between 20 Hz and 2 kHz. Tape recorder operation, identical for each axis, consisted of the following:

23 minutes record without vibration,
12 minutes record with vibration,
15 minutes record without vibration.

Thus the data was recorded in the following manner:

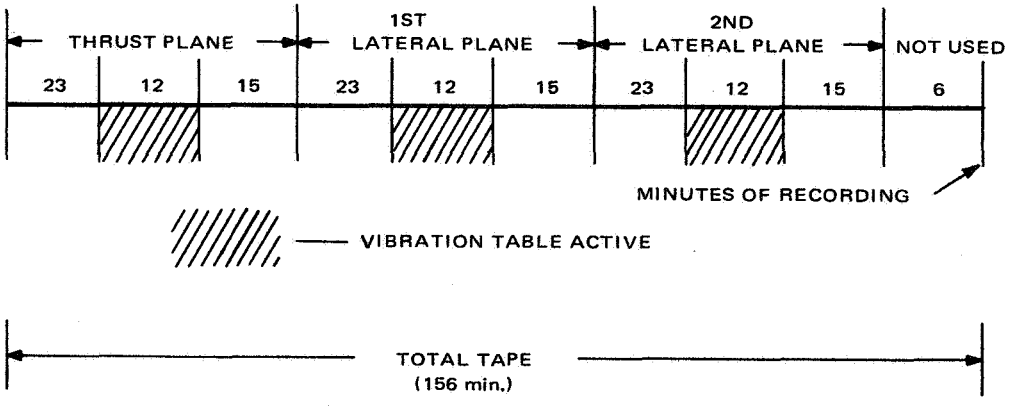

During the continuous recording operation 5 tape tracks were recorded with the following respective signals:

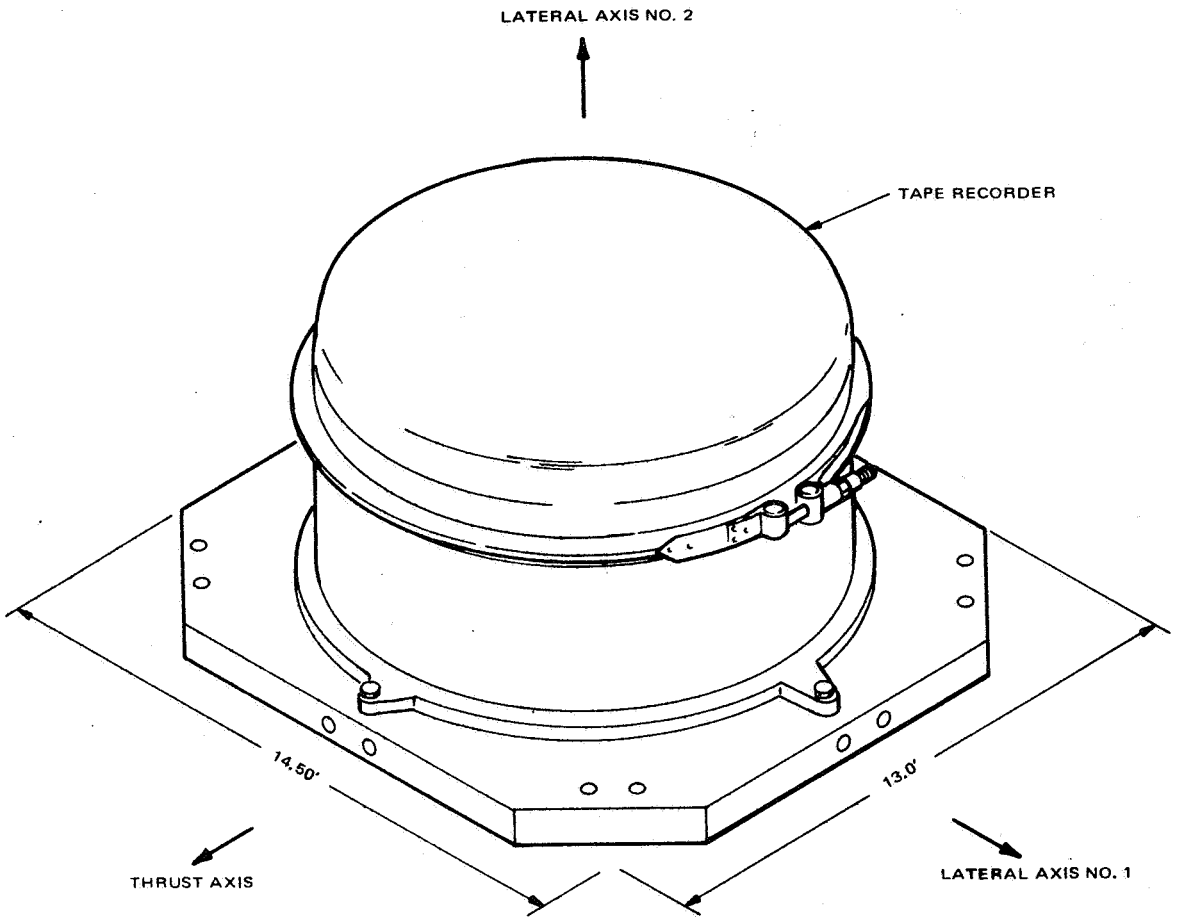

Figure I-1. Vibration Fixture and Axis Identification

- A 3750 bits/sec. biphase pattern (IRIS).
- A 3750 cps square wave signal, synchronous with the IRIS signal.
- A 1000 bits/sec. biphase pattern (special).
- A 500 bits/sec. biphase pattern (special).
- A 3750 cps carrier "marker" signal which was recorded during vibration only.

C. DATA SUMMARY

A summary of pertinent test data is tabulated in Table I-1. The parameters are listed in the left column and are numbered for future reference. The data is arranged in four columns: Typical Non-vibrational Performance, 1st Shake, "2nd Shake, and 3rd Shake, respectively. The order of shake number is in the original test-record sequence and is reversed during normal playback.

Mechanical operation of the tape recorder was satisfactory during vibration exposures.

TABLE I-1. TAPE-TRANSPORT LIVE-VIBRATION TEST RESULTS

Parameter	Typical Non-Vib. Perform.	1st Shake	2nd Shake	3rd Shake
1. Vibration Data, Axis and Approximate Recorder Reference (see Fig. I-1)	--	Thrust, Tape Motion Under Playback Head	1st Lateral, Tape Motion Under Record Head	2nd Lateral, Reel Axis
2. Minutes After Start Record	35-73	23-35	73-85	123-135
3. Percent of Operate Time - (Nom.)	--	14.4-21.9	45.6-53.1	76.9-84.4
3.75 kHz Clock				
4. Typical Playback Rate (kHz)	119.8	93.6	90	94.8
5. Non Vib/Vib (%)	--	128	133	126.5
1 kHz Biphase				
6. Typical Playback Rate (kHz)	23.5	23.75	36	29.29
7. Non Vib/Vib (%)	--	99	65	80
500 Hz Biphase				
8. Typical Playback Rate (Hz)	12.20	12.34	19.7	15.2
9 Non Vib/Vib (%)	--	99	62	80
FM Noise, 120 kHz Demod Out (Demod Linearity Range: 50 to 190 kHz)				
10. AC Output	12	460	430	400
11. Peak DC Levels (Min) (Max)	+1.0 --	-1.7 +1.6	-1.7 +1.6	-1.7 +1.6
Playback of Vibration Sequence				
12. Playback Time (sec)	22.5	23	14.8	16.2
13. Vib/Vib (%)	--	102	66	72
Total Playback Pulses (Line 12 × Playback Frequency)				
14. 3.75 kHz clock (kHz)	2,700	2,155	1,330	1,535
15. 1.0 kHz biphase (kHz)	528	546	533	475
16. 500 Hz biphase (kHz)	274	284	292	246
Calculated Transport Parameters				
17. Takeup Reel Tape Tension (oz)		9.0/8.2	6.6/7.1	7.3/7.8
18. Supply Reel Tape Tension (oz)		7.6/7.1	6.4/7.3	8.6/9.3
19. Capstan Torque-assumed zero friction (in-oz)		-2.8/-2.2	-0.4/+0.4	+2.6/+3.0

D. CONCLUSIONS

The most striking recorder performance change observed was the slowdown of the tape during the 2nd and 3rd vibrations.

The most pertinent evidence is shown in the data in lines 12 and 13 of Table I-1. Any loss in average recording tape speed would appear as a reduced playback interval. A 12-minute recording sequence should appear as 22.5 seconds in playback. The playback of the first shake appeared as 23 sec. or 102 percent of the nominal value. This is a small difference, and could easily be due to experimental error. It could also, however, be due to a 2 percent forward slip of the tape since the negator torque tended to overdrive the tape relative to the capstan at this time. The second shake playback time was 6 percent of nominal, and the third shake playback time was 72 percent of nominal.

Additional indications of tape slow-down are shown in line 4 which lists the playback frequency of the constant frequency clock. Nominally, this should be 120 kHz, and the non-vibrational value of 119.8 kHz is quite normal for HDRSS units. This frequency was obtained by a one second digital count of pulses in the playback signal at the limiter output. The digital count or apparent frequency of the same signal recorded during vibration was reduced between 20 and 25 percent below nominal. (The instantaneous display of the carrier signal showed a high level of time base instability and/or instantaneous loss of pulses.) The frequency reduction could have been caused by a speedup in recording tape speed, a loss of recorded pulses due to tape leaving the head, or a loss of pulses due to intermittent tape slowdown, such that the momentary signal packing density exceeded the resolution capability of the head-tape characteristic. To explore this last possibility it is of interest to examine the behavior of lower packing density tracks.

Although no long wavelength square waves were recorded, some insight into the speed during record can be gained by examining the lower frequency biphase signals. A random biphase pattern will produce fewer counts than a bit-rate square wave since one square wave count is lost for each phase reversal. For the test bit pattern, however, a 1 second period counts should be practically identical since the biphase patters were 100-bit words repetitive at intervals of 3.2 milliseconds for the special 32 KBS signal (1 KBS record) and 6.4 milliseconds for the special 16 KBS (500 BPS record), respectively. The non-vibrational playback counts of the biphase patterns were 23.5 kHz for the 32 KBS signal and 12.2 kHz for the 16 KBS signal (73.5 percent and 78 percent of the respective bit rates). The 500 BPS signal had a different pattern than the 1000 BPS, and this alone could account for the $2\frac{1}{2}$ percent difference between the two count reduction ratios. What is most pertinent is the fact that both counts increased when played back during the record-during-vibration signals, in direct contrast to the 120 kHz clock signal. There is good correlation between the two

long wavelength biphase non-vibrate count ratios for each vibration interval (lines 7 and 9). One factor that influenced tape speed was the rotation of the playback motor due to intermittent slippage of the brake which was observed during vibration. This rotation reduces the speed at which the capstan is driven. The action of the planetary drive mechanism was such that rotation of the playback motor during record affects the capstan rpm by 1/10 playback motor rpm. Although the playback motor moved in all vibration planes, the amount increased during successive vibrations. Visual estimates of the rate of rotation during each vibration and the effect or capstan speed are as follows:

Vibration	Playback Motor Rotation Observed	Reduction in Nominal Capstan Speed
1st	Very Slight	Negligible
2nd	6 - 11 rpm	2.4 - 4.4 percent
3rd	45 - 100 rpm	18 - 40 percent

Tentative conclusions drawn from the limited test data are:

- The average tape speed change was due to slippage of tape about the capstan, slippage of the playback motor brake, or, slippage of mylar belts. Experience suggests that the speed differences not directly attributable to playback motor movement are due to tape slippage.
- Tape jitter was extremely high with excursions exceeding the IRIS pulse length (179×10^{-6} inches). Therefore, cancellation of input pulses due to overlap of recoding on the tape occurred. The zero crossing excursions were less than the 1 kHz pulse wavelength (670×10^{-6} inches) except possibly during the third vibration.
- There was no positive evidence of loss of head-tape contact.

APPENDIX II

ANALYSIS OF ANALOG CHANNELS PERFORMANCE PARAMETERS

A. INTRODUCTION

Analysis of the performance parameters for the Image Dissector (ID) channel, High Resolution Infrared (HRIR) channel, and the flutter and wow (F&W) of the Time Code (TC) channel consists of the following:

- Signal-to-Noise Calculations
- Amplitude Response
- Linearity Calculations
- Drift Calculations
- Differential Phase Delay and TV Element Displacement Analysis for the ID Channel
- Sync Reliability Analysis for the ID Channel

B. SIGNAL-TO-NOISE RATIO

1. Analysis of Effect of Composite Noise on the Demodulated Output of an Ideal Frequency Discriminator

The input to the discriminator for sinewave FM modulation is

$$v = E_c \cos(\omega_c t + m \sin \omega_m t) + n_1(t) \qquad (1)$$

where m is the modulation index, ω_c is carrier angular velocity, ω_m is angular velocity of modulation signal and n_1 (t) is the noise voltage. If the noise voltage is ignored, the output from the discriminator is*

$$v_0 = k\frac{d}{dt}(m \sin \omega_m t) \qquad (2)$$

---

*Brown and Glazier, Signal Analysis, Reinhold, 1964, p. 188.

where k is the proportionality constant of the discriminator in volts per cycle of deviation, or

$$v_0 = k\omega_m m \cos \omega_m t \tag{3}$$

The corresponding output signal power in a one ohm resistor is therefore:

$$\text{Output signal power} = \tfrac{1}{2}k^2\omega_m^2 m^2 \tag{4}$$

If the noise $n_1(t)$ in equation (1) is either white Gaussian noise or triangular Gaussian noise, then $n_1(t)$ can be expressed as

$$n_1(t) = x_1(t) \cos \omega_c t + y_1(t) \sin \omega_c t \tag{5}$$

When the above noise is present and the modulation absent, equation (1) becomes:

$$v = E_c \cos \omega_c t + x_1(t) \cos \omega_c t + y_1(t) \sin \omega_c t \tag{6}$$

which may be expressed as:

$$v = A(t) \cos \left[\omega_c t + \theta(t)\right] \tag{7}$$

where

$$\theta(t) = \tan^{-1} \frac{y_1(t)}{E_c + x_1(t)} \tag{8}$$

If the input carrier-to-noise ratio is large ($E_c/n_1(t) > 10$), then

$$\theta(t) \simeq \frac{y_1(t)}{E_c} \tag{9}$$

and the output signal is

$$v_0 = \frac{k}{E_c} \frac{dy_1(t)}{dt} \tag{10}$$

If $y_1(t)$ corresponds to white flat Gaussian noise, then:

$$y_1(t) = \sum_{r=1}^{N} a_r \sin (\omega_r t + \phi_r) \tag{11}$$

and

$$v_0 = \frac{k}{E_c} \sum_{r=1}^{N} \omega_r a_r \cos (\omega_r t + \phi_r) \tag{12}$$

The discriminator noise output thus consists of a set of components, the rth one having angular frequency ω_r and rms amplitude $k\omega_r a_r/\sqrt{2}E_c$. The rms noise voltage is thus proportional to the frequency of the component considered. The average power delivered to a one ohm resistor by the rth component is $k^2\overline{a_r^2}\omega_r^2/2E_c^2$ and is associated with a frequency interval of width d_f centered on $\omega_r/2\pi$.

The output noise has a power density $G_0(f)$ where:

$$G_0(f)d_f = \frac{4\pi^2k^2f^2\overline{a_r^2}}{2E_c^2} \tag{13}$$

If the discriminator input frequency band covers $f_c - \frac{1}{2}B$ to $f_c + \frac{1}{2}B$, where

B = the predetection bandwidth, then

$$\frac{\overline{a_r^2}}{2} = \frac{\overline{y_1^2(t)}}{\left(\frac{B}{2\overline{d_f}}\right)} \tag{14}$$

and

$$G_0(f)d_f = \frac{4\pi^2k^2f^2\overline{y_1^2(t)}2df}{BE_c^2} \tag{15}$$

If the highest modulating frequency is b, then the total output noise power is:

$$\int_0^b G_0(f)d_f = \frac{8\pi^2k^2\overline{y_1^2(t)}}{BE_c^2}\int_0^b f^2d_f \tag{16}$$

$$\int_0^b G_0(f)d_f = \frac{8\pi^2k^2\overline{y_1^2(t)}b^3}{3BE_c^2} \tag{17}$$

Now consider the case where the input noise to the discriminator is comprised of white noise $n_1(t)$ and triangular noise $n_2(t)$ (i.e., from the output of another discriminator). Equation (6) becomes

$$v = E_c \cos \omega_c t + x_1(t) \cos \omega_c t + y_1(t) \sin \omega_c t + Kf_0y_0(t) \tag{18}$$

where $Kf_0y_0(t)$ is the triangular noise at the output of a discriminator.

Following a similar analysis for equations (7), (8), (9), and (10) we obtain for equation (10).

$$v_0 = \frac{k}{E_c} \frac{d\left[y_1(t) + Kf_0 y_0(t)\right]}{dt} \tag{19}$$

and

$$v_0 = \frac{k}{E_c}\left[\frac{dy_1(t)}{dt} + \frac{Kf_0 dy_0(t)}{dt}\right] \tag{20}$$

Introducing expansions similar to equation (11) for $y_1(t)$ and $y_0(t)$

$$y_1(t) = \sum_{r=1}^{N} a_{1r} \sin(\omega_r t + \phi_{1r}) \tag{21}$$

$$y_0(t) = \sum_{r=1}^{N} a_{0r_0} \sin(\omega_{r_0} t + \phi_{0r_0}) \tag{22}$$

Substituting these into equation (20), then

$$v_0 = \frac{k}{E_c}\left[\sum_{r=1}^{N} \omega_r a_{1r} \cos(\omega_r t + \phi_{1r}) \sum_{r_0=1}^{N} Kf_0 \omega_{r_0} a_{0r} \cos(\omega_{r_0} t + \phi_{0r_0})\right] \tag{23}$$

The output noise has a power density $G_0(f)$ where:

$$G_0(f)df = \frac{8\pi^2 k^2}{BE_c^2}\left[f^2\overline{y_1^2(t)} + 2f_0^2 f^2 \overline{y_1(t)y_0(t)} + f_0^2 f^2 \overline{y_0^2(t)}\right] df \tag{24}$$

The second term in equation (24) averages to zero since the noise sources $y_0(t)$ and $y_1(t)$ are independent.

The total output noise power for highest modulating frequency b is

$$\int_0^b G_0(f)\, df = \frac{8\pi^2 k^2}{BE_c^2}\,\overline{y_1^2(t)} \int_0^b f^3 df + \frac{8\pi^2 k^2}{BE_c^2} K^2 \overline{y_0^2(t)} \int_{f_{sc}-b}^{f_{sc}+b} f_0^2 f^2 df \tag{25}$$

The following translation process applies to the second term in equation (25).

$$f_0^2 = (f - f_{sc})^2 \text{ when } (f_{sc} \le f \le f_{sc} + b) \tag{26}$$

$$f_0^2 = (f + f_{sc})^2 \text{ when } (f_{sc} - b \le f \le f_{sc}) \tag{27}$$

$$f_0^2 = (f - f_{sc})^2 + (f + f_{sc})^2 \text{ when } (f_{sc} - b \le f \le f_{sc} + b) \tag{28}$$

$$f_0^2 = 2(f^2 + f_{sc}^2) \text{ when } (f_{sc} - b \le f \le f_{sc} + b) \tag{29}$$

Thus:

$$\int_0^b G_0(f)df = \frac{8\pi^2k^2}{3BE_c^2}\overline{y_1^2(t)}b^3 + \frac{16\pi^2k^2K^2}{BE_c^2}\overline{y_0^2(t)}\int_{f_{sc}-b}^{fsc+b} f_2(f^2+f_{sc}^2)d_f \qquad (30)$$

$$\int_0^b G_0(f)df = \frac{8\pi k^2}{3BE_c^2}\overline{y_1^2(t)}b^3 + \frac{16\pi k^2K^2}{BE_c^2}\overline{y_0^2(t)}\left[\frac{f^5}{5} + f_{sc}^2\frac{f^3}{3}\right]_{f_{sc}-b}^{f_{sc}+b} \qquad (31)$$

$$\int_0^b G_0(f)df = N_1 + N_2 \qquad (32)$$

where

N_1 is the first term of equation (31). This term* is the noise power at the output of a FM discriminator due to white flat Gaussian noise at the input.

N_2 is the second term of equation (31). This term is the noise power at at the output of the second FM discriminator due to white flat Gaussian noise at the input to the first discriminator.

Therefore, it can be concluded from equation (32) that the superposition theorem is valid for high signal-to-noise ratios.

2. SNR Calculations in a FM/FM Channel

Consider the FM/FM channel shown in Figure II-1.

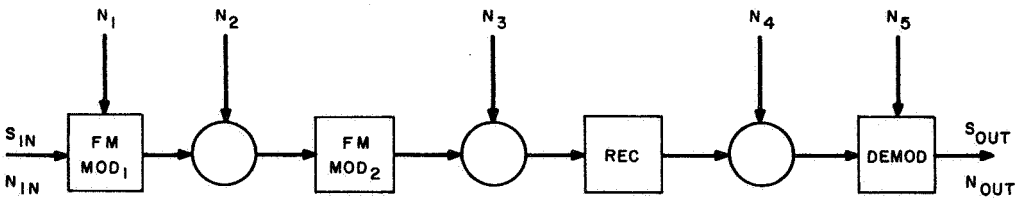

Figure II-1. Typical FM/FM Channel

*Brown and Glazier, Signal Analysis, Reinhold, 1964, p. 190.

Where N_1 is the noise introduced by the tape recorder. (This is measured directly in the baseband domain by connecting a doubler-demodulator combination at the tape recorder output, and then measuring the rms noise at the output of the calibrated demodulator.)

N_2 is the noise introduced by the multiplexer.

N_3 is the link noise.

N_4 is the noise introduced by the demultiplexer and other units such as the Mincom tape recorder.

N_5 is the noise introduced by the FM demodulator.

The procedure for calculating the net SNR at the output of the ID or HRIR channels is to compute the signal-to-noise ratios at the output video demodulator for each noise effect and then calculate the composite SNR at the components. To determine the SNR at the video demodulator output for the link, the FM/FM improvement factor is added to the link CNR and in the case of the multiplexer and demultiplexer, the FM improvement factor is added to the signal-to-noise ratios for these circuits. The SNR of the input signal, tape recorder, and video demodulator are given or measured at the video demodulator output. The SNR calculations in the subsequent sections do not include the effect of amplitude degradation with increasing signal frequency. However, the calculations are consistent with Nimbus A practices, where the signal is a d-c level and the noise is measured at the demodulator output using a true reading RMS voltmeter.

a. ID Channel SNR Calculations

The SNR contributions of the spacecraft tape recorder, multiplexer/demultiplexer, fm/fm link, video demodulator, and extraneous noise to the overall SNR value, are delineated as follows:

(1) Spacecraft Tape Recorder. The signal-to-noise ratio of the HDRSS spacecraft tape recorder is estimated to be as good as the Nimbus A tape recorder which had a minimum SNR of 35 db black-to-white/rms in a demodulated bandwidth of 0 to 60 kHz.

(2) Multiplexer/Demultiplexer. The multiplexer/demultiplexer cross talk effect is estimated from Nimbus A filter design as 45 db signal rms/noise rms. The power supply noise effect (excluding cross-talk) is arbitrarily assigned 37 db signal rms/noise rms. The overall combined SNR for the multiplexer is 36.4 db rms/rms measured at the output of the demultiplexer.

The FM improvement factor of the video demodulation is calculated from the standard FM improvement formula.

$$\text{FM improvement factor} = \frac{3}{2}\left(\frac{\Delta f_{sc}}{f_m}\right)^2 \frac{B}{f_m} \qquad (33)$$

where

Δf_{sc} is the peak frequency deviation of the subcarrier.

f_m is the cutoff frequency of the low pass post detection filter.

B is the bandwidth of the multiplexer channel.

The following values apply to the ID channel:

$\Delta f_{sc} = 4.8 \times 10^4$ Hz

$B = 1.3 \times 10^5$ Hz

$f_m = 6 \times 10^4$ Hz

Using these values in equation (33), then the

$$\text{FM improvement factor} = \frac{3}{2}\left(\frac{4.8 \times 10^4}{6 \times 10^4}\right)^2 \frac{1.3 \times 10^5}{6 \times 10^4} = 3.2 \text{ db}$$

The signal-to-noise ratio at the channel output for the multiplexer/demultiplexer is 36.4 + 3.2 = 39.6 db rms signal/rms noise.

This corresponds to 46.0 db black-to-white signal/rms noise.

(3) FM/FM Link. The signal-to-noise ratio for a fm/fm link is given by the following expression.*

$$SNR = \frac{3}{4} \frac{(\Delta f_{rf})^2 (\Delta f_{sc})^2 \cdot B_{if} \cdot CNR}{(f_m)^3 (f_{sc})^2 \left[1 + \left(\frac{3}{5}\right)\left(\frac{f_m}{f_{sc}}\right)^2\right]} \qquad (34)$$

*Radio Corporation of America, Astro-Electronics Division, Final Report for APT Camera/Tape Recorder Study, Contract NAS5-3772, Princeton, N.J., March 4, 1964 to July 10, 1964, p. 85.

where

SNR is the ratio of rms signal to rms noise, for sinusoidal modulation at the output of the low pass signal post detection filter.

f_m is the cutoff frequency of the low pass post detection filter.

CNR is the ratio of rms signal to rms noise at the input to the RF discriminator.

B_{if} is the bandwidth in which CNR is measured.

f_{sc} is the nominal center frequency of the subcarrier.

Δf_{sc} is the peak frequency deviation of the subcarrier.

Δf_{rf} is the peak frequency deviation of the RF carrier which is apportioned to this subcarrier.

The following values* apply to the ID channel:

$\Delta f_{rf} = 300$ kHz

$\Delta f_{sc} = 4.8 \times 10^4$ Hz

$f_m = 6 \times 10^4$ Hz

$f_{sc} = 4.65 \times 10^5$ Hz

$B_{if} = 3 \times 10^6$ Hz

CNR = 18.1 db rms/rms

Substituting these values in equation (34), then

$$\text{SNR} = 10 \log_{10} \left\{ \frac{3 (300 \times 10^3)^2 (4.8 \times 10^4)^2 (3 \times 10^6)}{4 (6 \times 10^4)^3 (4.65 \times 10^5)^2 \left[1 + (0.6) \left(\frac{6 \times 10^4}{4.65 \times 10^5} \right)^2 \right]} \right\} + 18 \text{ db}$$

$= 27.9$ db rms/rms

This corresponds to 34.4 db black-to-white signal-rms noise.

*Refer to Appendix III, Table III-1.

(4) Video FM Demodulator. A SNR performance of 46 db minimum black-to-white signal-rms noise in a 0 to 60 kHz bandwidth can be expected from the demodulator since Nimbus A circuit noise measurements* from the multiplexer input to the demodulator output was not less than 46 db black-to-white rms.

(5) Extraneous Noise Effect. The extraneous noise such as interconnecting cable noise is arbitrarily estimated as 40 db black-to-white signal/rms noise in a 0 to 60 kHz output bandwidth.

---

*Radio Corporation of America, Astro-Electronics Division, Test Log, Calibration Curves, and Photometric Calibration, Flight Model Camera F-3, Contract NAS5-877, Princeton, N.J., June 3, 1964, Para. 4.8.4.3.1.

(6) Overall SNR Summary

TABLE II-1. SUMMARY OF ID CHANNEL SNR

Channel Component	SNR, Black-to-White Signal/rms noise (db)
Spacecraft Tape Recorder	35.0
Multiplexer/Demultiplexer	46.0
FM/FM Link	34.4
Video FM Demodulator	46.0
Extraneous Noise	40.0
Net Channel SNR	37.2
Sensor SNR	34.0
Overall SNR	33.4

b. HRIR Channel SNR Calculations

The SNR contributions of the spacecraft tape recorder, multiplexer/demultiplexer, fm/fm link, Mincom tape recorder (Model G 100), HRIR demodulator, and extraneous noise to the overall SNR value are delineated as follows:

(1) Spacecraft Tape Recorder. The signal-to-noise ratio of the spacecraft tape recorder for the HRIR channel should be improved over the ID channel because of less bandwidth. The SNR is estimated as 36 db minimum black-to-white signal/rms noise in a demodulated bandwidth of 0 to 11.5 kHz.

(2) Multiplexer/Demultiplexer. The HRIR multiplexer-demultiplexer channel is similar to the ID channel. Therefore, the multiplexer/demultiplexer ID channel SNR of 36.4 db rms/rms at the output of the demultiplexer is applicable to the HRIR channel. The following values* apply in calculating the HRIR demodulator improvement factor from equation (33):

$$\Delta f_{sc} = 6.88 \times 10^3 \text{ Hz}$$

$$B = 3.25 \times 10^4 \text{ Hz}$$

$$f_m = 2.88 \times 10^3 \text{ Hz video}$$

*Refer to Appendix III, Table III-1.

$$\text{FM improvement factor} = \frac{3}{2}\left(\frac{6.88\times10^3}{2.88\times10^3}\right)^2 \frac{3.25\times10^4}{2.88\times10^3} = 19.8 \text{ db}$$

The signal-to-noise ratio at the channel output for the multiplexer/demultiplexer is 36.4 db + 19.8 db = 56.2 db rms/rms. This corresponds to a 65.2 db black-to-white signal/rms noise at the HRIR video demodulator output.

(3) FM/FM Link. For convenience in link SNR calculation, consider an HRIR demodulator operating at four times the normal speed connected in front of the Mincom tape recorder.

Referring to equation (34), the following values* apply for the HRIR channel:

$$\Delta f_{rf} = 2.0\times10^5 \text{ Hz}$$
$$\Delta f_{sc} = 2.752\times10^4 \text{ Hz}$$
$$f_m = 1.15\times10^4$$
$$f_{sc} = 6.3\times10^5$$
$$B_{if} = 3.0\times10^6$$
$$\text{CNR} = 18.1$$

Substituting these values in equation (34), then

$$\text{SNR} = 10\log_{10}\left\{\frac{3\,(2.00\times10^3)^2\,(2.752\times10^4)^2\,(3.0\times10^6)}{4\,(1.15\times10^4)^3\,(6.3\times10^5)^2\,[1+(0.6)\,(1.15\times10^4/6.3\times10^5)]}\right\}$$

$$+ 18.1 \text{ db} = 38.6 \text{ db rms/rms}$$

This corresponds to 47.6 db black-to-white signal/rms noise.

(4) Mincom Tape Recorder. The HRIR signal bandwidth at the output of the demultiplexer is between 135.68 kHz to 213.76 kHz. The signal-to-noise ratio of the tape recorder was calculated as 30 db rms/rms from noise level curves for the Mincom tape recorder. The applicability of C-100 series noise curves was confirmed in a telephone conversation with Mr. David A. Bixler, Technical Proposal Supervisor, Mincom Division of the 3M Company, Camarillo, California.

*Refer to Appendix III, Table III-1.

(5) HRIR Video FM Demodulator. The SNR of the HRIR demodulator is similar to the ID demodulator and therefore should have a minimum SNR of 46 db black-white/rms in a 0 to 2.88-kHz demodulated output bandwidth.

(6) Extraneous Noise. The extraneous noise (cable noise, etc.,) is arbitrarily estimated as 40 db minimum black-to-white signal/rms noise in a 0-to 2.88-kHz output bandwidth.

(7) Overall SNR Summary

TABLE II-2. SUMMARY OF HRIR CHANNEL SNR

Channel Component	SNR, Black-toWhite Signal/rms noise (db)
Spacecraft Tape Recorder	36.0
Multiplexer/Demultiplexer	56.2
FM/FM Link	47.6
Mincom Tape Recorder	58.8
HRIR Demodulator	46.0
Extraneous Noise	40.0
Net Channel SNR	34.0
Sensor SNR	35.0
Overall SNR	31.4

c. F&W SNR Calculations

The SNR contributions of the spacecraft tape recorder, multiplexer/demultiplexer, fm/fm link, flutter and wow (F&W) demodulator, and extraneous noise to the overall SNR value, are delineated as follows:

(1) Spacecraft Tape Recorder. A signal-to-noise ratio of 48 db* rms/rms was measured at the output of the breadboard tape recorder time code channel. Allowing a margin of 10 db, the SNR is given as 38 db rms/rms in a bandwidth 32 kHz centered about 80 kHz at the output of the tape recorder.

* Radio Corporation of America, Astro-Electronics Division, Final Report on Breadboard Phase of the APT Camera/Tape Recorder Study, Contract NAS5-3772, Princeton, N.J., May 5, 1966, P 75.

The following values apply to the F&W channel:

$$\Delta f_{sc} = 0.8 \times 10^3 \text{ Hz}$$
$$B = 3.2 \times 10^4 \text{ Hz}$$
$$f_m = 1.0 \times 10^3 \text{ Hz}$$

Using these values in equation (33), the

$$\text{FM improvement factor} = \frac{3}{2}\left(\frac{0.8 \times 10^3}{1.0 \times 10^3}\right)^2 \times \frac{3.2 \times 10^4}{1.0 \times 10^3} = 14.9 \text{ db}$$

Therefore, the SNR referred to the F&W demodulator output is 52.9 db rms/rms.

(2) Multiplexer/Demultiplexer. The combined effect of crosstalk noise and power supply noise in the time code channel of the multiplexer/demultiplexer is estimated as 36.4 db rms/rms. This corresponds to a SNR of 51.3 db (36.4 + 14.9) rms signal/rms noise at the F&W demodulator input.

(3) FM/FM Link. The following values* apply to the F&W channel:

$$\Delta f_{rf} = 7.5 \times 10^4 \text{ Hz}$$
$$\Delta f_{sc} = 0.8 \times 10^3 \text{ Hz}$$
$$f_m = 1 \times 10^3 \text{ Hz}$$
$$f_{sc} = 1.87 \times 10^5 \text{ Hz}$$
$$B_{if} = 3 \times 10^6 \text{ Hz}$$
$$\text{CNR} = 18.1 \text{ db}$$

Using these values in equation (34), the resultant SNR is a 41.7-db rms signal to rms noise to the F&W demodulator. During the time code modulation valleys, this number could be reduced by 11.5 db (worst case valley/peak ratio = 0.3) resulting in 30.2 db rms signal to rms noise.

(4) Flutter and Wow Demodulator. The SNR of the F&W demodulator is arbitrarily estimated as 40.0 db rms signal/rms noise in a 0 to 1.0 kHz bandwidth.

(5) Extraneous Noise. The extraneous noise effect in the F&W channel is arbitrarily estimated as 40 db rms signal/rms noise at the F&W demodulator output.

*Refer to Appendix III, Table III-1.

(6) Time Code Channel SNR Summary

TABLE II-3. SUMMARY OF TIME CODE CHANNEL

Channel Component	SNR, rms Signal/rms Noise (db)
Spacecraft Tape Recorder	52.9
Multiplexer/Demultiplexer	51.3
FM/FM Link	30.2
F&W Demodulator	40.0
Extraneous Noise	40.0
Net Channel SNR	29.3

C. AMPLITUDE RESPONSE

Analysis and calculations of amplitude degradation were performed at the highest signal frequency.

1. Amplitude Response Analysis

The effects of upper sideband attenuation and filtering on amplitude response in the tape recorder, multiplexer and demultiplexer are analyzed in the following paragraphs. Refer to Figure II-2.

a. Input Signal

The input signal is

$$V_{in} = \cos \omega t \qquad (35)$$

where $\omega/2\pi$ is the modulating frequency.

b. FM Modulator Output

The FM modulator output is

$$A = \sin \left(\omega_c t + m \sin \omega t\right) \qquad (36)$$

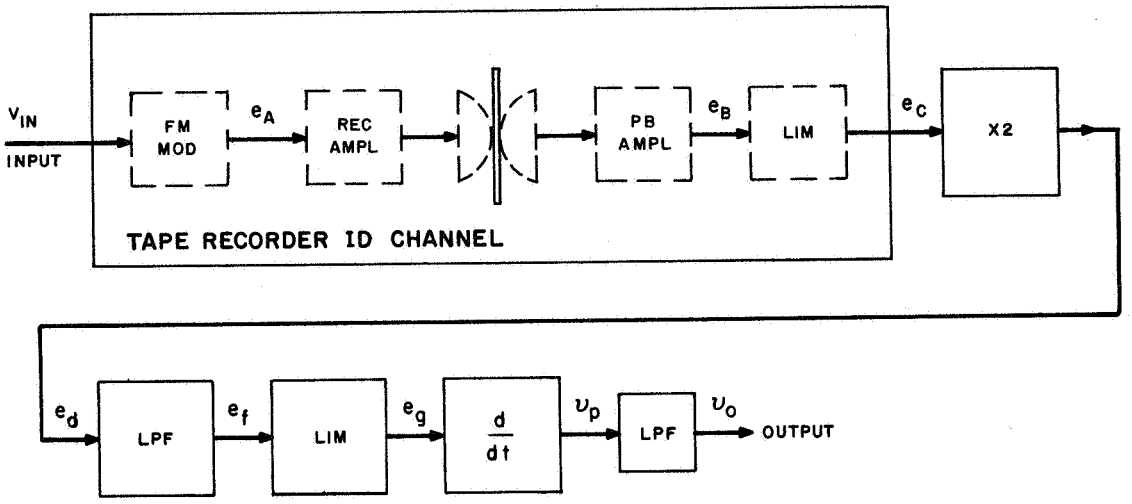

Figure II-2. HDRSS ID Channel, Block Diagram

where

$\omega_c/2$ is the subcarrier frequency

m is the modulation index (ratio of subcarrier deviation to modulating frequency 16.8 kHz/51.2 kHz = 0.33)

For a low modulation index ($m < 0.6$), equation (36) can be represented by:

$$e_A = J_0(m) \sin \omega_c t + J_1(m) \sin(\omega_c + \omega)t - J_1(m) \sin(\omega_c - \omega)t \qquad (37)$$

c. Playback Amplifier Output

The record and playback processes introduce phase and amplitude variations in equation (37). Then:

$$e_B = J_0(m) \sin \omega_c t + a\, J_1(m) \sin [\omega_c t + (\omega t + \phi_A)] - b\, J_1(m) \sin [\omega_c t - (\omega t - \phi_B)] \quad (38)$$

where

ϕ_A and ϕ_B are the upper and lower sidebands respective phase shifts with respect to the carrier, and a and b are the amplitude response factors.

Equation (38) can be rearranged after expanding the sine and cosine terms to give:

$$e_B = \{J_0(m) + J_1(m) [a \cos (\omega t + \phi_A) - b \cos (\omega t - \phi_B)]\} \cdot \sin \omega_c t + J_1(m) [a \sin (\omega t + \phi_A) + b \sin (\omega t - \phi_B)] \cos \omega_c t \quad (39)$$

Since

$$J_0(m) = J_0(0.33) \simeq 1 \text{ and } J_1(m) \simeq \frac{m}{2} \simeq \frac{0.33}{2} = 0.165$$

$$e_B = J_0(m) \sin \omega_c t + \frac{m}{2} [a \sin (\omega t + \phi_A) + b \sin (\omega t - \phi_B)] \cos \omega_c t \quad (40)$$

$$e_B = J_0(m) \sin \omega_c t + \frac{m}{2} [(a \cos \phi_A + b \cos \phi_B) \sin \omega t + (a \sin \phi_A - b \sin \phi_B) \cos \omega t] \cos \omega t \quad (41)$$

$$e_B = J_0(m) \sin \omega_c t + \frac{m}{2} [a^2 + b^2 + 2ab \cos (\phi_A + \phi_B)]^{\frac{1}{2}} \cdot \sin (\omega t + y) \cos \omega t \quad (42)$$

where

$$y \text{ is } \tan^{-1} \frac{a \sin \phi_A - b \sin \phi_B}{a \cos \phi_A + b \cos \phi_B} \quad (43)$$

$$e_B = P_1 \sin \omega_c t + Q_1 \cos \omega t \tag{44}$$

where

$$P_1 = J_0(m) \tag{45}$$

$$Q_1 = \frac{m}{2}\left[a^2 + b^2 + 2ab \cos(\phi_A + \phi_B)\right]^{\frac{1}{2}} \cdot \sin(\omega t + y) \tag{46}$$

$$e_B = (P_1^2 + Q_1^2)^{\frac{1}{2}} \sin\left(\omega_c t + \tan^{-1}\frac{Q_1}{P_1}\right) \tag{47}$$

d. Tape Recorder Limiter Output

The output of an ideal limiter is given by:*

$$y(z) = \frac{4K}{\pi}\left[\cos z - \frac{1}{3}\cos 3z + \ldots\right] \tag{48}$$

where

$$z = \omega_c t + \tan^{-1}\frac{Q_1}{P_1} \tag{49}$$

$$e_C = \cos\left(\omega_c t + \tan^{-1}\frac{Q_1}{P_1}\right) - \frac{1}{3}\cos 3\left(\omega_c t + \tan^{-1}\frac{Q_1}{P_1}\right) + \ldots \tag{50}$$

e. Doubler Output

The doubler output is

$$e_d = \cos\left(2\omega_c t + 2\tan^{-1}\frac{Q_1}{P_1}\right) - \frac{1}{3}\cos 6\left(\omega_c t + \tan^{-1}\frac{Q_1}{P_1}\right) + \ldots \tag{51}$$

$$e_d \simeq \cos\left(2\omega_c t + 2\frac{Q_1}{P_1}\right) + \ldots \tag{52}$$

$$e_d = \cos\left\{2\omega_c t + m\left[a^2 + b^2 + 2ab\cos(\phi_A + \phi_B)\right]^{\frac{1}{2}} \sin(\omega t + y)\right\} + \ldots \tag{53}$$

$$e_d = \cos\left[2\omega_c t + m' \sin(\omega t + y)\right] + \ldots \tag{54}$$

---

* W. Bennet, Data Transmission, McGraw Hill, 1965, p 169.

where

$$m' = m \left[a^2 + b^2 + 2ab \cos (\phi_A + \phi_B) \right]^{\frac{1}{2}} \quad (55)$$

f. Low Pass Filter Output

All frequency components above $2\omega_c$ will be attenuated by the low pass filter.

Consider a rotation of axis of first term in equation (54) then,

$$e_d = \sin \left[2\omega_c t + m' \sin (\omega t + y) \right] \quad (56)$$

$$e_d = J_0 (m') \sin \omega_c t - J_1 (m') \sin (2\omega_c t - \omega t - y) + J_1 (m') \sin (2\omega_c t + \omega t + y) \quad (57)$$

The third term is attenuated by the low pass filter, therefore the output $e_d = e_f$.

$$e_f = J_0 (m') \sin \omega_c t - J_1 (m') \sin (2\omega_c t - \omega t - y) \quad (58)$$

Equation (57) can be rearranged after expanding the second term to give:

$$e_f = \left[J_0 (m') - J_1 (m') \cos (\omega t + y) \right] \sin 2\omega_c t + J_1 (m') \sin (\omega t + y) \cos 2\omega_c t \quad (59)$$

$$e_f = P_2 \sin 2\omega_c t + Q_2 \cos 2\omega_c t \quad (60)$$

where

$$P_2 = J_0 (m') - J_1 (m') \cos (\omega t + y) \quad (61)$$

and

$$Q_2 = J_1 (m') \sin (\omega t + y) \quad (62)$$

then

$$e_f = (P_2^2 + Q_2^2)^{1/2} \sin \left(2\omega_c t + \tan^{-1} \frac{Q_2}{P_2} \right) \quad (63)$$

g. Limiter Output

Applying equation (48) to equation (63)

$$e_g = \cos\left(2\,\omega_c t + \tan^{-1}\frac{Q_2}{P_2}\right) - \frac{1}{3}\cos 3\left(2\,\omega_c t + \tan^{-1}\frac{Q_2}{P_2}\right) + \ldots \qquad (64)$$

The low pass filter will attentuate the second and higher terms in equation (64).

h. Discriminator Output

The discriminator output

$$v_p = \frac{D}{2\pi}\,\frac{\partial}{\partial t}\left(\tan^{-1}\frac{Q_2}{P_2}\right) \qquad (65)$$

where $D/2\pi$ is the discriminator constant

$$v_p = \frac{D}{2\pi}\,\frac{P_2\frac{\partial Q_2}{\partial t} - Q_2\frac{\partial P_2}{\partial t}}{P_2^2 + Q_2^2} \qquad (66)$$

where

$$P_2 = J_0(m') - J_1(m')\cos(\omega t + y) \qquad (67)$$

$$\frac{\partial P_2}{\partial t} = \omega\, J_1(m')\sin(\omega t + y) \qquad (68)$$

$$Q_2 = J_1(m')\sin(\omega t + y) \qquad (69)$$

$$\frac{\partial Q_2}{\partial t} = \omega\, J_1(m')\cos(\omega t + y) \qquad (70)$$

Substituting equations (67), (68), (69), and (70) into equation (66):

$$\begin{aligned} v_p = \frac{D}{2\pi}\,\{&\left[J_0(m') - J_1(m')\cos(\omega t + y)\right]^2 \\ &+\left[J_1(m')\sin(\omega t + y)\right]^2\}^{-1}\ \left[J_0(m')\right. \\ &\left. - J_1(m')\cos(\omega t + y)\right]\left[\omega\, J_1(m')\cos(\omega t + y)\right] \\ &-\left[J_1(m')\sin(\omega t + y)\right]\left[\omega\, J_1(m')\sin(\omega t + y)\right]\} \end{aligned} \qquad (71)$$

$$v_p = \frac{D\omega J_1(m')}{2\pi\left[J_0^2(m') + J_1^2(m')\right]} \left\{ 1 + \frac{2J_0(m')J_2(m')}{J_0^2(m') + J_1^2(m')} \cos(\omega t + y) \right.$$

$$\left. + \frac{4J_0^2(m')J_1^2(m')}{\left[J_0^2(m') + J_1^2(m')\right]^2} \cos^2(\omega t + y) + \cdots \right\}$$

$$\cdot \left\{ J_0(m') \cos(\omega t + y) - J_2(m') \right\} \tag{72}$$

$$= \frac{D\omega J_2(m')}{2\pi\left[J_0^2(m') + J_2^2(m')\right]^3} \left\{ -J_1^3(m')\left[1 + 3J_0^2(m')\right] \right.$$

$$+ J_0(m')\left[J_0^4(m') + 2J_0^2(m')J_1^2(m') - J_1^4(m')\right] \cos(\omega t + y)$$

$$\left. + \cdots \right\} \tag{73}$$

j. Output Signal

The low pass filter, cutting off at $\omega/2\pi$, eliminates all Fourier terms above the fundamental term cos $(\omega t + y)$ in equation (73), for $J_0^2(m') >> J_1^2(m')$.

Then the output signal after final filtering becomes

$$v_p \simeq \frac{D\omega J_2(m')}{2\pi J_0^6(m')} \left\{ -J_1^3(m')\left[1 + 3J_0^2(m')\right] \right.$$

$$\left. + J_0^5(m') \cos(\omega t + y) \right\} \tag{74}$$

For

$$J_0(m') \simeq 1$$

$$v_p \simeq \frac{D\omega J_2(m')}{2\pi} \left[-4J_1^3(m') + \cos(\omega t + y) \right] \tag{75}$$

Equation (75) shows that the effect on the baseband signal caused by upper sideband amplitude and phase transfer characteristics in the tape recorder is the same as that caused by similar transfer characteristics in the lower sideband even when the upper sideband signal is attenuated after the tape recorder output.

Consider the case where the tape recorder amplitude characteristic is flat up to the subcarrier frequency and then drops off rapidly and that the phase shift of the lower sideband with respect to the subcarrier is negligible, then m' in equation (55) after substituting a = 0, b = 1, and $\phi_B = 0$, becomes

$$m' = m \tag{76}$$

The amplitude term of equation (74) becomes

$$\frac{D\omega}{2\pi} J_1(m') \simeq \frac{D\omega}{2\pi} \bullet \frac{m}{2} \tag{77}$$

If $a = b = 1$ and $\phi_A = \phi_B = 0$, then from equation (55)

$$m' = 2m \tag{78}$$

and the amplitude term of equation (75) becomes

$$\frac{D\omega}{2\pi} J_1(m') \simeq \frac{D\omega}{2\pi} \bullet m \tag{79}$$

Therefore, in comparing (77) to (79) a 6 db loss of signal amplitude can result by complete attenuation of the upper sideband in the tape recorder.

The following conclusions result from the analysis:

- The effect on the baseband signal caused by upper sideband amplitude and phase transfer characteristics in the tape recorder is the same as that caused by similar transfer characteristics in the lower sideband even when the upper sideband signal is attenuated after the tape recorder output.
- A 6 db loss in amplitude of the baseband signal can result by complete attenuation of the upper sideband within the tape recorder. This is in addition to the 6 db loss by upper sideband attenuation after the tape recorder output.
- The tape recorder amplitude and phase transfer characteristics of the upper and lower sidebands have an effect on the dc component of the baseband signal.
- The tape recorder amplitude and phase transfer characteristics of the upper and lower sidebands have an effect on the differential phase delay of the baseband signal.

2. ID Channel Amplitude Response

The maximum contributions by the spacecraft tape recorder, multiplexer/demultiplexer and ID Demodulator to signal amplitude degradation in the ID channel are delineated as follows:

a. Spacecraft Tape Recorder

The spacecraft tape recorder has been specified to have a maximum amplitude attenuation of -2 db at the highest signal frequency when measured at the output of a calibrated demodulator.

b. Multiplexer/Demultiplexer

The multiplexer/demultiplexer contributes -6.0 db maximum amplitude degradation due to upper sideband filtering. The Nimbus A multiplexer/demultiplexer amplitude ripple specification is 6 db peak-to-peak over the bandwidth which can result in an additional 6 db amplitude degradation.

c. ID Demodulator

The amplitude response of a TOS AVCS modulator, TOS-type doubler, and AVCS Video Demodulator was measured -3 db down at highest modulating frequency. The reference was taken as dc black-to-white levels. The ID demodulator amplitude degradation was specified as -3 db down at 51.2 kc.

d. ID Channel Amplitude Degradation

TABLE II-4. SUMMARY OF ID CHANNEL AMPLITUDE RESPONSE

Channel Component	Amplitude Response at 51.2 kHz	
	Specified (db)	Expected (db)
Spacecraft Tape Recorder		-2.0
Multiplexer/Demultiplexer		
Upper Sideband Suppression		-6.0
Ripple Effect		-6.0
ID Demodulator		-3.0
Overall Amplitude Response (Total)		-17.0

One black level grey step, 2.6 percent of black-to-white scale, has been selected as the limit of resolution. This level corresponds to -31.7 db down from full black-to-white scale. If the ID sensor is down no more than -6 db at 1600 Hz, the overall ID channel has a margin of 8.7 db above limiting resolution.

3. HRIR Channel Amplitude Response

The maximum contributions by the spacecraft tape recorder, multiplexer/demultiplexer, Mincom tape recorder and HRIR demodulator to signal amplitude degradation in the HRIR channel are delineated as follows:

a. Spacecraft Tape Recorder

The spacecraft tape recorder has been specified to have a maximum amplitude attenuation of -2.5 db at the highest signal frequency when measured at the output of a calibrated demodulator which is down 1 db at 51.2 kHz.

b. Multiplexer/Demultiplexer

The multiplexer/demultiplexer amplitude ripple specification is 6 db peak-to-peak over the channel bandwidth. Theoretically, a 6 db amplitude degradation is possible; however, most of the signal energy is distributed in several spectral components above and below the subcarrier frequency, therefore, it is extermely unlikely that a worse case amplitude degradation of -6 db would occur. A more realistic amplitude degradation value of -3 db is used in the analysis.

c. Mincom Tape Recorder

The amplitude ripple specification of the Mincom tape recorder is ±3 db over the HRIR bandwidth. The same rationale for the multiplexer/demultiplexer amplitude degradation is applicable to the Mincom tape recorder. An amplitude degradation value of -3 db is used in the analysis.

d. HRIR Demodulator

The amplitude degradation of the HRIR demodulator has been specified as -1.0 db maximum at the highest signal frequency.

e. HRIR Channel Amplitude Degradation

TABLE II-5. SUMMARY OF HRIR CHANNEL AMPLITUDE RESPONSE

Channel Component	Amplitude Response at	
	Specified (db)	Expected (db)
Spacecraft Tape Recorder		-2.5
Multiplexer/Demultiplexer		-3.0
Mincom Tape Recorder		-3.0
HRIR Demodulator		-1.0
Overall Amplitude Response (Total)		-9.5

Since there is no existing grey scale limiting resolution specification for the HRIR channel, one linear grey step, 12.5 percent (-18 db) of black-to-white scale, has been selected as the limit of resolution. The sensor is specified to be down no more than -6 db at 360 Hz. Therefore, there is an overall margin of 2.5 db above the limiting resolution specification.

D. LINEARITY CALCULATIONS

1. Basis of Calculation

The modulator and demodulator are the only channel components associated with linearity deviation. This deviation from linearity is defined as the percent black-to-white deviation from a best straight line fit to the actual output/input line. From Nimbus A practice a good linear fit to the data was obtained by the eye; however, if the eye method should prove inadequate the method of least squares as applied to regression theory can be used to find a best linear fit* to the data.

2. ID Channel Linearity

a. ID FM Modulator

The linearity specifications were established on the basis of what performance can be expected from a modulator of this type (modified Nimbus A HRIR modulator).

---

* Burington and May, Handbook of Probability and Statistics with Tobbe, McGraw Hill 1958, Chapter XII.

The specification for the linearity limits of the ID Modulator are shown in Figure II-3.

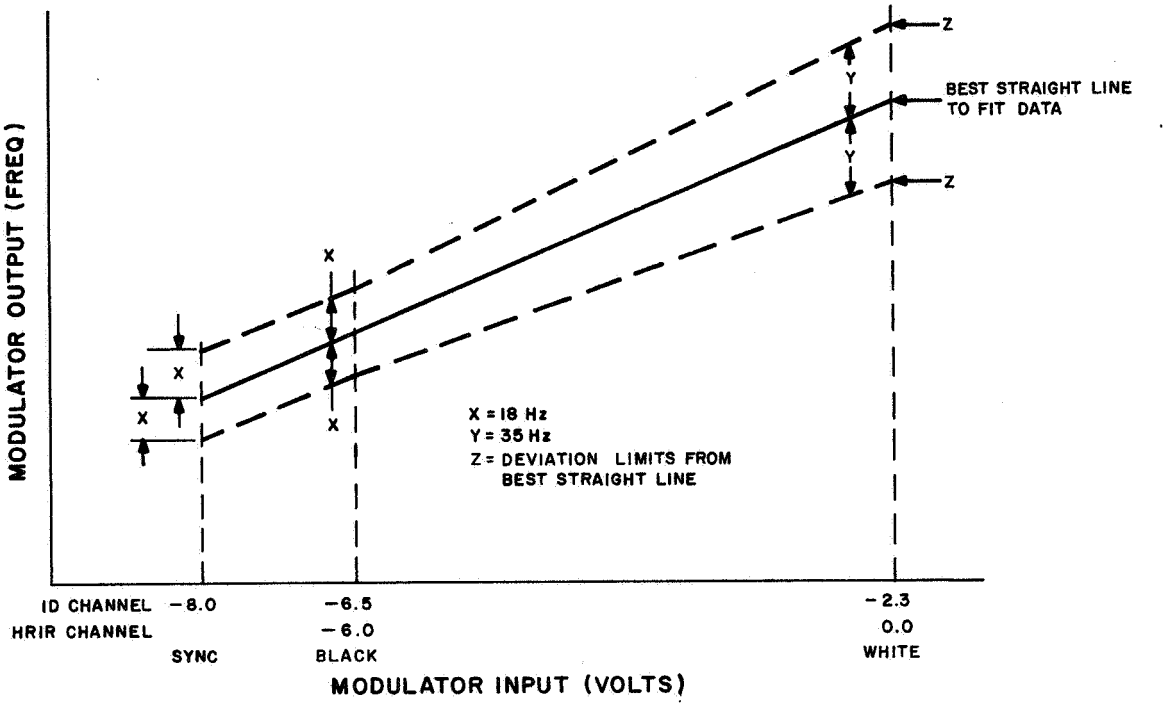

Figure II-3. ID and HRIR Modulator Linearity Specifications

The linearity limits (see Figure II-3) in terms of percent black-to-white scale are based on the following modulator characteristics:

Input Level	Output Frequency (Hz)	Specified Deviation Limits From Best Straight Time (Hz)
White	3675	35
Black	2625	18
Diff (black-to-white)	1050	

Linearity in percent of black-to-white scale equals

White	$35/1050 \times 100 = 3.3$
Black	$18/1050 \times 100 = 1.7$

b. Demodulator

The demodulator linearity limits are arbitrary specified as follows:

Level	Deviation from Best Straight Line in Percent of Black-to-White Scale
White	1.0
Black	1.0

c. ID Channel Linearity

TABLE II-6. SUMMARY OF ID CHANNEL LINEARITY

Channel Component	Black-to-White Ratio (%)	
	White Level	Black Level
Modulator	3.3	1.7
Demodulator	1.0	1.0
Overall Linearity (Maximum)	4.3	2.7

The overall objective linearity limits from the best straight line presented at the system conceptual design review were:

Black level: one black level gray step, 2.6 percent black-to-white scale

White level: two black level gray step, 5.2 percent black-to-white scale

The difference between the system maximum of 2.7 percent and the system objective 2.6 percent for the black level is not considered a significant difference.

3. HRIR Channel Linearity

a. HRIR FM Modulator

The HRIR FM Modulator is the same type as the ID modulator. The specification on the linearity limits of the HRIR Modulator are the same as the ID modulator and are shown in Figure II-3

The linearity limits (see Figure II-3) in terms of percent black-to-white scale are based on the following modulator characteristics:

Input Level	Output Frequency (Hz)	Specified Deviation Limits From Best Straight Time (Hz)
White	3160	35
Black	2300	18
Diff (black-to-white)	860	

Linearity in percent of black-to-white scale becomes

White	$35/860 \times 100 = 4.1$
Black	$18/860 \times 100 = 2.1$

b. Demodulator

The demodulator linearity limits are arbitrary specified as follows:

Level	Deviation from Best Straight Line in Percent of Black-to-White Scale
White	1.0
Black	1.0

c. ID Channel Linearity

TABLE II-7. SUMMARY OF HRIR CHANNEL LINEARITY

Channel Component	Black-to-White Ratio (%)	
	White Level	Black Level
Modulator	4.1	2.1
Demodulator	1.0	1.0
Overall Linearity (Maximum)	5.1	3.1

The overall objective linearity limits from the best straight line presented at the system conceptual design review were:

Black level: one ID black level grey step 2.6 percent black-to-white scale

White level: two ID black level grey step 5.2 percent black-to-white scale

It was also pointed out at the design review that RCA could not meet the black level objectives which were not derived from HRIR.

E. DRIFT CALCULATIONS

1. Basis of Calculations

A channel component plot of output versus input could change either by aging or by an ambient temperature change. Drift is defined as the difference between the best straight line as defined in Paragraph D1 and the nominal output versus input line. This difference is expressed in percent of black-to-white scale and is taken as a measurement of drift. The drift characteristic specified and the linearity characteristic stated in Paragraph D1 permits practical identification of these effects. The channel components contributing to drift are the FM modulator, tape recorder transport, multiplexer, demultiplexer, Mincom tape recorder, and demodulator.

2. ID Channel Drift Calculations

a. ID FM Modulator

The drift specifications were established on the basis of what performance can be expected from a modulator of this type. (Modified Nimbus A HRIR Modulator).

The specifications on the drift limits of the ID Modulator are shown in Figure II-4.

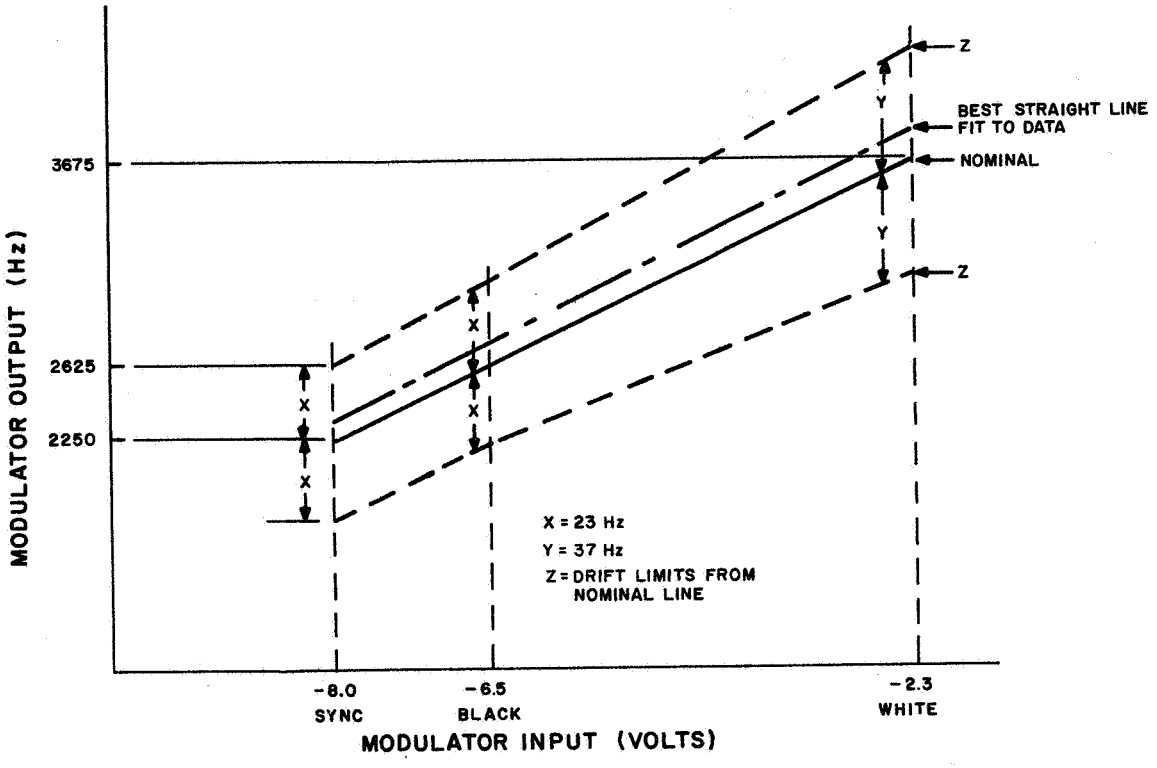

Figure II-4. ID Modulator Drift Specifications

The drift limits (see Figure II-4) in terms of percent black-to-white scale are based on the following modulator characteristics:

Input Level	Output Frequency (Hz)	Specified Deviation Limits From Nominal Line (Hz)
White	3675	37
Black	2625	23
Diff (black-to-white)	1050	

Drift in percent of black-to-white scale becomes

White	$37/1050 \times 100 = 3.5$
Black	$23/1050 \times 100 = 2.2$

b. Tape Recorder Transport

The maximum drift of the playback/record ratio is specified as ±0.5 percent.

Level	Drift in Percent of Black-to-White Scale
White	$0.5 \times \frac{3675}{1050} = 1.7$
Black	$0.5 \times \frac{2625}{1050} = 1.3$

c. Multiplexer/Demultiplexer

The frequency stability of the local oscillator in the multiplexer or demultiplexer is ±160 Hz. The oscillator is the same as the oscillator in Nimbus A equipment and has a frequency difference of 67200 Hz ($2 \times 32 \times 1050$) between the black and white levels. Then the maximum drift for the multiplexer and demultiplexer in percent black-to-white scale is

$$2 \times \frac{160}{67200} \times 100 = 0.5 \text{ percent.}$$

d. Demodulator

The maximum drift of the ID demodulator is arbitrary specified as ±1.0 percent black-to-white scale.

e. ID Channel Overall Drift

TABLE II-8. SUMMARY OF ID CHANNEL DRIFT

Channel Component	Black-to-White Ratio (%)	
	White Level	Black Level
Modulator	3.5	2.2
Tape Recorder	1.7	1.3
Multiplexer/Demultiplexer	0.5	0.5
Demodulator	1.0	1.0
Overall Drift (max)	6.7	5.0

The overall objective ID drift limits from the nominal line presented at the system conceptual design review review were:

Black Level: One black level grey step, 2.6 percent black-to-white scale.

White Level: Two black level grey steps, 5.2 percent black-to-white scale.

The channel drift values exceed the objective values. The following is derived from the rms sums of the values in Table II-8:

Black Level 2.8 percent

White Level 4.0 percent

The black level ID objective is not achieved because the local oscillator designs in the Nimbus A multiplexer and demultiplexer do not take full advantage of the crystal tolerance. It is possible to improve the design of the local oscillator and reduce the drift by a factor of 2. The actual drift of the ID demodulator in a controlled temperature environment is unknown and is probably less than the 1.0 percent specification value. If the modulator drift value were also reduced by a factor of 2, the black level rms drift sums would meet the objective value of 2.6 percent.

3. HRIR Channel Drift

a. HRIR FM Modulator

The HRIR FM Modulator, drift limits are approximately proportional to the drift values of the ID Modulator and are shown in Figure II-5.

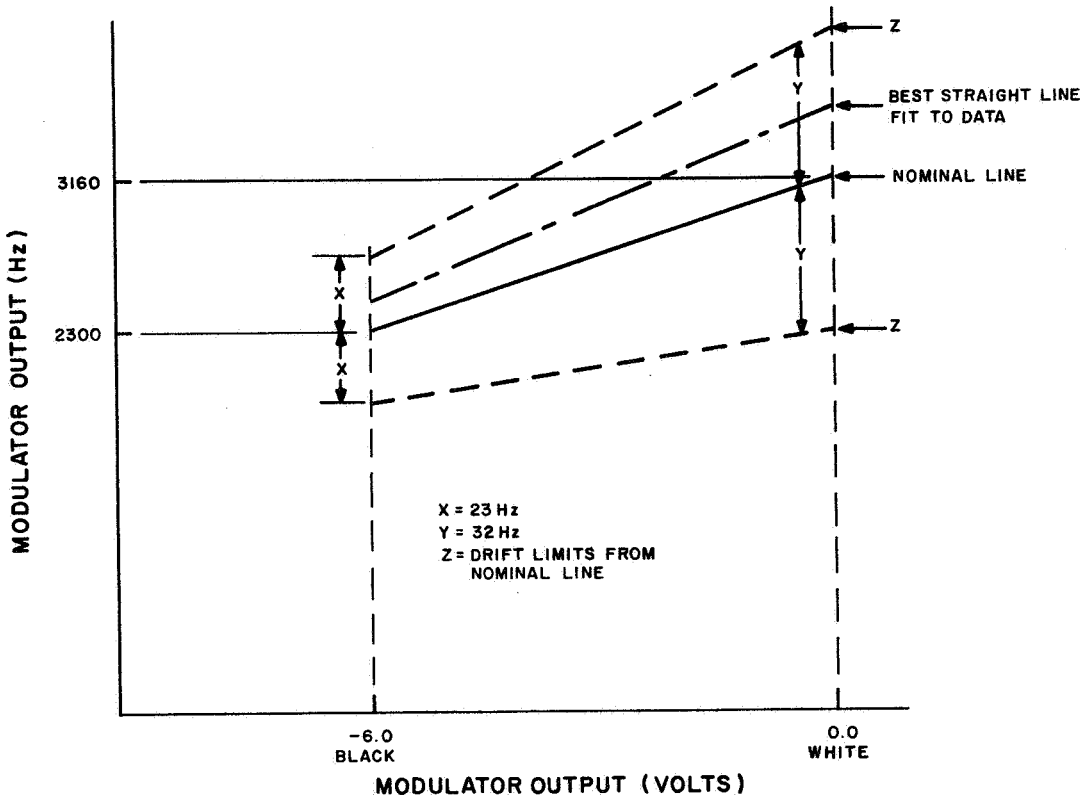

Figure II-5. HRIR Modulator Drift Specifications

The drift limits (see Figure II-5) in terms of percent black-to-white scale are based on the following modulator characteristics:

Input Level	Output Frequency (Hz)	Specified Deviation Limits From Nominal Time (Hz)
White	3160	32
Black	2300	23
Diff (black-to-white)	860	

Drift in percent of black-to-white scale becomes

White	$32/860 \times 100 = 3.7$
Black	$23/860 \times 100 = 2.7$

b. Spacecraft Tape Recorder

The maximum drift of the playback/record ratio is specified as ±0.5 percent.

Level	Drift in Percent of Black-to-White Scale
White	$0.5 \times \frac{3160}{860} = 1.9$
Black	$0.5 \times \frac{2300}{860} = 1.3$

c. Multiplexer/Demultiplexer

The stability of the local oscillator in the multiplexer or demultiplexer HRIR channel is ±160 Hz. The oscillator is the same as the oscillator in Nimbus A and has a frequency difference of 55040 ($2 \times 32 \times 860$) between black and white levels. Then the maximum drift for the multiplexer and demultiplexer in percent black-to-white scale is

$$2 \times \frac{160}{55040} \times 100 = 0.6 \text{ percent}$$

d. Mincom Tape Recorder

The maximum drift on the playback/record ratio is 0.15 percent.* At the output of the Mincom tape recorder, the white level frequency is

$$\frac{2 \times 32 \times \text{Modulator Frequency}}{\text{Record/Playback Ratio}}$$

$$= \frac{2 \times 32 \times 3160}{4} = 50560 \text{ Hz.}$$

Similarily, the black level is

$$\frac{2 \times 32 \times 2300}{4} = 36800 \text{ Hz.}$$

---

* Taken from specification on the Mincom G-100 Tape Recorder.

The frequency difference between black-to-white at the output of Mincom tape recorders

$$= \frac{55040}{4} = 13760 \text{ Hz.}$$

Drift for the tape recorder now equals the Record/Playback rates × Level Frequency/Playback Frequency Difference.

The percent white level drift becomes

$$0.15 \times \frac{50560}{13760} = 0.6 \text{ percent, and}$$

the black level drift becomes

$$0.15 \times \frac{36800}{13760} = 0.4 \text{ percent.}$$

e. Demodulator

The maximum drift of the HRIR demodulator is arbitrary, specified as ±1.0 percent black-to-white scale.

f. HRIR Channel Overall Drift

TABLE II-9. SUMMARY OF HRIR CHANNEL DRIFT

Channel Component	Black-to-White Ratio (%)	
	White Level	Black Level
Modulator	3.7	2.7
Spacecraft Tape Recorder	1.9	1.3
Multiplexer/Demultiplexer	0.6	0.6
Mincom Tape Recorder	0.6	0.4
Demodulator	1.0	1.0
Overall Drift (max)	7.8	6.0

The overall objective HRIR drift limits from the nominal line presented at the system conceptual design review were:

Black Level: One black level grey step, 2.6 percent black-to-white scale.

White Level: Two black level grey steps, 5.2 percent black-to-white scale.

The maximum HRIR channel drift values exceed the objective values. The rms sum of the values in Table II-9 yields the following:

Black Level	3.2 percent
White Level	4.3 percent

On an rms sum basis, the black level objective is not obtained. However, as stated in Paragraph D.3.c, the grey scale resolution requirements for HRIR are unknown and the 2.6 percent objective has been borrowed from the ID objective.

F. DIFFERENTIAL PHASE DELAY AND TV ELEMENT DISPLACEMENT ANALYSIS

1. Analysis

a. Input Signal

Referring to the block diagram of Figure II-2, the input signal is given by:

$$v_{in} = \cos \omega t \tag{80}$$

where $\omega/2\pi$ is the modulating frequency.

b. FM Modulator Output

$$e_A = \sin (\omega_c t + m \sin \omega t) \tag{81}$$

where

$\omega/2\pi$ is the subcarrier frequency

m is the index modulation (ratio of subcarrier deviation to modulating frequency 16.8 kHz/51.2 kHz - 0.33).

For a low index modulation ($m < 0.6$) equation (81) can be represented* by:

$$e_A = J_0(m) \sin \omega_c t + J_1(m) \sin(\omega_c + \omega)t - J_1(m) \sin(\omega_c - \omega)t \quad (82)$$

c. Playback Amplifier Output

The record and playback processes introduce phase and amplitude variations in equation (3). Then:

$$e_B = J_0(m) \sin \omega_c t + a J_1(m) \sin [\omega_c t + (\omega_c t + (\omega t + \phi_A)] - b J_1(m) \sin [\omega_c t - (\omega t - \phi_B)] \quad (83)$$

where

ϕ_A and ϕ_B are the upper and lower sidebands respective phase shifts with respect to the carrier, and

a and b are the amplitude response factors.

Assuming that the amplitude response of the tape recorder is approximately flat, equation (83) for low index of modulation becomes:

$$e_B = \sin \omega_c t - \frac{m}{2} \sin [\omega_c t + (\omega t + \phi_A)] - \frac{m}{2} \sin [\omega_c t - (\omega t - \phi_B)] \quad (84)$$

Equation (84) can be rearranged to give

$$e_b = \left[1 - m \sin \left(\omega t + \frac{\phi_A - \phi_B}{2}\right) \sin \frac{\phi_A + \phi_B}{2}\right] \sin \omega_c t + \left[m \sin \left(\omega t + \frac{\phi_A - \phi_B}{2}\right) \cos \frac{\phi_A + \phi_B}{2}\right] \cos \omega t \quad (85)$$

$$e_B = P_1 \sin \omega_c t + Q_1 \cos \omega_c t \quad (86)$$

---

* J. Hancock, An Introduction to the Principles of Communication Theory, McGraw Hill, 1961, p 56.

where:

$$P_1 = 1 - m \sin\left(\omega t + \frac{\phi_A - \phi_B}{2}\right) \sin\frac{\phi_A + \phi_B}{2} \tag{87}$$

$$Q_1 = m \sin\left(\omega t + \frac{\phi_A - \phi_B}{2}\right) \cos\frac{\phi_A + \phi_B}{2} \tag{88}$$

$$e_B = (P_1^2 + Q_1^2)^{\frac{1}{2}} \sin\left(\omega_c t + \tan^{-1}\frac{Q_1}{P_1}\right) \tag{89}$$

d. Tape Recorder Limiter

The output of an ideal limiter is given by:*

$$y(z) = \frac{4K}{\pi}\left[\cos z - \frac{1}{3}\cos 3z + \ldots\right] \tag{90}$$

where:

$$z = \omega_c t + \tan^{-1}\frac{Q_1}{P_1}$$

$$e_C = \cos\left(\omega_c t + \tan^{-1}\frac{Q_1}{P_1}\right) - \frac{1}{3}\cos 3\left(\omega_c t + \tan^{-1}\frac{Q_1}{P_1}\right) + \ldots \tag{91}$$

e. Doubler Output

The doubler output is

$$e_d' = \cos\left(2\omega_c t + 2\tan^{-1}\frac{Q_1}{P_1}\right) - \frac{1}{3}\cos 6\left(\omega_c t + \tan^{-1}\frac{Q_1}{P_1}\right) + \ldots \tag{92}$$

f. Demultiplexer Output

All components except the first will be attenuated by the multiplexer/demultiplexer circuits.

$$e_f = \cos\left(2\omega_c t + 2\tan^{-1}\frac{Q_1}{P_1}\right) \tag{93}$$

---

* W. Bennet, Data Transmission, McGraw Hill, 1965, P. 169.

Consider a rotation of axis of equation (93):

$$e_f = \sin\left(2\,\omega_c t + 2\tan^{-1}\frac{Q_1}{P_1}\right) \tag{94}$$

For low index of modulation, $P_1 = 1$ and equation (94) becomes:

$$e_f = \sin\left[2\,\omega_c t + 2\,m\cos\frac{\phi_A + \phi_B}{2}\sin\left(\omega t + \frac{\phi_A - \phi_B}{2}\right)\right] \tag{95}$$

$$e_f = J_0(m^1)\sin 2\,\omega_c t - J_1(m^1)\sin\left(2\,\omega_c - \omega t - \frac{\phi_A - \phi_B}{2} - y\right) \tag{96}$$

where

y is the phase shift of the lower sideband when passing through the multiplexer/demultiplexer circuits with respect to the subcarrier, and

$$m' = 2\,m\cos\frac{\phi_A + \phi_B}{2}$$

$$e_f \simeq \left[J_0(m') - J_1(m')\cos\left(\omega t - \frac{\phi_A - \phi_B}{2} - y\right)\right]\sin^2\omega_c t + \left[J_1(m')\sin\left(\omega t - \frac{\phi_A - \phi_B}{2} - y\right)\right]\cos^2\omega_c t \tag{97}$$

(98)

where:

$$P_2 = J_0(m') - J_1(m')\cos\left(\omega t - \frac{\phi_A - \phi_B}{2} - y\right) \tag{99}$$

$$Q_2 = J_1(m')\sin\left(\omega t - \frac{\phi_A - \phi_B}{2} - y\right) \tag{100}$$

(101)

g. Limiter Output

Applying equation (90) to equation (101):

$$e_g = \cos\left(2\,\omega_c t + \tan^{-1}\frac{Q_2}{P_2}\right) - \frac{1}{3}\cos 3\left(2\,\omega_c t + \tan^{-1}\frac{Q_2}{P_2}\right) + \ldots \tag{102}$$

The low pass filter will eliminate the second and higher terms in equation (102).

h. Discriminator Output

$$v_p = \frac{D}{2\pi} \frac{\partial}{\partial t} \left(\tan^{-1} \frac{Q_2}{P_2} \right) \tag{103}$$

where $D/2\pi$ is the discriminator constant.

$$v_p = \frac{D}{2\pi} \frac{P_2 \frac{\partial Q_2}{\partial t} - Q_2 \frac{\partial P_2}{\partial t}}{P_2^2 + Q_2^2} \tag{104}$$

where:

$$P_2 = J_0(m') - J_1(m') \cos\left(\omega t - \frac{\phi_A - \phi_B}{2} - y\right) \tag{105}$$

$$\frac{\partial P_2}{\partial t} = \omega J_1(m') \sin\left(\omega t - \frac{\phi_A - \phi_B}{2} - y\right) \tag{106}$$

$$Q_2 = J_1(m') \sin\left(\omega t - \frac{\phi_A - \phi_B}{2} - y\right) \tag{107}$$

$$\frac{\partial Q_2}{\partial t} = \omega J_1(m') \cos\left(\omega t - \frac{\phi_A - \phi_B}{2} - y\right) \tag{108}$$

Substituting equations (105), (106), (107), and (108) into equation (104):

$$v_p = \left\{ \frac{-D\omega J_1(m')}{2\pi \left[J_0(m') + J_1^2(m') - 2 J_0(m') J_1(m') \cos\left(\omega t - \frac{\phi_A - \phi_B}{2} - y\right) \right]} \right\} \cdot \left\{ J_0(m') \cos\left(\omega t - \frac{\phi_A - \phi_B}{2} - y\right) + J_1(m') \left[\sin^2\left(\omega t - \frac{\phi_A - \phi_B}{2}\right) y - \cos^2\left(\omega t - \frac{\phi_A - \phi_B}{2} - y\right) \right] \right\} \tag{109}$$

j. Output Signal

The low pass filters, cutting off at $\omega/2\pi$, eliminates all Fourier terms above the fundamental, i.e., $\cos(\omega t\ \phi_A - \phi_B/2)$ in equation (109).

$$v_0 = \frac{A_0}{2} + A_1 \cos\left(\omega t - \frac{\phi_A - \phi_B}{2} - y\right) \tag{110}$$

where

$$A_0 = \frac{\omega}{\pi}\int_{-\frac{\pi}{\omega}}^{\frac{\pi}{\omega}} v_0\, dt \tag{111}$$

$$A_1 = \frac{\omega}{\pi}\int_{-\frac{\pi}{\omega}}^{\frac{\pi}{\omega}} v_0 \cos \omega t\, dt \tag{112}$$

It is seen from equations (110), (111), and (112) that the output signal is a translated sinewave. The video signal delay is given by the rate of change of phase angle in equation (110) with respect to ω, then the

$$\text{video signal delay} = \frac{\Delta\left[\frac{\phi_A - \phi_B}{2} + y\right]}{\Delta\omega} \tag{113}$$

$$= \frac{1}{2}\left(\frac{\Delta\phi_A}{\Delta\omega} - \frac{\Delta\phi_B}{\Delta\omega}\right) + \frac{\Delta y}{\Delta\omega} \tag{114}$$

If $\delta\phi_A/\Delta\omega$ and $\delta\phi_B/\Delta\omega$ are defined as the deviations from the slope of the best straight line approximation to the phase transfer characteristic of the tape recorder at $\omega_c + \omega$ and $\omega_c - \omega$ respectively, and similarly $\delta y/\Delta\omega$ is defined as the deviation from the slope of the best straight line approximation to the phase transfer characteristics of the multiplexer and demultiplexer circuits, then the nonlinear signal delays is given by:

$$\text{nonlinear video signal delay} = \frac{1}{2}\left(\frac{\delta\phi_A}{\Delta\omega} - \frac{\delta\phi_B}{\Delta\omega}\right) + \frac{\delta y}{\Delta\omega} \tag{115}$$

At the output of the demodulator, the highest modulating frequency is 51.2 kHz One period at this frequency corresponds to 2 TV elements, then $\frac{1}{2}$ TV element is $\frac{1}{4}$ $(1/51.2 \times 10^3) = 4.9$ microseconds.

The Nimbus A multiplexer and demultiplexer circuits equalize the signal to within ±5 microseconds. Therefore, the tape recorder should not be permitted to degrade this value by any significant amount.

Equation (31) shows that the phase changes of the lower sideband, while passing through the mux/demux, are reflected one-to-one in the baseband signal and the algebraic average of the phase changes of the upper and lower sidebands are reflected into the baseband signal.

2. Sync Jitter Calculation in the ID Channel

The line-to-line sync pulse jitter effect is equal to the sum of the channel input sync jitter (as seen at the output) plus the noise effect on the sync pulse rise time. The input sync jitter and rise time specifications for HDRSS is ±25 microseconds and 200 microseconds respectively. The specified SNR at the video demodulator output is 30 db black-to-white/rms measured in a 0 to 51.2 kHz bandwidth. Thus, the sync pulse jitter effect is

$$\pm\frac{1}{32}\times \text{input sync jitter} + 2.8 + \text{net sync pulse rise time/SNR}$$

$$= \pm\frac{1}{32}\times \text{input sync jitter} + 2.8 + \left[(\text{channel rise time})^2 + \left(\frac{1}{32}\times \text{input sync rise time}\right)^2\right]^{\frac{1}{2}}/\text{SNR}$$

$$= \pm\frac{1}{32}\times 25\times 10^{-6} + 2.8 + \left[\left(\frac{0.5}{51.2\times 10^3}\right)^2 + \left(\frac{1}{32}\times 200\times 10^{-6}\right)^2\right]^{\frac{1}{2}}/31.5$$

$$= \pm 2.0 \text{ microseconds or approximately } \pm 0.2 \text{ TV elements}$$

where 2.8 is the ratio of black-to-white and black-to-sync scales.

3. Overall TV Element Displacement

If the tape recorder and video modulator were each differential-phase delay equalized to within ±2.5 microseconds, then the overall channel TV element displacement would be as shown in Table II-10.

TABLE II-10. SUMMARY OF TV ELEMENT DISPLACEMENT

Parameter	Displacement* (TV Elements)
F&W Demodulator Nonlinearity	±0.07
F&W Phase Effect	±0.24
F&W Noise Effect	±0.11
Tape Recorder Video Differential Phase Delay	±0.25
Video Demodulator Differential Phase Delay	±0.25
Multiplexer/Demultiplexer Differential Phase Delay	±0.2
Sync Pulse Jitter Effect	±0.2
TV Element Displacement (Total)	±0.53

* The optimistic case assumes a ±2 μsec equalization in the multiplexer/demultiplexer and a ±2.5 μsec equalization for each the tape recorder and video demodulator. Actual conditions in the multiplexer/demultiplexer may reach ±5 μsec equalization and the tape recorder and demodulator delays may exceed ±2.5 μsec.

G. ID CHANNEL SYNC RELIABILITY ANALYSIS

The composite noise at the ID channel output is not flat but the amplitude characteristics is assumed to be approximately Gaussian because of the large numbers of independent noise sources that make up the composite noise. A list of ID channel components and the percent black-to-white scale of linearity and drift are shown in Table II-11.

The margin for noise peaks is calculated as follows:

Parameter	Percent Black-to-White Scale
Sync Height	36.0 (specified)
Linearity and drift (-2 × 10.2)	-20.4 (from Table II-11)
Undershoot (10 percent of 36.0)	- 3.6 (specified)
Sync Gate (tolerance)	- 2.0 (estimate)
Total Peak-to-Peak Noise Allowance	10.00

TABLE II-11. ID CHANNEL LINEARITY AND DRIFT VALUES

Channel Component	Percent Black-to-White Scale
Input Signal	$\pm \frac{0.14100}{4.2} = \pm 2.5$
Modulator	$\pm (1.7 + 2.2) = \pm 3.9$
Spacecraft Tape Recorder	$\pm (0 + 1.3) = \pm 1.3$
Multiplexer/Demultiplexer	$\pm (0 + 0.5) = \pm 0.5$
Demodulator	$\pm (1.0 + 1.0) = \pm 2.0$
Total	± 10.2

The most probable regions of interference with sync are shown in Figure II-6.

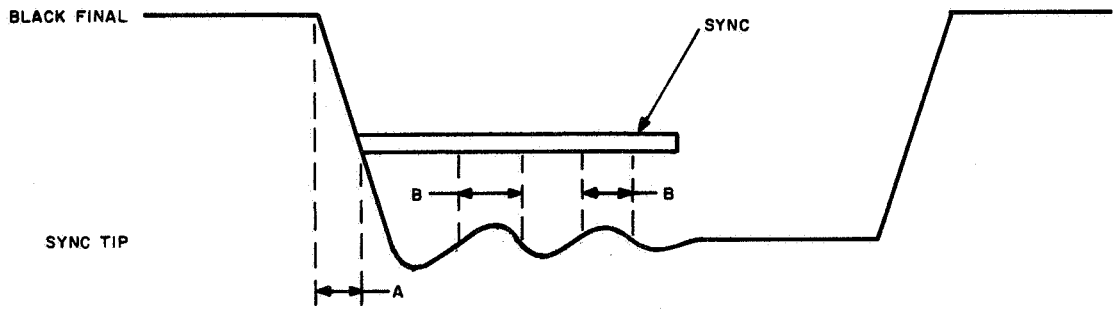

Figure II-6. Probable Regions of Sync Interference

Fraction of Line Period = (A + 2B) × 128 (lines per second) where:

$$A = 2B = \frac{1}{BW} = \frac{1}{60 \times 103} = 16.7 \times 10^{-6} \text{ sec.}$$

Fraction of line period $= (33.4 \times 10^{-6}) \times 128 = 4.28 \times 10^{-3}$.

The channel output noise is 3.5 percent (29.2 db) of black-to-white scale.

The peak noise allowance to rms noise is $\underline{N} = \frac{\frac{1}{2}(10.0)}{3.5} = 1.4$.

Since one-sided peaks are of interest here, this ratio can be doubled to 2.8. The fraction of the time exceeding 2.8 is 0.0052 as given in Burlington Tables. The fraction of lines with sync interference is then calculated by the product of the fraction of lines period times 0.0026

$$= 4.28 \times 10^{-3} \times 0.0052$$

$$= 2.2 \times 10^{-5}$$

Since there are 800 lines per picture, the fraction of pictures with sync interference is $2.2 \times 10^{-5} \times 800 = 1.8 \times 10^{-2}$. This is approximately one sync interference per 100 pictures.

The following conclusions result from the analysis:

- The video signal is delayed by an amount equal to the average delay time of the upper and lower sidebands with respect to the subcarrier in the tape recorder.
- The video signal is delayed by an amount equal to the delay of the lower sideband with respect to the subcarrier in multiplexer and demultiplexer.
- It has been extablished, during a HDRSS system design review, that the maximum displacement of an element on one line to an adjacent element on the next line of one TV element after flutter and wow correction is acceptable. Based on Nimbus A practice, the definition of the measurement of TV element displacement is: for a simulated vertical line (at the modulator input) or imaged vertical line (at the camera input) of unspecified but constant intensity and unspecified but constant width, having an unspecified but constant rise time (the transition from the surrounding field to the line itself) at the input to the system, the expected maximum displacement at the output of the system for corresponding elements on adjacent horizontal scan lines shall be equal to or less than $\pm\frac{1}{2}$ TV element displacement from the best line which describes the display information. Measurements of the residual TV element displacement on 70-mm kinescope pictures were made using Nimbus A flight and ground station equipment in accordance with the above technique were within $\pm\frac{1}{2}$ TV elements. These measurements were made without simulating the effect of link noise on TV element displacement. In addition, the intra-channel differential phase delay effects on elemental displacement could not be observed in the pictures because corresponding elements on adjacent lines had the same differential delay and, therefore, no relative displacement (for the defined measurement signal).

The Nimbus A multiplexer/demultiplexer AVCS channels are equalized to within ±5 microseconds differential phase delay, which is approximately equal to $\pm\frac{1}{2}$ TV element period. Differential phase delay measurements made on two AVCS channels of a Nimbus A multiplexer/demultiplexer (see Figure II-7) were within ±2 microseconds for 89 percent of the channel bandwidth. At upper and lower channel frequency extremes, the differential phase delay increases respectively to plus and minus 5 microseconds.

- An analysis of TV element displacement* including an estimated flutter spectrum showed a maximum picture elemental displacement of + 0.27 TV elements. This analysis included the effect of F&W and the video channels, and the F&W channel noise effect but did not include the video intra-channel differential phase delay and the line-to-line sync pulse jitter. Furthermore, if the arithmetic sum were used (for the three effects considered in the cited study) instead of the rms sum, the displacement would be ±0.42 TV elements.

---

* Radio Corporation of America, Astro-Electronics Division, Final Report for APT Camera/Tape Recorder Study, Contract NAS5-3772, March 4, 1964 to July 10, 1964, p 84.

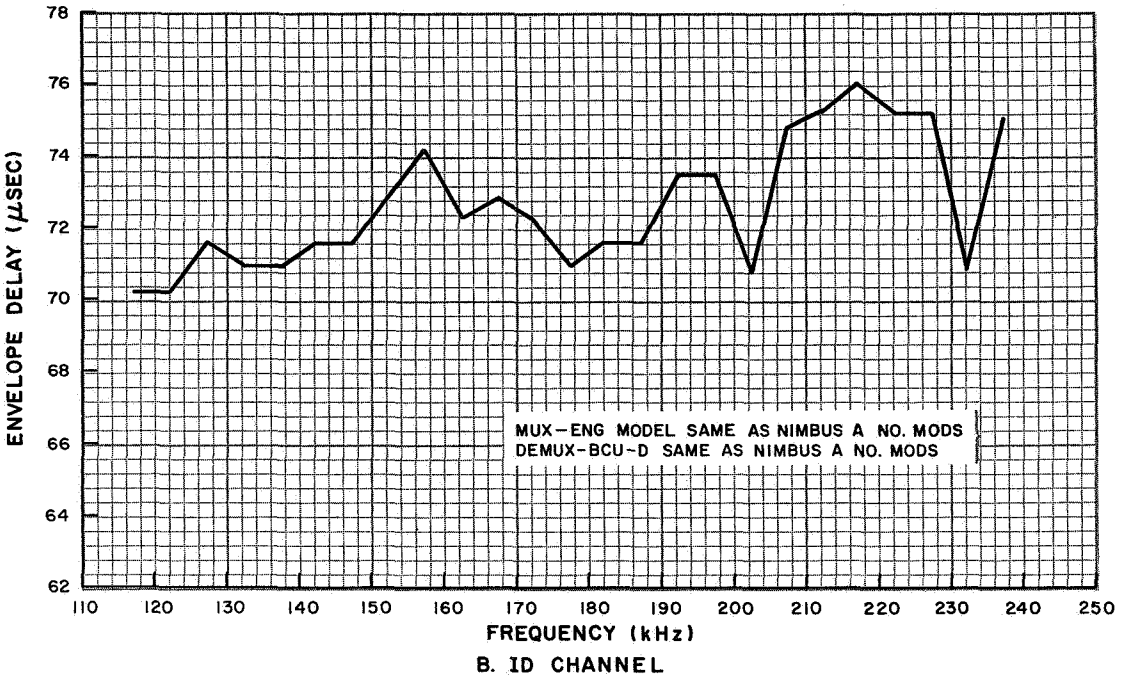

Figure II-7. Envelope Delay Versus Frequency

APPENDIX III
ANALYSIS OF IRIS CHANNEL DATA

A. INTRODUCTION AND SUMMARY

1. Introduction

Analysis of the biphase channel performance characteristics was performed using the parameters of the IRIS channel. Analyses of the following characteristics are presented in this appendix:

- Biphase channel input signal-to-noise ratio
- Intersymbol interference
- Timing error and biphase repeater/signal conditioner bandwidth
- Bit-error-rate as a function of tape dropouts.

2. Summary

The IRIS channel performance degradations, as predicted by the analysis presented in subsequent paragraphs of this appendix, are summarized in Table III-1. These degradations are added to the theoretical signal-to-noise ratio (SNR) required for a bit-error-rate (BER) of 1×10^{-5}; the result is a SNR that the RF link must provide to support a BER of 1×10^{-5}. The basis for each value is presented in the reference cited.

TABLE III-1. SUMMARY OF IRIS CHANNEL SNR REQUIREMENT

Parameter	Loss (db)	Reference
Multiplexer/Demultiplexer Amplitude Response	- 2.0	Contract Specifications
Tape Recorder Limiter Output SNR	0.0	Para. A2a
Multiplexer/Demultiplexer Intersymbol Interference	-10.0	Para. A2b
Interface Signal Variations	- 3.2	Para. A2c
SUB TOTAL	-15.2	
Timing Error Loss	- 1.2	Para. A2d
TOTAL LOSS	-16.4	
Signal Conditioner SNR Requirement	-14.8*	Para. B
RF Link Power Requirement =	31.2*	

*Defined as peak/rms

a. Tape Recorder Limiter Output SNR

The tape recorder output SNR is specified at 46 db $\frac{p\text{-}p}{rms}$ minimum in the limiter bandwidths. This SNR corresponds to 37 db rms/rms. It is measured in the limiter bandwidth which is an order of magnitude larger than the overall channel bandwidth, and the noise appears on the "flats" of the limiter signal.

The tape recorder SNR of 37 db rms/rms will produce no appreciable degradation of the r-f link SNR.

b. Intersymbol Interference

Intersymbol interference was obtained by computer simulations of the IRIS channel. The simulation yielded a distorted demultiplexer output wave form for a given "square pulse" binary word into the multiplexer. The processing action of the signal conditioner was also considered. The analysis and system design was based on a sampling type signal conditioner (the Dynatronics signal conditioner selected was a reset-integration type). The loss due to intersymbol interference for the sampling type signal conditioner was calculated at 10 db. Refer to Paragraph C.

c. Interface Signal Variations

Interface signal variations are due to the tolerances on the impedance values, voltage levels, and transmitter deviation sensitivity. The tolerances specified include long-term variations. An equivalent circuit is shown on Figure III-1, and a variation of ±10 percent on the deviation sensitivity of the FM transmitter is assumed. The multiplexer gain is adjusted to obtain a 3.36 ±0.34 volt p-p open circuit voltage when the input voltage of 6.5 ±0.01 volts p-p is applied to the input through a resistor of 10000 ±10 ohms.

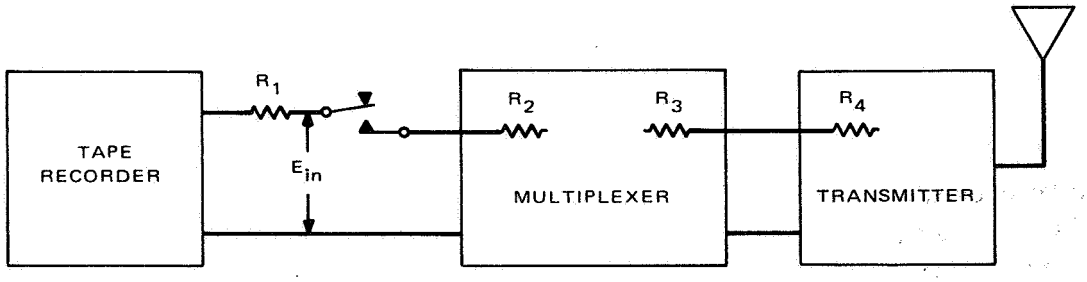

E_{in} = 6.5 ± 0.65 VPP
R_1 = 1000 ± 50 Ω
R_2 = 1000 ± 100 Ω (± 5%)
R_3 600 ± 6Ω
R_4 600 ± 6Ω
Trans Deviation = ± 10% (assumed)

Figure III-1. Block Diagram for Signal Variation Calculation

The nominal signal loss from the open circuit tape recorder to transmitter deviation is 0.250 K (voltage ratio), where K = the nominal multiplexer gain. The worst case loss:

$$L = \begin{pmatrix}\text{Tape Recorder}\\ \text{Voltage Level}\end{pmatrix} \times \begin{pmatrix}\text{Tape Recorder/}\\ \text{Multiplexer}\\ \text{Interface Ratio}\end{pmatrix} \times \begin{pmatrix}\text{Multiplexer/}\\ \text{Transmitter}\\ \text{Interface Ratio}\end{pmatrix} \times \begin{pmatrix}\text{Multiplexer}\\ \text{Gain}\end{pmatrix} \times \begin{pmatrix}\text{Transmitter}\\ \text{Sensitivity}\end{pmatrix}$$

$$= 0.90 \times \frac{950}{2000} \times \frac{540}{1080} \times 0.90\,K \times 0.90 = 0.173$$

The relative loss is $\frac{0.250}{0.173} = 3.2$ db.

d. Timing Errors

The specified peak-timing errors for the parameters listed in Table III-2 are first converted to rms by dividing by a crest factor of 4, a value commonly used for such conversions. The total rms timing error (σ, is then calculated and used to determine the timing error loss:

$$L = \cos 2\pi\sigma$$

In the interest of being on the conservative side, the timing error loss (L) is calculated for a value of 3σ. Thus,

$$L = \cos 2\pi(3\sigma)$$

The tape recorder contributes most of the timing errors. The tape recorder cumulative timing error of 1.3 percent rms is the contribution due to flutter components which are not tracked by the signal conditioner phase-lock loop for a bandwidth setting of 2.8 percent of bit rate ($\approx$3600 Hz). The bandwidth setting is the frequency at which the Dynatronics signal conditioner has an open-loop gain of 0 db, and corresponds loosely to the maximum frequency the loop will track. The "cumulative flutter jitter" specification of the tape recorder is 0.1 microseconds rms or 1.3 percent of 1 bit for components in the band of 3.0 kHz to 60 kHz (those not tracked by the loop). The tape recorder pre-limiter SNR of 26 db p-p/rms produces an rms jitter of 1.6 percent at the limiter output. Jitter is related to the rms/rms SNR by

$$\frac{\Delta T}{T} = \frac{1}{2\pi}\sqrt{\frac{N}{2S}}$$

TABLE III-2. IRIS CHANNEL TIMING ERRORS

Parameter	Timing Error			Remarks
	% Peak*	% rms	Ref.	
Static Asymmetry				
Tape Recorder and Input Source	±1.5	0.375	See Note 1	
Multiplexer/Demultiplexer	±1.0	0.250		
rms sum		0.450		
Bit-to-Bit Jitter (due to clock jitter and pattern shift)				
Input Source	±0.5	0.125	See Note 2	
Tape Recorder	±6.0	1.5	See Note 1	
Multiplexer/Demultiplexer	---	---		Included in inter-symbol interference Paragraph III-C
rms sum		≈1.5		
Cumulative Timing Error (due to tape recorder flutter into Dynatronics Signal Conditioner at 2.8 percent bandwidth setting)		1.3		Refer to text
Timing Jitter (due to pre-limiter SNR of 26 db-p-p/rms)		1.6	See Note 2	
Static Phase Shift (Dynatronics Signal Conditioner at 2.8 percent Bandwidth Setting)		0.8		Refer to text
TOTAL RMS SUM (σ)		2.7		
3σ VALUE		8.1		
SIGNAL LOSS DUE TO TIMING ERROR			See Note 3	1.2 db

*Divided by a crest factor of 4 = % rms

Note 1. HDRSS Tape Recorder Specification, PS-1849826

Note 2. Contract NAS5-3772 Contract Specification (as amended)

Note 3. The equivalent loss due to timing error is defined as $L = \cos\theta$. This expression is plotted in db versus θ (percent of bit period) in Figure III-2.

The static phase shift error due to frequency drifts is given by the formula

$$\frac{\Delta T}{T} = \left(\frac{1}{2\pi}\right) \frac{\Delta f}{\frac{G}{2\pi}} = \frac{\Delta f}{G}$$

Where Δf = the total frequency shifts = ±0.54 percent (data drift = 0.02 percent, VCO drift-assumed = ±0.02 percent, and tape recorder drift = ±0.5 percent; and G = the dc loop gain of the Signal Conditioner second order tracking loop.

For 2.8 percent bandwidth, the dc loop gain $G = 2\pi \times 1.41 \times 10^4$ based on open-loop characteristics of the Dynatronics signal conditioner.

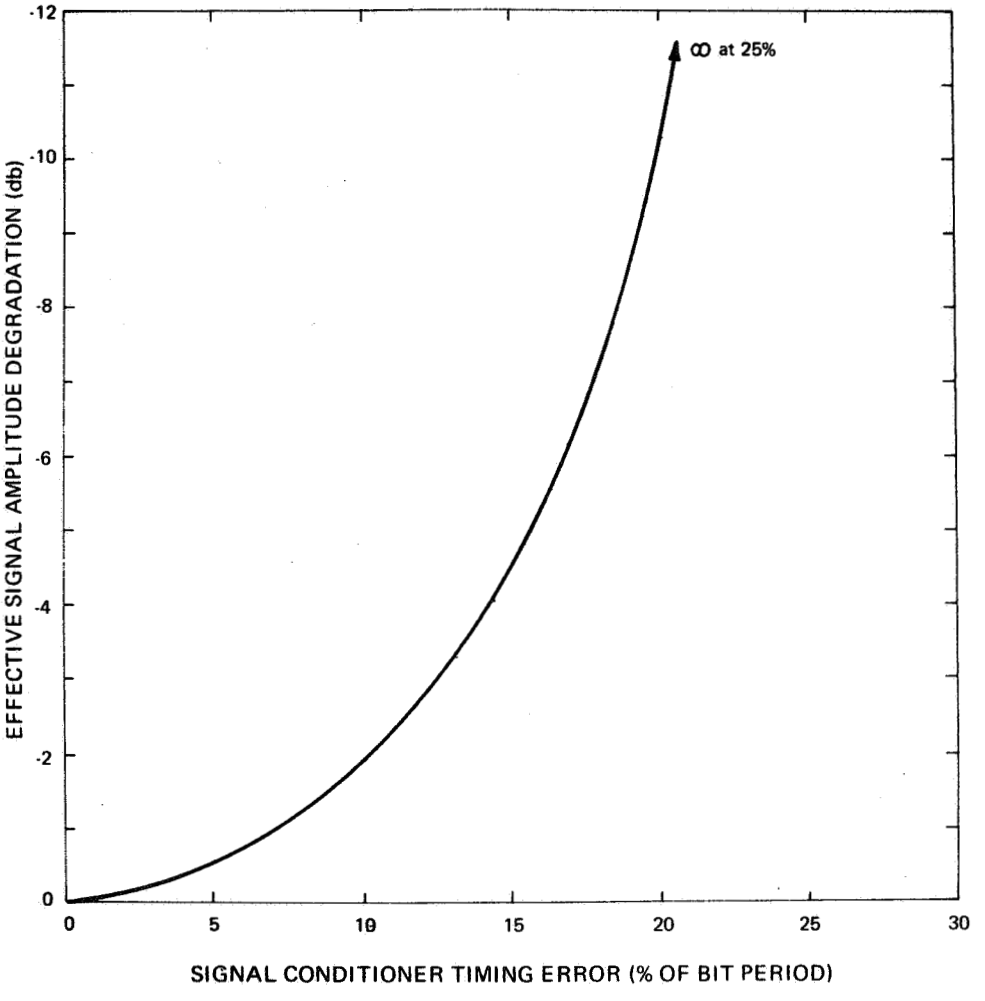

Figure III-2. IRIS Channel Timing Error Losses

B. ANALYSIS OF BIPHASE CHANNEL INPUT SNR

1. General

The input signal-to-noise-ratio (SNR) requirement is calculated for the IRIS channel where the noise density is parabolic low-pass, i.e., the frequency components extend from d-c to a cut-off frequency f_c. The SNR calculations are made for the special situation where a periodic sequence of square pulse binary "ones" are transmitted: 1111... . This represents the optimum situation for the signal conditioner - any word composed of "ones" and "zeros" will suffer from intersymbol interference which produces SNR degradation. The analysis of intersymbol interference and the results of computer simulations are discussed in Paragraph C. Paragraph B deals with the zero intersymbol interference situation. The derivations yield the relationship between the input and peak signal-to-noise-ratios of the reset integrator at the decision time T. The calculated SNR is verified against experimental results for the low-pass noise spectrum case.

2. Biphase Coding Format

The biphase coding format considered herein is defined as shown on Figure III-3. The biphase format is the product-modulation of non-return to zero (NRZ) data onto a square wave subcarrier at twice the NRZ bit rate frequency. A binary "0" is obtained from a binary "1" by 180° phase reversal the square wave carrier. The biphase format has a zero crossing in the middle of each bit. There is a strong clock frequency component which is easily extracted by a phase lock loop (PLL).

3. Analysis of System Characteristics

The system considered in this analysis is illustrated in the Figure III-4. The system is idealized in the sense that the only degrading factor taken into consideration is the link-additive noise; the transmitter uses frequency modulation. Filters F_{11} and F_{12} strongly attenuate all signal components above 1.1 × the bit rate (1.1b).

4. Signal Conditioner for Biphase Data

The signal conditioner (Dynatronics Model BSC-7B) operates on the biphase data, as shown on Figure III-5. The signal into the conditioner is the useful signal plus additive channel noise. The useful signal wave form is a quasi-sinusoid wave form resulting from the effect of channel bandwidth limitation on the square input wave form.

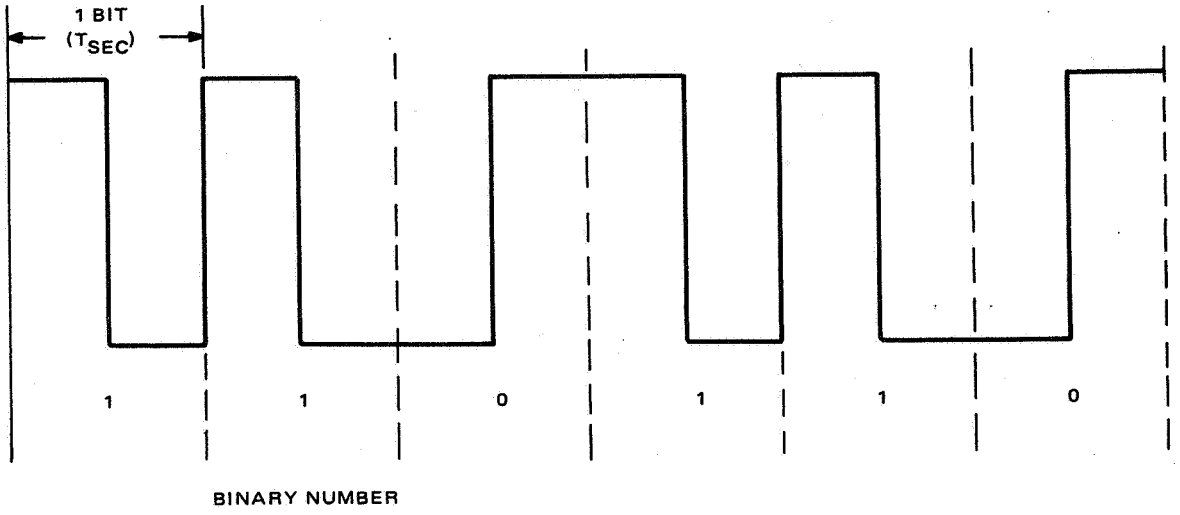

Figure III-3. Definitive Biphase Format

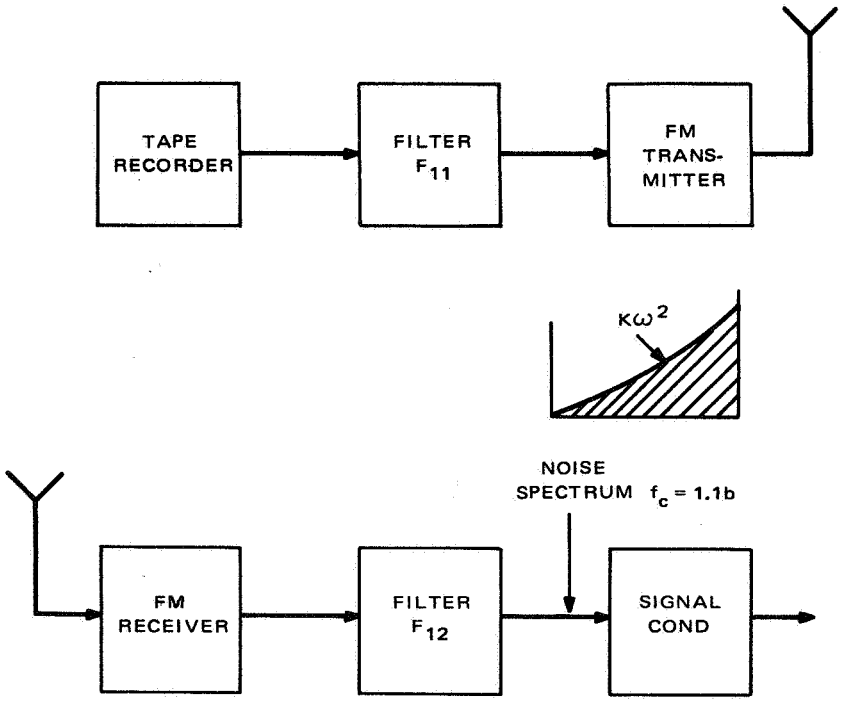

Figure III-4. IRIS Channel, Simplified Block Diagram

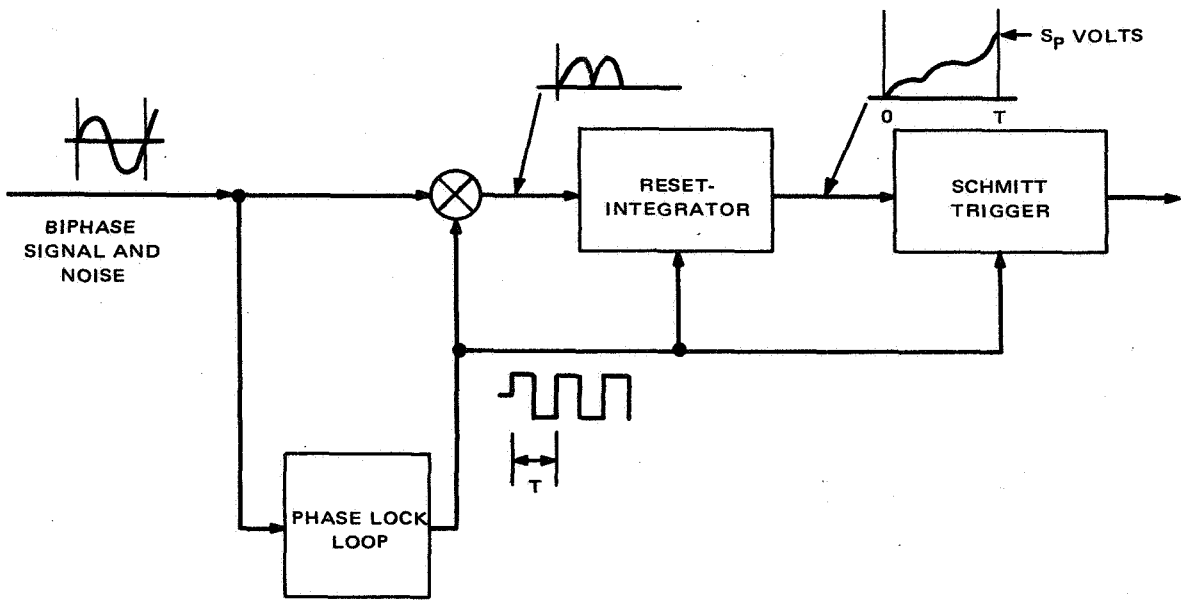

Figure III-5. Signal Conditioner, Block Diagram

a. Signal Level at Reset Integrator Output

The start of the integrator period is determined by the clock. For the periodic sequence of binary "ones" assumed in this analysis, the signal into the decoder is a sine wave $f(t) = A \sin \omega_b t$. There is no timing error between the data and the clock.

At time $t = T$ the voltage level S_p at the reset integrator output is:

$$S_p = 2\int_0^{\frac{T}{2}} \left(A \sin \omega_b t\right) dt = \frac{4A}{\omega_b}$$

This voltage operates a Schmitt trigger whose output is a binary "one" if S_p is positive or a binary "zero" if S_p is negative. The operation of the Schmitt trigger is inhibited until the decision time t = T determined by the clock.

b. Calculation of the Variance of the Signal Level at the Reset Integrator Output

Due to presence of noise, the integrator voltage at time T is a random variable whose mean is $S_p = \frac{4A}{\omega_b}$. The variance of the random variable has to be calculated. If the variance is denoted by N_0, then the probability of error is given by:

$$P_e = \frac{1}{2} E_{RFC} \left(\frac{S_p^2}{2N_0} \right)$$

Where E_{RFC} is the complementary error function.

This expression assumes that the noise is Gaussian distributed. Note that $\frac{S_p^2}{2N_0}$ could be called the average signal-to-noise-power-ratio at the reset integrator output at time t = T; however this SNR cannot be measured directly by the ususal method with a true rms meter.

At time $t = T^+$ the integrator is reset to zero (capacitor discharged) and the integration over the next bit starts.

The stationary noise process into the signal conditioner, is denoted by $\hat{n}(t)$. The output of the integrator at time t = T is $\hat{\gamma} = S_p + \hat{v}$.

Where

$$\hat{v} = \int_0^{\frac{T}{2}} \hat{n}(t)\, dt + \int_{\frac{T}{2}}^{T} \left[-\hat{n}(t) \right] dt$$

The mean value $\hat{v}_0$ is $E(\hat{v}_0) = 0$.

The variance of $\hat{v}_0$ is:

$$E(\hat{v}_0^2) = E\left[(v_1 + v_2)^2\right]$$

Where

$$E(\quad) = \text{expected value of } (\quad)$$

and

$$\hat{v}_1 = \int_0^{\frac{T}{2}} \hat{n}(t)\, dt$$

$$\hat{v}_2 = \int_{\frac{T}{2}}^{T} -\hat{n}(t)\, dt$$

Therefore

$$E(\hat{v}_0^2) = N_0 = 2\sigma^2 (1 + p)$$

Where

$$p = \frac{(E\ v_1 v_2)}{\sigma_1 \sigma_2} = \text{correlation function of}$$

$\hat{v}_1$ and $\hat{v}_2$.

For worst case calculation, $p = 1$ and $N_0 = 4\sigma^2 = 4\ E\left(\upsilon_1{}^2\right)$.

The reset integrator over a time interval $(0, \gamma)$ has an impulse response $h(t)$ given by:

$$h(t) = 0 \qquad t < 0$$

$$h(t) = 0 \qquad t < \gamma$$

$$h(t) = 1 \qquad 0 \leq t \leq \gamma$$

If the noise applied to the integrator is denoted by $\hat{n}(t)$, and if this noise process is Gaussian and stationary, then the noise level at time $t = \gamma$ is a random variable $(\hat{\upsilon}_0)$ whose variance (N_0) is given by:

$$N_0 = E\left[\hat{\upsilon}_0{}^2\right] = E\left[\int_0^{\gamma} \hat{n}(t)\ dt\right]\left[\int_0^{\gamma} \hat{n}(\alpha)\ d\alpha\right]$$

Where

$E[\ ]$ = expected value of, and the mean of $\hat{\upsilon}_0{}^2$ is assumed zero.

Therefore:

$$N_0 = \int_0^{\gamma}\int_0^{\gamma} E\left[\hat{n}(t)\hat{n}(\alpha)\right]\ dt\ d\alpha$$

$$N_0 = \int_0^{\gamma}\int_0^{\gamma} R_n(t_1\alpha)\ dt\ d\alpha$$

Where

$R_n(t_1\alpha)$ is the auto correlation function of the noise $[\hat{n}(t)]$. Since $\hat{n}(t)$ is stationary, then

$$R_n(t_1\alpha) = R_n(t - \alpha).$$

$$N_0 = \int_0^{\gamma}\int_0^{\gamma} R_n(t-\alpha)\, dt\, d\alpha$$

$$N_0 = \int_0^{\gamma} d\lambda \int_{-\lambda}^{\gamma-\lambda} R_n(\upsilon)\, d\upsilon$$

$$= \int_{-\infty}^{\infty} h(\lambda)\, d\lambda \int_{-\infty}^{\infty} h(\upsilon+\lambda)\, R_n(\upsilon)\, d\upsilon$$

Where

$$t - \alpha = \upsilon \text{ and } t = \lambda$$

If $\psi(\omega)$ (watts/Hz) is the double-sided power spectral density of the input noise $[\hat{n}(t)]$, then by definition:

$$R_n(\upsilon) = \frac{1}{2\pi} \int_{-\infty}^{\infty} \psi_n(\omega)\, e^{j\omega\upsilon}\, d\omega$$

$$N_0 = \frac{1}{2\pi} \iiint h(\lambda)\, h(\upsilon+\lambda)\, \psi_n(\omega)\, e^{j\omega\upsilon}\, d\omega\, d\upsilon\, d\lambda$$

$$N_0 = \frac{1}{2\pi} \iiint h(\lambda)\, h(\Theta)\, \psi_n(\omega)\, e^{j\omega\Theta}\, e^{-j\omega\lambda}\, d\omega\, d\lambda\, d\Theta$$

Where

$$\upsilon + \lambda = \Theta$$

$$N_0 = \frac{1}{2\pi} \int_{-\infty}^{\infty} H(\omega)\, H(-\omega)\, \psi_n(\omega)\, d\omega$$

$$N_0 = \frac{1}{2\pi} \int_{-\infty}^{\infty} |H(\omega)|^2 \psi_n(\omega)\, d\omega$$

The final expression looks quite similar to the expression for noise output of a filter with frequency response $H(\omega)$ and whose input is a stationary process $\hat{n}(\alpha)$ with power density $\psi(\omega)$. However it must be pointed out, that $\hat{N}_0$ is a sample of a non-stationary random process since the integrator is dumped every γ seconds and has to "charge up" from zero at each integration. In this case however, the results are exactly the same as for the stationary case and it is correct to treat the reset-integrator as a filter.

Where $H(\omega)$ is the Fourier transform of the reset integrator impulse response; $\psi_n(\omega)$ is the noise power density (watts/Hz) at the signal conditioner input. Note that for calculations, the hypothetical reset integrator integrates from 0 to T/2. The impulse response of the reset integrator (0 - T/2) is shown in Figure III-6.

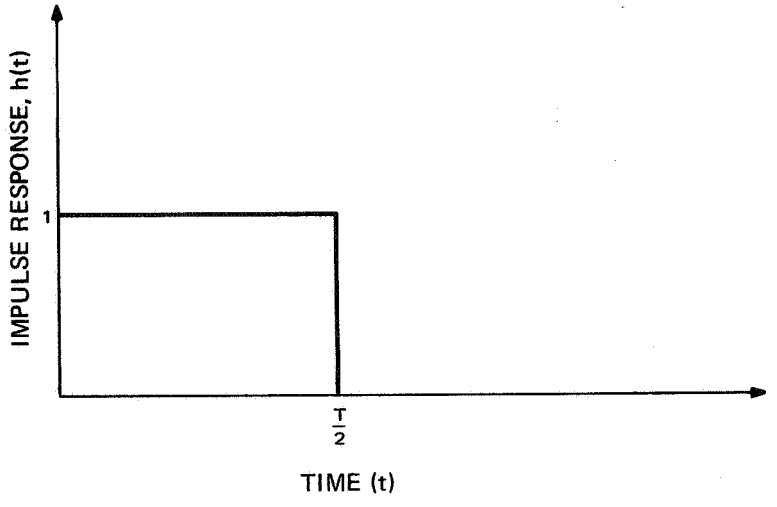

Figure III-6. Impulse Response of Reset Integrator (0, T/2)

For an input f(t), the output g(t) is

$$g(t) = \int_{-\infty}^{\infty} f(\tau)\, h(t-\tau)\, d\tau = \int_{t-\frac{T}{2}}^{t} f(\tau)\, d\tau$$

$$g\left(\frac{T}{2}\right) = \int_{0}^{\frac{T}{2}} f(t)\, dt$$

Then:

$$H(\omega) = \int_{0}^{\frac{T}{2}} e^{-j\omega t}\, dt = \frac{1 - e^{-j\omega \frac{T}{2}}}{j\omega}$$

$$\left| H(\omega) \right|^2 = \left(\frac{2 \sin \omega \frac{T}{4}}{\omega} \right)^2 = \frac{T^2}{4} \frac{\sin^2 \left(\frac{\omega\tau}{4} \right)}{\left(\frac{\omega T}{4} \right)^2}$$

Therefore the variance N_0 is:

$$N_0 = 4E \hat{v}_1^2 = T^2 \int_{-\infty}^{\infty} \frac{\sin^2 \omega \frac{T}{4}}{\left(\frac{\omega T}{4} \right)^2} \psi_n(\omega)\, df$$

Where

$$f = \frac{\omega}{2\pi} .$$

Also note that the units of $\psi_n(\omega)$ are watts/Hz (assuming a 1 ohm load). Also $\psi_n(\omega)$ is double-sided, i.e., it covers both negative and positive frequencies.

The noise density for IRIS extends from vdc to a cut-off frequency fc = 1.1b. The double sided noise density is $\psi_n(N) = \frac{K}{2}\omega^2$ (watts/Hz). Alternatively the single sided density is $\psi(\omega) = K\omega^2$.

Let N_1 be the noise power in bandwidth f_c at the input to the signal conditioner. The input signal is a sine wave of peak amplitude A volts and bit rate frequency.

$$N_1 = \frac{1}{2\pi}\int_0^{\omega_c} K\omega^2 d\omega = \frac{K\omega_c^3}{3}$$

$$N_0 = K \times 8 \times \left(\omega_c - \frac{2}{T}\sin \pi R\right)$$

Where

$$R = \frac{f_c}{f_b} = 1.1$$

It has been shown previously that: $S_p = \frac{4A}{\omega_b} = \frac{2A}{\pi} T.$

Therefore

$$\frac{A^2}{N_1} = \frac{S_p^2}{N_0} \frac{\left(\frac{\pi}{2}\right)^2 24}{\omega_c^2 T}\left(1 - \frac{2}{\omega_c T}\sin \pi R\right)$$

$$\left(\frac{A^2}{N_1}\right) = \left(\frac{S_p^2}{N_0}\right) 1.36$$

or

$$\left(\frac{A^2}{N_1}\right)_{db} = \left(\frac{S_p^2}{N_0}\right)_{db} + 1.34 \text{ db}$$

For a desired probability of error (P_e) of 1×10^{-6},

$$\left(\frac{S_p^2}{N_0}\right)_{db} = 13.5 \text{ db peak/rms.}$$

The required input SNR into the signal conditioner is then:

$$\left(\frac{A^2}{N_1}\right)_{db} = 13.5 + 34 \text{ db} = 14.8 \text{ db peak/rms}$$

5. Experimental Confirmation of Calculations

Bit-error-rate (BER) measurements have been performed on the signal conditioner in the presence of parabolic noise simulating the IRIS channel noise. The results are shown on Figure III-7.

The conditions of the test were the following:

- Parabolic noise.
- The square-pulse biphase signal was pre-filtered by a linear-phase filter with gentle skirt attenuation.
- Signal to noise ratio is measured through a sharp cutoff filter whose bandwidth is 1.0b.

Signal-to-noise-ratio was measured with the pattern 010101... applied to the signal conditioner. This pattern yields a one-half bit rate sine wave through the sharp cutoff filter. A true rms-meter was used for these measurements.

In order to make a comparison with the calculated SNR, it is necessary to:

- Correct the calculated SNR for a bandwidth equal to 1.0b. The calculated SNR is in a bandwidth = 1.1b (connection +1.3 db, with parabolic noise).
- Correct the calculated SNR for the difference in reference signals used. In the calculation a 1111... pattern was used. In the measurement, a 0101... pattern was used (correction is 0 db, since the integral of

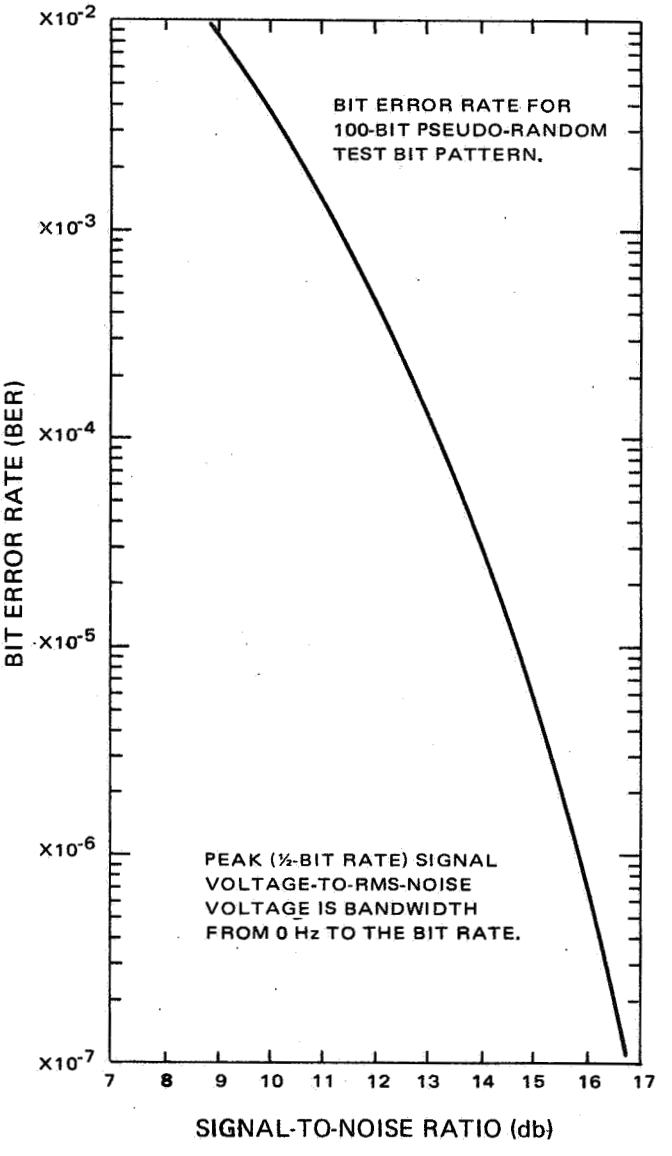

Figure III-7. BER vs. SNR Performance

the $\frac{1}{2}$ bit rate sine wave is equal to the integral of the 1-bit rate sine wave over the bit interval, after inversion of the second half of the bit).

- Correct the measured SNR for any intersymbol interference. The bit error rate measurement was performed with a 100-bit random pattern. The correction for the measured SNR was found to be negligible ($\approx$ 0 db).

An eye pattern test was performed with 100-bit word which indicated a negligible amount of eye closure. The eye pattern was obtained by displaying the input wave form to the signal conditioner on an oscilloscope which was externally triggered by the clock signal.

For a bit error rate of 1×10^{-6} the following results were obtained:

Calculated SNR	=	14.8 db peak/rms in 1.1b.
Bandwidth correction	=	1.3 db
TOTAL		16.1 db peak/rms in 1.0b.
Measured SNR	=	15.8 db in 1.0b.

The calculated and measured SNR requirement agree within 0.3 db.

C. ANALYSIS OF INTERSYMBOL INTERFERENCE

This analysis was performed in order to determine the degradation in signal-to-noise-ratio in the IRIS channel contributed by intersymbol interference. Intersymbol interference is caused by the limited channel bandwidth and by the amount of differential-time-delay distortion (DTD). Intersymbol interference is also sensitive to the shape of the time delay response. The response curve assumed in this analysis is expected to yield worst case results.

1. Criterion of Degradation

The eye pattern aperture which is the criterion used by most workers in the field of digital communications, is used here. This criterion is very useful for a filter and a sample type of signal conditioner.

The eye aperture is the ratio of the smallest sample to the reference sample which is near the peak of the sinusoidal wave form obtained at the input to the signal conditioner when a periodic sequence of 1's is transmitted. The sine wave frequency is the bit rate frequency (120 kHz/sec).

The eye pattern is obtained experimentally by displaying the wave form on an oscilloscope. The sweep frequency is adjusted to display one or two bits and is synchronized with the clock extracted from the incoming data. Due to channel bandwidth limitations the wave form of the received data does not have sharp edges, but is rounded into a quasi-sine wave.

The oscilloscope display then resembles an eye as seen on Figure III-8. The relative eye aperture in db is given by: $20 \log_{10} A_0/A_1$.

2. IRIS PCM Format

The PCM format is the biphase level as shown in Figure III-9.

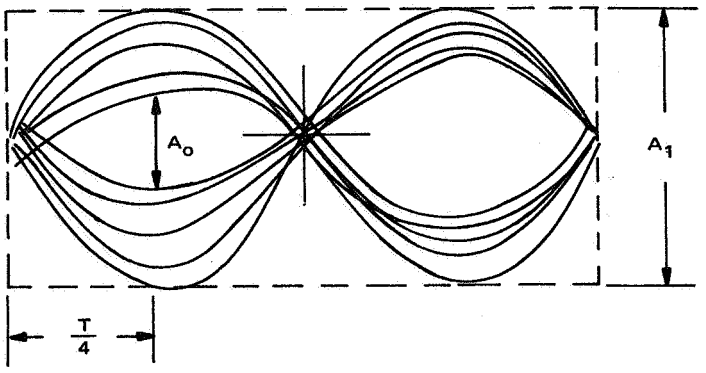

Figure III-8. Eye Pattern (1 bit displayed)

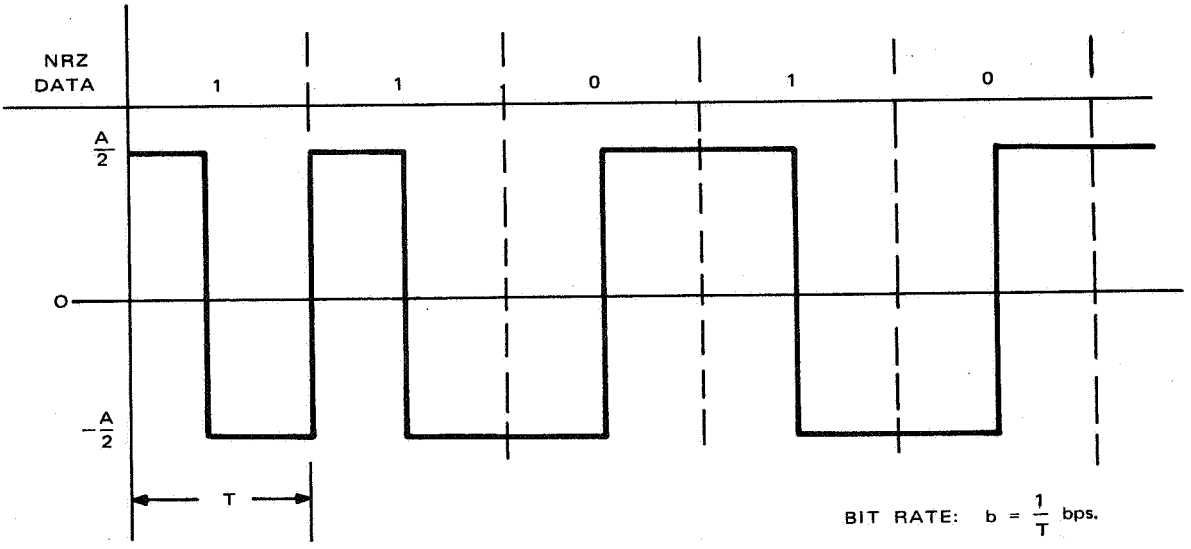

Figure III-9. Biphase Level Format

3. IRIS Channel Characteristics

The portion of the IRIS channel considered is from the input to the multiplexer to the output of the equalizer following the demultiplexer. However, degradations introduced by the FM link are not considered. The characteristics of the channel, shown on Figure III-10, are:

IRIS Data Rate:	120 kb/sec
Bandwidth:	0.1b to 1.1b

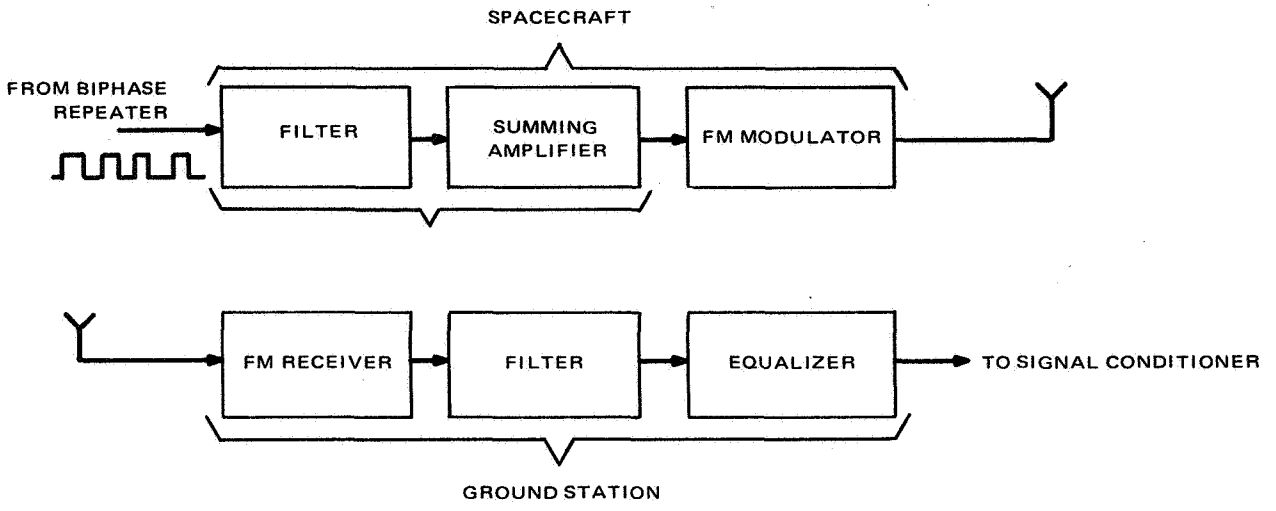

Figure III-10. IRIS Channel, Simplified Block Diagram

IRIS Multiplexer Filter: ±0.5 db from 0.1b to 1.1b
-20 db at 151 kHz (min)
-45 db (min) at 171 kHz and beyond.

4. IRIS Channel Assumptions

a. Amplitude Response

The amplitude response of the channel is assumed to be flat from d-c to 1.1b with sharp cut-off at 1.1b (see Figure III-11).

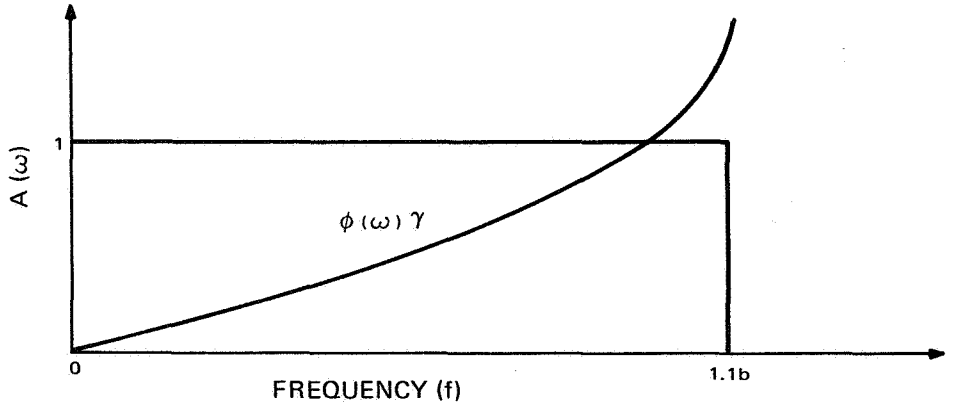

Figure III-11. Assumed Amplitude and Phase Characteristics of IRIS Channel

The justifications for this assumption are:

- Below 0.1b the power spectral density of a biphase level signal is smaller than -14.7 db as referred to the peak value of the spectrum[1].
- The amplitude of the IRIS multiplexer filter is specified to be flat within ±0.5 db up to 1.1b. (This limit has been changed since to 1.0b in the IRIS filter specification with 6 db maximum attenuation at 1.1b. This change is not expected to change the results of the computation substantially.)
- Attenuation at 171 kHz and beyond is specified to be -45 db minimum for the IRIS filter. Assuming that an identical filter exists on the ground equipment, the overall attenuation will be at least -90 db at 171 kHz and beyond. At 151 kHz the multiplexer filter attenuation is specified to be -20 db minimum. This yields an overall -40 db minimum attenuation at 151 kHz. The skirt of the overall response rolls off at about 240 db/octave beyond 132 kHz.

b. Time Delay Response

The group delay $T_g(\omega)$ was taken as having a cosine shape.

$$T_g(\omega) = \frac{\partial \phi}{\partial \omega} = A - K\alpha \cos \alpha\omega \qquad (1)$$

This yields the phase response $\phi(\omega)$:

$$\phi(\omega) = A\omega - K \sin \alpha\omega \qquad (2)$$

and the time delay, $T_d(\omega)$, becomes:

$$T_d(\omega) = \frac{\phi}{\omega} = A - \frac{K}{\omega} \sin \alpha\omega \qquad (3)$$

$T_d(\omega)$ is plotted on Figure III-12.

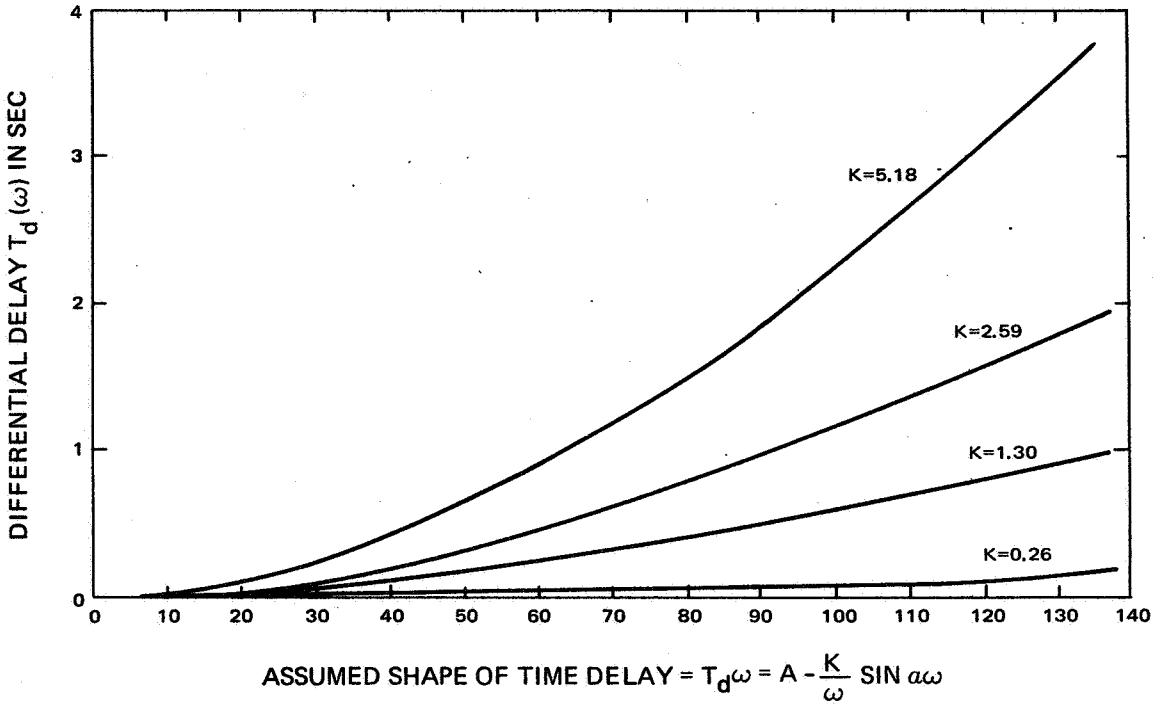

Figure III-12. Time Delay Response, IRIS Channel

The preceding assumption is justified on the following basis:

- Published group delay responses[2] of Chebyscheff filters show a cosine type of variation. The group delay responses of other sharp cut-off filters are expected to have similar shapes due to the relationship between phase and amplitude responses of minimum phase networks.

- Theoretical work[3] has shown that the cosine group delay is close to the worst shape of group delay for a channel with rectangular amplitude characteristics.

- Preliminary tests on an IRIS filter breadboard have yielded a time delay curve similar to Equation (3), but with a somewhat sharper rise at high frequencies.

Another assumption made is that the equalized group delay also has a cosine shape with a quarter cycle between d-c cutoff (f_c), i.e., there are no ripples in the time delay over the passband. The shape considered yields the maximum interference in the vicinity of the pulse[3].

c. Input Wave Form

The input bit stream is assumed to be a stream of pulses with perfectly sharp edges. The actual pulses have a 1.0 microsecond rise time. The assumed pulses will produce an output rise time slightly faster than in actuality. The ripples are not expected to be much different due to the narrowness of the filter bandwidth.

5. Paired Echo Analysis

The method of analysis was as follows:

- The response of the perfectly equalized filter was calculated for an input pulse of width T/2 and peak amplitude A, where T is the bit duration.

- The response of the channel with a given amount of time delay distortion was then calculated using the paired echo analysis[4-5]. The time delay curves are shown on Figure III-12.

- The response of the system to the binary sequence was then calculated. This was done by replacing each square pulse by the distorted wave form and adding the contributions of each distorted pulse at different values of time. The simulation was first performed with binary word A for 4 values of differential time delay.

$$\text{Word A} = 111111111100011011000101 0 \quad \ldots \quad (4)$$

After analysis of results obtained with word A, word B is as follows:

$$\text{Word B} = 111111110111111110000000 \quad \ldots \quad (5)$$

The series of 1's, at the beginning of each word, were selected to yield a sinusoidal steady-state output. Their frequency is equal to the bit rate. This steady-state output was used as time and amplitude reference for the determination of the location and level of the subsequent samples. In other words, the clock was assumed synchronized to this sinusoid. This is equivalent to assuming that the time constant of the clock extraction circuit was greater than the duration of the 25-bit word. This corresponds to a loop bandwidth of 5 kHz.

Words A, and B are the types of words that are considered worst for the biphase level signal.[6,7]

Samples were taken in each bit-cell at 1/4 T and 3/4 T, where T is the bit duration. The degradation of each sample is calculated using the peak sinusoidal level as reference. The results are discussed later in this Appendix. Word B yielded worse degradations than word A; the worst degradation occurred in the 0 imbedded in the series of 1's.

The impulse response h(t) of the idealized (perfectly equalized) channel was calculated as follows:

$$h(t) = \frac{1}{2\pi}\int_{-\omega c}^{\omega_c} e^{j\omega t}\, d\omega = \frac{1}{\pi}\,\frac{\sin \omega_c t}{t} \tag{6}$$

The response to a single square pulse of amplitude A and width $\frac{T}{2}$ was obtained by calculating the convolution integral.

$$g_1(t) = \int_{-\infty}^{\infty} f(t=\tau)\, h(\tau)\, d\tau \tag{7}$$

$$\left.\begin{aligned} f(\tau) &= 0 \text{ for } \tau < -\frac{T}{4} \text{ and } \tau > \frac{T}{4} \\ f(\tau) &= A \text{ for } -\frac{T}{4} < \tau < \frac{T}{4} \end{aligned}\right\} \tag{8}$$

The undistorted response was then

$$g_1(t) = \frac{A}{\pi}\int_{t-\frac{T}{4}}^{t+\frac{T}{4}} \frac{\sin \omega_c\tau}{\omega_c\tau}\, d(\omega_c\tau) \tag{9}$$

$$g_1(t) = \frac{A}{\pi}\left\{ \sin\left[\omega_c\left(t + \frac{T}{4}\right)\right] - \sin\left[\omega_c\left(t - \frac{T}{4}\right)\right]\right\} \qquad (10)$$

where

$$S_i(x) = \int_0^x \frac{\sin y}{y}\, dy = \text{sine integral of } x$$

The distorted pulse $g_{d_1}(t)$ is obtained as follows:

Let $G_1(\omega)$ be the Fourier transform of the undistorted pulse. The Fourier transform $G_{d_1}(\omega)$ of the distorted pulse is:

$$G_{d_1}(\omega) = G_1(\omega)\, e^{-j\Delta\phi(\omega)}$$

where

$$\Delta\phi(\omega) = -K \sin \alpha\omega$$

$\Delta\phi(\omega)$ = is the phase distortion.

The function $e^{jK \sin \alpha\omega}$ is expanded into a Fourier series over the range $= -\omega_c < \omega < \omega_c$. This is permissible because there are no signal components outside that range.

$$e^{jK \sin \alpha\omega} = J_0(k) + J_1(k)\, e^{j\alpha\omega} - J_1(k)\, e^{-j\alpha\omega}$$

$$+ J_2(k)\, e^{j2\alpha\omega} + J_2(k)\, e^{-j\alpha\omega} \ldots$$

$$G_{d_1} = G_1(\omega)\left[j_0(k) + J_1(k)\, e^{j\alpha\omega} - j_1(k)\, e^{-j\alpha\omega} \ldots\right]$$

i.e.,

$$g_{d_1}(t) = j_0(k)g_1(t) + j_1(k)g(t-\alpha) - j_1(k)g(t+\alpha$$

$$+ j_2(k)g(t-\alpha) + j_2(k)g(t+2\alpha) \ldots$$

Where

$$\alpha = \frac{1}{4f_c}; \text{ since } \alpha\omega_c = \frac{\pi}{2} \qquad (11)$$

and $J_n(k)$ is the nth order ordinary Bessel function. Equation (11) yields the distorted pulse.

Equation (10) shows that the echoes are spaced further apart if α is made larger. For n cycles in the pass-band from d-c to ω_c

$$\alpha\omega_c = 2n\pi$$

For a fixed peak-to-peak group delay, T_g peak-to-peak, the value of K is inversely proportional to α

$$K = \frac{T_{g\,(p\text{-}p)}}{2\alpha}$$

As the number of ripples increases, K decreases. $J_0(k)$ increases towards unity and the $J_n(k)$ for $n > 1$ decrease in value as K approaches zero. In addition, the echoes are moved away from the original pulse.

This shows that ripples in the equalized time delay have the effect of reducing the amount of intersymbol interference.

The calculations of equations (9) and (10) and the synthesis of the final wave form were all performed on an RCA-601 computer. The computer also supplied the wave form in graphical form as shown on Figures III-13 through III-22.

6. Evaluation of Computer Results

The calculation was made for four values of K corresponding to the following values of peak-to-peak-differential-time-delay (DTD) in microseconds (Refer to Table III-3).

TABLE III-3. DIFFERENTIAL TIME DELAY USED IN COMPUTATION

K (Radians)	ΔT (p-p) d.c to 1.1b μsec.	ΔT (p-p) d.c to 1.0b μsec.	ΔT (p-p) 0.5b to 1.06 μsec.
5.18	3.58	3.05	2.20
2.59	1.79	1.52	1.10
1.30	0.89	0.76	0.55
0.26	0.179	0.15	0.11

Where:

$\Delta T_{dc\text{-}1.1b} = 0.689 \times 10^{-6}$ Ksec.

$\Delta T_{dc\text{-}1.0b} = 0.588 \times 10^{-6}$ Ksec.

$\Delta T_{0.5b \text{ to } 1.0b} = 0.164 \times 10^{-6}$ Ksec.

7. Worst Sample Degradation (Single Sample Conditioner)

The output wave forms are displayed on Figures III-13 through III-22. The level of the smallest sample was measured as described under Paragraph C.5. The degradation with respect to the peak value of the sinusoid at the bit rate frequency is listed in Table III-4. This is the relative eye aperture as defined

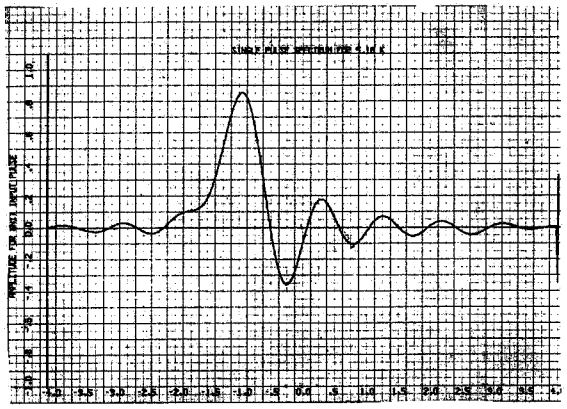

Figure III-13. Time-Response of Distorted Pulse, K = 5.18

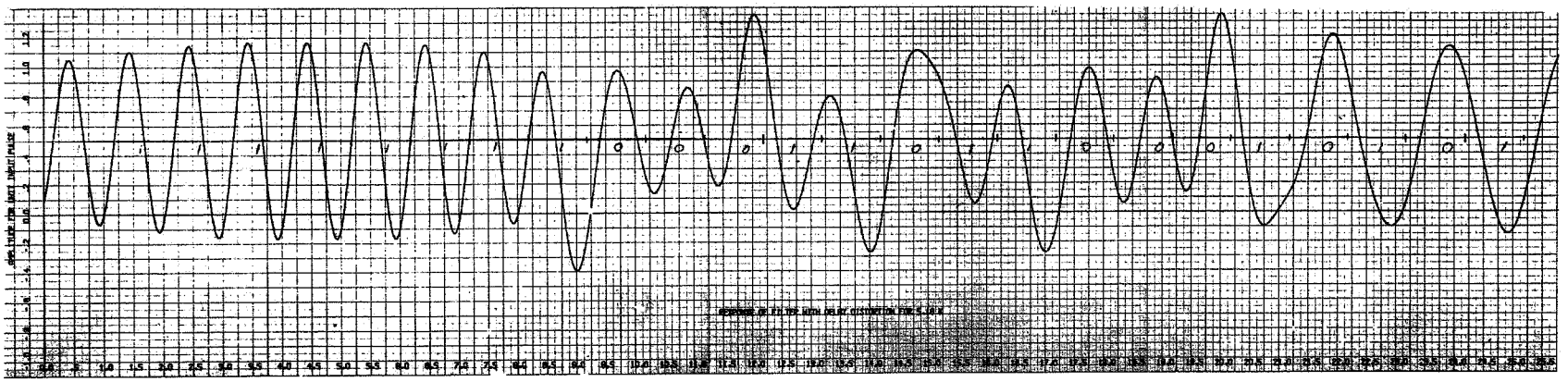

Test Conditions:

DTD between dc and 1.1b	=	3.58μsec
Worst left sample degradation	=	Reversed polarity
Worst right sample degradation	=	-8.2 db
Timing error (% bit length)	=	25%

Figure III-14. Calculated Response to Word A, K = 5.18

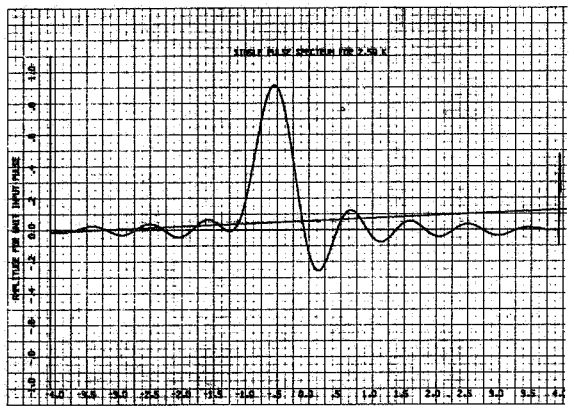

Figure III-15. Time Response of Distorted Pulse, K = 2.59

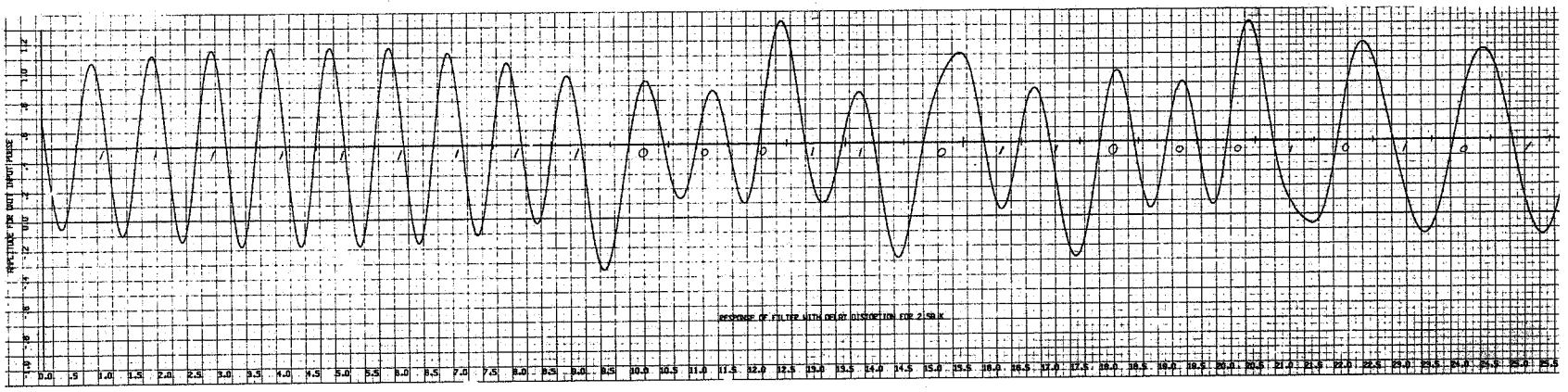

Test Conditions:

DTD (μsec) between dc and 1.1b	=	1.79 μsec
Left sample degradation	=	-14.2 db
Right sample degradation	=	-6.7 db
Timing error (% bit length)	=	17.5%

Figure III-16. Calculated Response to Word A, K = 2.59

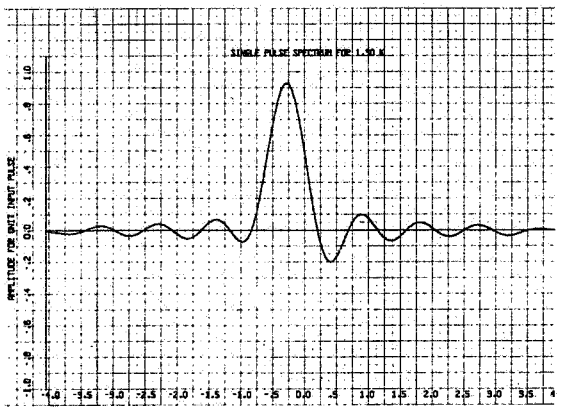

Figure III-17. Time Response of Distorted Pulse, K = 1.30

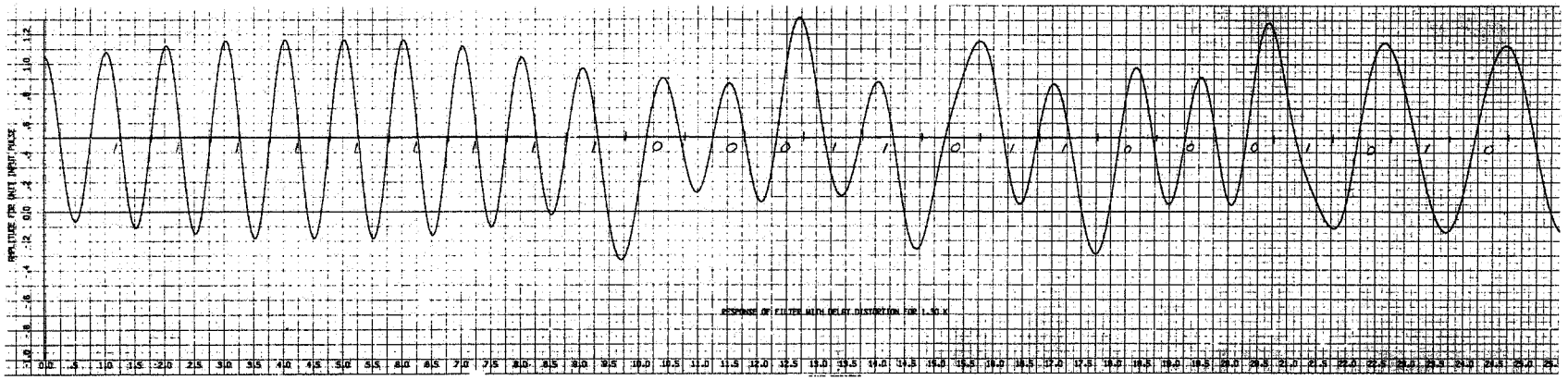

Test Conditions:

DTD (μsec between dc and 1.1b	=	0.89 μsec
Worst left sample degradation	=	-8.4 db
Worst right sample degradation	=	-5.8 db
Timing error (% bit length)	=	13.0%

Figure III-18. Calculated Response to Word A, K = 1.30

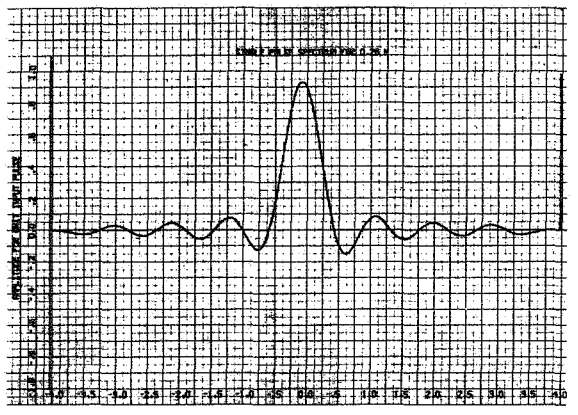

Figure III-19. Time Response of Distorted Pulse, K = 0.26

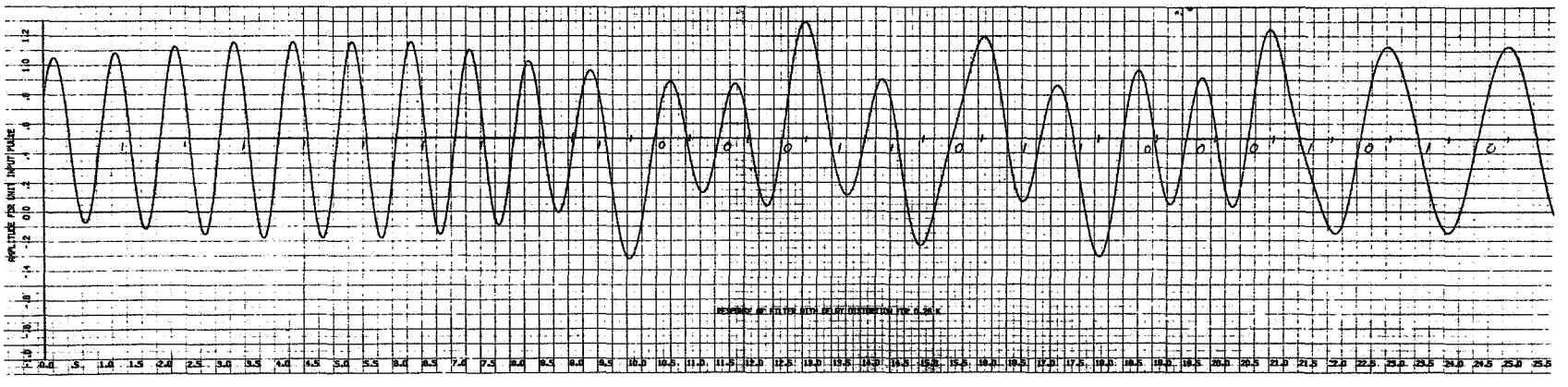

Test Conditions:

DTD between dc and 1.1b	=	0.18 μsec
Worst left sample degradation	=	-5.6 db
Worst right sample degradation	=	-5.6 db
Timing error (% bit length)	=	10.0%

Figure III-20. Calculated Response to Word A, K = 0.26

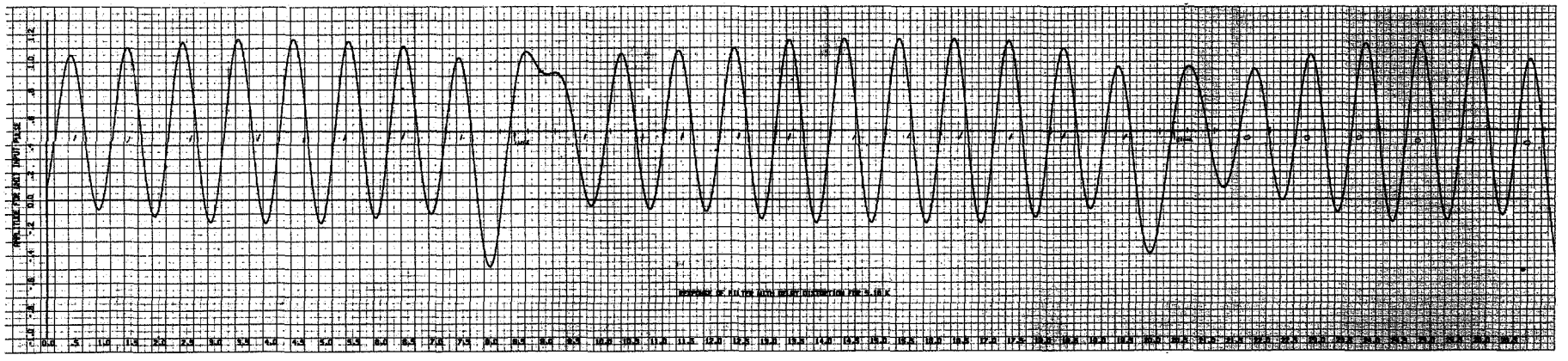

Test Conditions:

DTD between dc and 1.1b	=	3.58 μsec
Worst left sample degradation	=	Reversed polarity
Worst right sample degradation	=	-8.4 db
Timing error	=	32.5%

Figure III-21. Calculated Response to Word B, K = 5.18

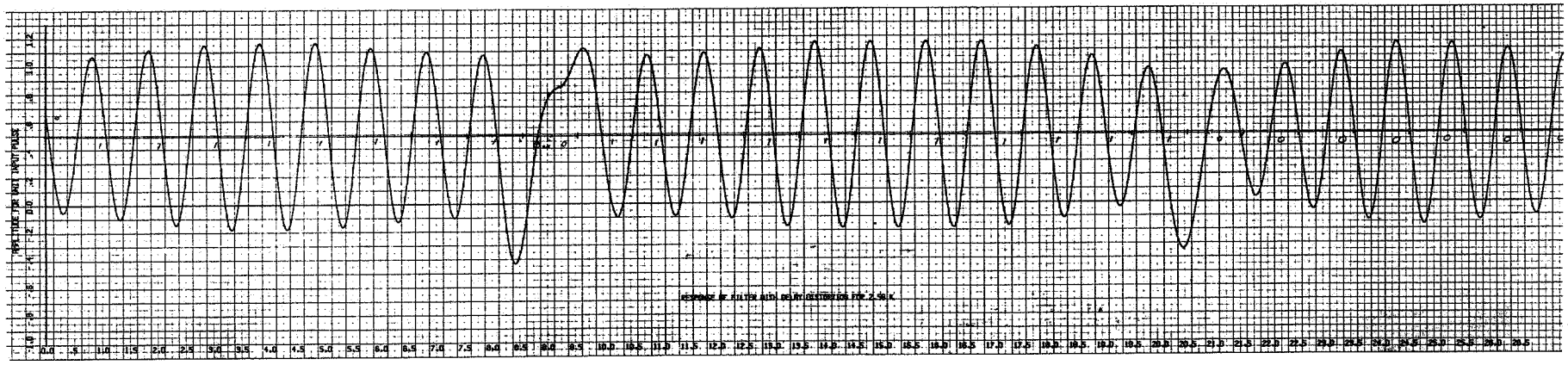

Test Conditions:

DTD between dc and 1.1b	=	1.79 μsec
Worst left sample degradation	=	-21.0 db
Worst right sample degradation	=	5.2 db
Timing error	=	25%

Figure III-22. Calculated Response to Word B, K = 2.59

in Paragraph C.1. In the computer simulation the peak-to-peak value A of the input pulses is normalized to unity.

The maximum timing error was also measured and is listed on Table III-5. In the biphase level format, a zero-axis crossing is expected in the center of every bit. The maximum displacement of the actual zero crossing from the expected crossing is the timing error. This error has been expressed as a percentage of bit duration.

TABLE III-4. COMPUTER RESULTS FOR WORDS A AND B

Word	K Radians	DTD (P-P) from 0.56 to 1.0b		Peak Reference at 1.0b	Smallest Sample (left)	Relative-Eye Aperture db
		μsec	% of T			
A	5.18	2.20	26.4	0.67	0.05 (wrong polarity)	-
A	2.59	1.10	13.2	0.67	0.13	-14.2
A	1.30	0.55	6.6	0.66	0.25	- 8.4
A	0.26	0.11	1.3	0.67	0.35	- 5.6
B	5.18	2.20	26.4	0.66	0.25 (wrong polarity)	-
B	2.59	1.10	13.2	0.67	0.06	-21.0

The results of Tables III-4 and III-5 clearly show that the results of word B are the worst case. The left sample is the worst case because the time delay chosen is an increasing function of frequency. Had it been a decrease in function of frequency, the right sample would be the worst case. Unless the signal conditioner has a way of decoding which half of the bit is consistently worse, its performance would have to be determined on the basis of the worst sample. The values of the smallest right samples are given in Table III-6. These samples do not necessarily occur in the same bit cell as the smallest left sample.

TABLE III-5. MEASURED TIMING ERROR (FROM COMPUTER RESULTS)

Word	K Radians	DTD (P-P) 0.5b to 1.0b		Measured Timing Error % of T
		μsec	% of T	
A	5.18	2.20	26.4	25.0
A	2.59	1.10	13.2	17.5
A	1.30	0.55	6.6	13.0
A	0.26	0.11	1.3	10.0
B	5.18	2.20	26.4	32.5
B	2.59	1.10	13.2	25.0

TABLE III-6. SMALLEST RIGHT AND LEFT SAMPLES

Word	K Radians	Peak Reference Level A_p	Smallest Right Level	Right Eye Aperture db	Left Eye Aperture db
A	5.18	0.67	0.26	-8.2	-
A	2.59	0.67	0.31	-6.7	-14.2
A	1.30	0.66	0.34	-5.8	- 8.4
A	0.26	0.67	0.35	-5.6	- 5.6
B	5.18	0.66	0.25	-8.4	-
B	2.19	0.67	0.37	-5.2	-21.0

8. Two-Sample-Conditioner

In the two sample conditioner, the 3/4 bit sample is subtracted from the $\frac{1}{4}$ bit sample. The decision that the transmitted bit is a "1" is made if the algebraic sum is positive. Otherwise the decision is that a "0" has been transmitted.

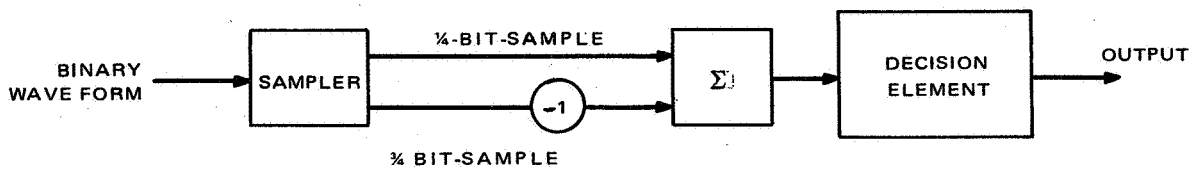

Figure III-23. Two-Sample Conditioner, Block Diagram

The signal-to-noise-ratio into the decision element (See Figure III-23) is calculated as follows:

Let A_p be the peak reference level obtained when the sequence 11111 is transmitted. For any other sequence the first sample is usually degraded by a factor (α) and the second sample by a factor (β).

Let the level of the first sample be: $A = \alpha A_p$

Let the level of the second sample be: $B = \beta A_p$

The peak-to-rms signal-to-noise-ratio for the first sample is:

$$SNR_1 = \frac{\alpha^2 A_p^{\,2}}{\sigma^2} \left(\frac{\text{Peak}}{\text{rms}}\right)^2 \qquad (12)$$

For the second sample, the peak-to-rms signal-to-noise-ratio is:

$$SNR_2 = \frac{\beta^2 A_p^{\,2}}{\sigma^2} \left(\frac{\text{Peak}}{\text{rms}}\right)^2 \qquad (13)$$

The rms noise level of the first sample is equal to the rms noise level of the second sample and is denoted by σ.

Let $n_1(t_0)$ be the instantaneous noise voltage at the first sample. The instantaneous noise voltage at the second sample will be $n_1\left(t_0 + \frac{T}{2}\right)$. The random noise process is denoted by $n_0(t)$.

The second sample is inverted and added to the first. The noise voltage at the decision device is then:

$$n(t) = n_1(t_0) - n_1\left(t_0 - \frac{T}{2}\right) \tag{14}$$

The noise power (or mean-square value of the noise) is:

$$N_0 = E\left[n^2\right] = E\left[n_1^2(t_0) + n_1^2\left(t_0 + \frac{T}{2}\right) - 2\,n_1(t_0)\,n_1\left(t_0 + \frac{T}{2}\right)\right] \tag{15}$$

where $E\left[\ \right]$ stands for expected (or ensemble average) value of . . . .

$$N_0 = N_1 + N_1 - 2\,R_d\left(\frac{T}{2}\right) \tag{16}$$

N_1 is the average noise power at each sample, i.e., $N_1 = \sigma_0^2$, $R_d(\tau)$ is the auto-correlation function of $n_1(t)$ defined as:

$$R_d(\tau) = E\left[n_1(t_0)\ n_1(t_0 + \tau)\right]$$

If the two noise samples are uncorrelated, then

$$R_d\left(\frac{T}{2}\right) = 0, \qquad \sqrt{N_0} = \sqrt{2}\sigma, \tag{17}$$

and

$$SNR_{1+2} = \frac{(\alpha - \beta)^2\ A_p^{\ 2}}{2\sigma^2} \quad \text{(uncorrelated noise samples)} \tag{18}$$

The correlation coefficient ρ is defined as

$$\rho = \frac{R_d(\tau)}{R_d(0)} = \frac{R_d(\tau)}{N_0}$$

Since $R_d(0) = N_1$

In general, the two samples are correlated to some degree and the correlation coefficient is evaluated as follows:

If the noise density were white, the equations could be written as:

$$\underset{\text{white}}{\rho(\tau)} = \frac{\sin \omega_c \tau}{\omega_c \tau} \tag{20}$$

$$\underset{\text{white}}{\rho \frac{\tau}{2}} = -0.0895 \tag{21}$$

However, the IRIS noise density is parabolic due to the frequency discriminator of the ground RF receiver and the auto-correlation is explained as follows:

The total noise power N_0 for the receiver bandwidth up to cutoff point ω_c is:

$$N_0 = \frac{1}{2\pi} \int_{-\omega_c}^{\omega_c} K\omega^2 \, d\omega \tag{22}$$

Where $K\omega^2 = S(\omega)$ is the double-sided power spectral density.

Auto-correlation is

$$R_d(\tau) = \frac{1}{2\pi} \int_{-\omega_c}^{\omega_c} K\omega^2 \, e^{j\omega\tau} \, d\omega$$

The correlation function $\rho(\tau)$ is given by

$$\rho(\tau) = \frac{R_d(\tau)}{N_0} = \frac{3}{2\omega_c^3} \left(\frac{2\omega_c^2}{\tau} \sin \omega_c \tau + \frac{4\omega_c}{\tau^2} \cos \omega_c \tau - \frac{4 \sin \omega_c \tau}{\tau^3} \right) \tag{24}$$

Where

$$\omega_c = 2\pi \times 1.1b$$

$$\tau = \frac{T}{2}$$

$$\rho\left(\tau = \frac{T}{2}\right) = -0.701$$

Equation (16) becomes

$$N_0 = 2N_i (1 - \rho) \tag{25}$$

Perfect correlation corresponds to $\rho = 1$. The samples are uncorrelated when: $\rho = 0$. ρ can also assume negative values.

The case where $\rho = -1$ (anti-correlation) will be the worst case and correspond to 3 db SNR degradation as compared to the case where $\rho = 0$.

In general:

$$SNR_{1+2} = \frac{(\alpha - \beta)^2 A_p^2}{2\sigma^2 (1-\rho)} \left(\frac{\text{peak}}{\text{rms}}\right)^2 \tag{26}$$

The auto-correlation function $R_d(\tau)$ is the inverse Fourier transform of the noise power spectral density $S(\omega)$

$$R_d(\tau) = \frac{1}{2\pi} \int_{-\infty}^{\infty} S(\omega)\, e^{j\omega\tau}\, d\omega \tag{27}$$

The total noise power is:

$$N = \frac{1}{2\pi} \int_{-\infty}^{\infty} S(\omega)\, d\omega \tag{28}$$

The two noise samples are strongly anti-correlated. This value of ρ produces 2-3 db SNR degradation with respect to the uncorrelated case ($\rho = 0$). It is only 0.7 db better than the perfectly anti-correlated case ($\rho = -1$). The case $\rho = -1$ is quite representative of the performance of the conditioner when supplied from a discriminator.

Table III-7 shows the values αA_p and βA_p of the left and right sample of the same bit cell which yield the worst degradation with respect to A_p for the two-sample conditioner. The SNR_{1+2} degradation is the factor $\frac{(\alpha - \rho)^2}{2(1 - \rho)}$ expressed in db.

TABLE III-7. SNR DEGRADATION OF TWO-SAMPLE CONDITIONER

Word	K Radians	DTD 0.5b to 1.0b μsec	Reference Level (A_p)	$\lvert\alpha A_p\rvert$ Left	$\lvert\beta A_p\rvert$ Right	SNR_{1+2} Degradation (db)	
						$\rho = 0$	$\rho = 1$
A	5.18	2.20	0.67	0.05 (Reverse)	0.26	-13.1	-16.1
A	2.59	1.10	0.67	0.18	0.31	- 5.3	- 8.3
A	1.30	0.55	0.66	0.25	0.34	- 4.0	- 7.0
A	0.26	0.11	0.67	0.35	0.38	- 2.2	- 5.2
B	5.18	2.20	.66	0.25 (Reverse)	0.42	-14.8	-17.8
B	2.59	1.10	0.67	0.06	0.37	- 6.9	- 9.9

9. Conclusions

The results of the computer simulation, for the single sample conditioner indicate the following:

- A conditioner using a single sample per bit wastes most of the information in the wave form.

- With a single sample per bit conditioner, -21 db degradation in signal-ratio is lost for a maximum DTD of ±0.55. from 0.5b to 1.0b.

- Even with a very tight equalization of ±0.05 μsec. between 0.5b to 1.0b, the relative eye aperture is -5.6 db for word A. This degradation is due to the limited bandwidth which yields a pulse response close to a $\frac{\sin x}{x}$ shape.

- The sample for the case K = 5.18 (±1.10 μsec. from 0.5b to 1.0b) is reversed in sign and will cause an error.

The proper conditioner for this channel must use the full information available in a bit cell.

The results for $\rho = -1$ listed in Table III-7 should be compared to the results shown on Table III-2 for a single sample conditioner. The degradations are expressed with respect to the same reference in both situations, namely

$$\frac{A_p^2}{\sigma^2}$$

The performance of the two-sample conditioner is decidedly superior for differential time delays corresponding to K = 1.30. Below this value of K the two-sample conditioner does not contribute as much improvement. For K = 0.26 only +0.4 db improvement is realized. This is due to the fact for K = 0.26, most of the intersymbol interference is contributed by the bandwidth limitation rather than time delay distortion.

If the DTD cannot be equalized to better than ±0.55 μsec. between 0.5b and 1.0b, then a two-sample conditioner is recommended. In that case, a 10 db signal-to-noise ratio degradation will be suffered.

D. PHASE ERROR AS A FUNCTION OF THE BIPHASE REPEATER

1. General

This analysis investigates the effects of time displacement error (phase error) of the repeater phase lock-loop (PLL) to the input jitter of the tape recorder; the jitter is the time-integral of the tape flutter. The maximum time displacement error (TDE) the loop can tolerate is ±25 percent of a bit period. Time displacement errors in excess of this value will produce one or more errors. However, about six percent of the TDE is contributed by the following:

bit pattern shift, ±0.3 percent; asymmetry, ±0.75 percent; and VCO offset, ±2.0 percent. The remaining ±19 percent is due to tape recorder flutter and is the maximum TDE limit on the minimum-loop bandwidth.

The phase-lock-loop is a second-order PLL with unity damping coefficient ($\epsilon = 1$). The flutter spectrum of the tape recorder is assumed similar to the flutter spectrum measured on the APT Tape Recorder Breadboard model, except for the flutter levels which have been increased by 20 percent.

2. Analysis of Phase-Lock-Loops

The analyses of the PLL are based on the block diagram shown on Figure III-24.

The input phase $\phi_{in}(t)$ and the output phase $\phi_o(t)$ are phase deviations from the reference phase determined by the average input bit rate. The phase error is

$$\phi_e(t) = \phi_{in}(t) - \phi_o(t)$$

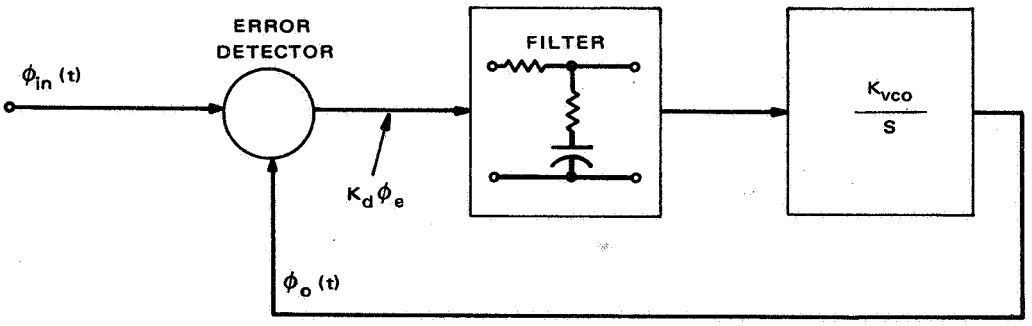

Figure III-24. Phase-Lock-Loop, Block Diagram

If the signals were sinusoidal, the input waveform would be expressed as

$$f_{in}(t) = A \cos\left[\omega_c t + \phi_{in}(t)\right],$$

and the output waveform would be expressed as

$$f_o t = B \cos\left[\omega_c + \phi_o(t)\right].$$

The average rate of zero crossings is

$$f_c = \frac{\omega_c}{2\pi}$$

The small signal transfer function is:

$$H(s) = \frac{\Phi_o(s)}{\Phi_i(s)} = \frac{G\frac{T_2}{T_1}(s + \frac{1}{T_2})}{s^2 + \left[\frac{GT_2 + 1}{T_1}\right]S + \frac{G}{T_1}} \qquad (1)$$

where $G = K_d K_{VCO}$ = dc loop gain

T_2 = small time constant of filter $F(s)$

T_1 = large time constant of filter $F(s)$

$$F(s) = \frac{1 + T_2 S}{1 + T_1 S} \quad \text{(filter transfer function)}$$

The loop transfer function can be rewritten as:

$$H(s) = \frac{2\epsilon\omega_n S^1 + \omega_n^2\left(1 - \frac{1}{G}\right)}{S^2 + 2\epsilon\omega_n S + \omega_n^2} \qquad (2)$$

usually $G >> 1$ (typical $G \approx 10^4$)

Therefore

$$H(s) = \frac{2\epsilon\omega_n S + \omega_n^2}{S^2 + 2\epsilon\omega_n S + \omega_n^2} \qquad (3)$$

where, ϵ = damping coefficient

ω_n = loop natural frequency (rps) = $\sqrt{\frac{G}{T_1}}$

$$2\epsilon\omega_n = \frac{G\,T_2 + 1}{T_1} = \frac{G\,T_2}{T_1}$$

For the repeater, ϵ will be chosen to be unity ($\epsilon = 1$). This selection of ϵ yields a reasonable compromise between flatness of the amplitude (frequency deviation vs frequency) response of the loop and adequate pull-in-time — A larger ϵ yields a longer pull-in-time.

$$H(s) = \frac{2\omega_n S + \omega_n^2}{S^2 + 2\omega_n S + \omega_n^2} ; \epsilon = 1 \qquad (4)$$

The phase error transfer function is:

$$G(s) = \frac{\Phi_e(s)}{\Phi_{in}(s)} = 1\text{-}H(s)$$

$$G(s) = \frac{s^2}{(s + \omega_n)^2} ; \epsilon = 1 \qquad (5)$$

$$G(\omega) = \frac{\omega^2}{\omega^2 + \omega_n^2} \qquad (6)$$

Let the input phase be sinusoidal:

$$\phi_{in}(t) = A \sin \omega_i t$$

The output phase will be

$$\phi_o(t) = B \sin (\omega_i t + \theta_i)$$

$$B = A\left| G(\omega_i)\right|$$

$$B = \frac{A\,\omega_i^2}{\omega_i^2 + \omega_n^2} = \frac{A\left(\frac{f_i}{f_n}\right)}{\left(\frac{f_i}{f_n}\right) + 1} \qquad (7)$$

$\left|G(\omega)\right|$ is plotted as a function of $\frac{f_i}{f_n}$ on Figure III-25.

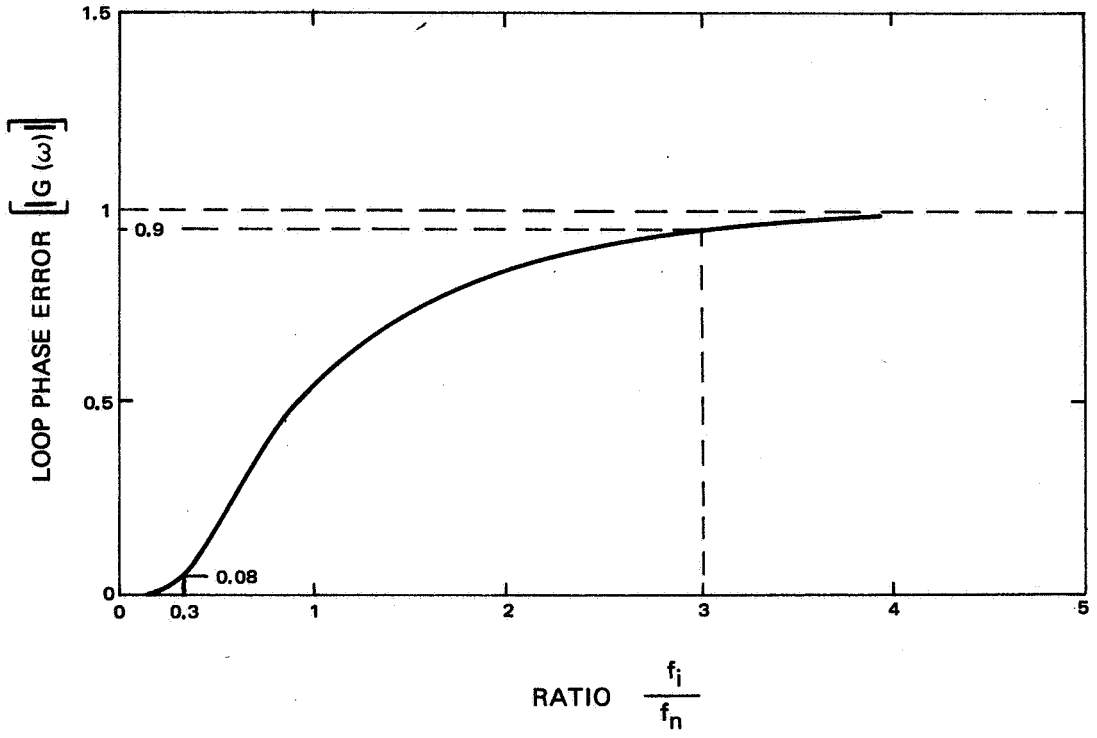

Figure III-25. Loop-Phase-Error Transfer Function

Noise Bandwidth:

The single-sided noise bandwidth of the loop is defined as

$$B_L\,(\text{cps}) = \int_0^\infty \left|H(f)\right|^2 df$$

$$B_L\,(\text{cps}) = \frac{\omega_n\,(1 + 4\epsilon^2)}{8\epsilon}\;;\;(\omega_n = \text{rps}) \qquad (8)$$

$$\text{For } \epsilon = 1;\; \boxed{B_L(\text{cps}) = \frac{5}{8}\,\omega_n} \qquad (9)$$

General expression for phase-error transfer function:

When ϵ is not equal to unity

$$G(\omega) = \frac{\omega^2}{\sqrt{\omega^4 + \omega_n{}^4 + 2\omega_n{}^2\,\omega^2\,(2\epsilon^2 - 1)}} \qquad (10)$$

Tape jitter components:

A typical tape flutter spectrum is as shown in Figure III-26.

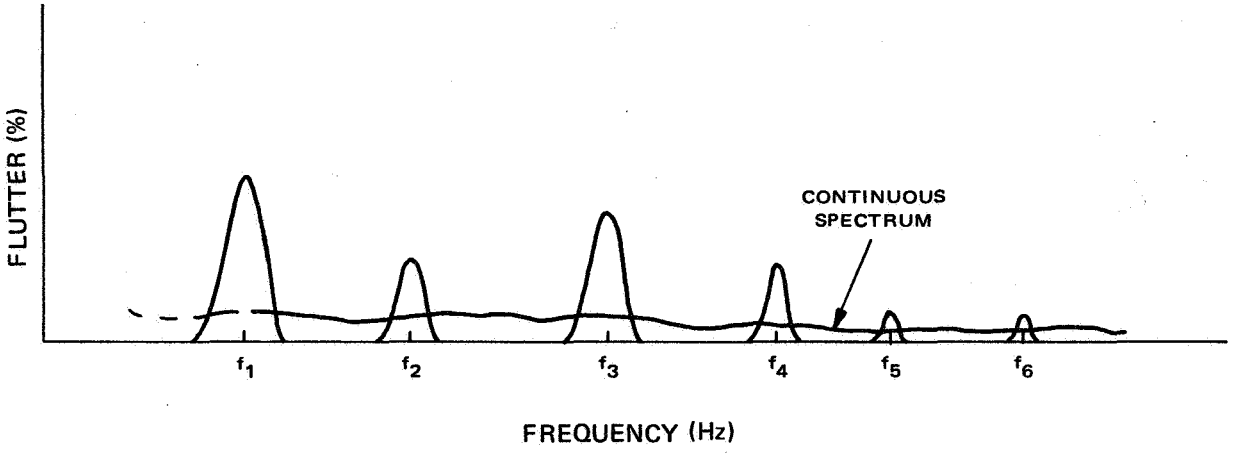

Figure III-26. Typical Tape Flutter Spectrum

The spectrum has large peaks at quite well defined frequencies f_1, f_2, f_3 ... f_n. There is also a continuous spectrum which is negligible except at very high frequencies.

Let the following periodic signal be recorded. Its frequency is f_c (Hz). Let us assume that this signal is expressed by:

$$g_R(t) = \cos \omega_c t$$

On playback the signal will be:

$$g_p(t) = \cos \omega_c t + \phi_i(t)$$

where $\phi_i(t)$ is the time-varying jitter in radians and is defined as

$$\phi_i(t) = \frac{a_1}{\omega_1} \sin \omega_1 t + \frac{a_2}{\omega_2} \sin \omega_2 t + \ldots t \frac{a_n}{\omega_n} \sin \omega_n t \qquad (11)$$

The flutter $\Delta f(t)$ is given by:

$$\Delta f(t) = \frac{1}{2\pi}\frac{d\phi_i}{dt} = \frac{1}{2\pi}\left[a_1 \cos \omega_1 t + a_2 \cos \omega_2 t + \ldots \; a_m \cos \omega_m t\right] \tag{12}$$

The percentage of instantaneous flutter is:

$$\% \text{ flutter} = 100 \times \frac{\Delta f(t)}{f_c} = 100\left(\frac{a_1}{2\pi f_c}\cos \omega_1 t + \frac{a_2}{2\pi f_c}\cos \omega_2 t + \ldots +\right)$$

$$\% \text{ flutter} = 100\left(\frac{a_1}{\omega_c}\cos \omega_1 t + \frac{a_2}{\omega_c}\cos \omega_2 t + \ldots + \ldots\right)$$

In order to generalize the above expressions some phase must be assigned to each sinusoidal component.

$$\% \text{ flutter} = 100\left[\frac{a_1}{\omega_c}\cos \omega_1 t + \frac{a_2}{\omega_c}\cos \omega_2 t + \theta_2) + \ldots + \frac{a_m}{\omega_c}\cos (\omega_m + \theta_m)\right] \tag{13}$$

The general expression for the jitter is then:

$$\phi_i(t) = \frac{a_1}{\omega_1}\sin \omega_1 t + \frac{a_2}{\omega_2}\sin (\omega_2 t + \theta_2) + \ldots + \frac{a_m}{\omega_c}\sin (\omega_c t + \theta_m) \tag{14}$$

The phase error $\phi_e(t)$ of the phase-lock-loop is given by:

$$\phi_e(t) = \frac{a_1}{\omega_1}\left|G(\omega_1)\right| \sin (\omega_1 t + \alpha_1) + \frac{a_2}{\omega_2}\left|G(\omega_2)\right| \sin (\omega_2 t + \alpha_2) + \ldots \tag{15}$$

The expected peak values of flutter are those measured on the APT tape recorder breadboard increased by 20 percent.

3. Bandwidth Calculations

The bandwidths were determined by trial and error. The following bandwidths were selected for IRIS and MRIR:

(a) IRIS Channel

Natural frequency: $f_n = 400$ Hz

Noise bandwidth: $B_L = 1.57$ kHz $\quad \epsilon = 1$

3db bandwidth: $f_{3db} = 1.0$ kHz

Once the damping coefficient ϵ is fixed at $\epsilon = 1$ the loop flutter handling capability is completely determined either by the natural frequency, the noise bandwidth or the 3 db bandwidth.

In order to obtain an expression for the 3 db bandwidth in terms of the noise bandwidth, the amplitude response $[|H(\omega)|]$ was approximated by an RC low-pass filter. The relationship between the 3 db bandwidth f_{3db} and the noise bandwidth of a one-stage low-pass RC filter is the following:

$$f_{3db\,(RC)} = \frac{2}{\pi} B_L \; ; \epsilon = 1 \qquad (16)$$

This expression is a fairly accurate one for the phase-lock-loop with $\epsilon = 1$. This expression has been checked against one derived from the amplitude response curve[8], and the following relationship was obtained:

$$\omega_{3db} = 2.48\, \omega_n \quad (\epsilon = 1) \qquad (17)$$

Combining equations (9) and (17),

$$B_{L(cps)} = \frac{5}{8} \frac{\omega_{3db}}{2.48} = 1.01 \times \frac{\pi}{2} \times f_{3db} \qquad (18)$$

Equation (16) is therefore sufficiently accurate.

In the biphase repeater specification, the 3 db bandwidth has been specified. Also a bound of ±1.0 db has been specified on the flatness of the loop amplitude response. This bound automatically requires that $\epsilon \geq 1$. However, the specification of acquisition time restricts the value of ϵ to be about unity ($\epsilon \approx 1$).

Using equation (15), the peak TDE expected from the IRIS repeater is calculated to be ±21.2 percent of one bit duration. The calculations are tabulated in Table III-8. This value of peak TDE exceeds the maximum of ±19 percent by about 10 percent. It has not been judged necessary to repeat the bandwidth calculations because the tape flutter spectrum estimate is conservative. Also, some fine bandwidth adjustment will certainly have to be performed when the tape recorder is mated with the repeater.

TABLE III-8. IRIS REPEATER PHASE ERROR (BIT RATE = 120 kb/sec)

Flutter Frequency (Hz)	Peak Tape Jitter $\lvert\phi_{in}\rvert$ (radians)	$\lvert G(\omega)\rvert = \frac{\lvert\phi_e(\omega)\rvert}{\lvert\phi_{in}(\omega)\rvert}$	$\lvert\phi_e(\omega)\rvert$ (radians - peak)	$\phi_e(\omega)$ (radians - rms)
26	20.8	0.004	0.083	0.0034
110	3.26	0.071	0.231	0.026
180	1.99	0.169	0.336	0.055
300	0.72	0.361	0.260	0.038
600	0.36	0.694	0.249	0.031
1800	0.18	0.95	0.170	0.015
			1.329	0.168 = 0.41 rms

Peak phase error = ±1.329 rad = ±21.2 percent of 1 bit duration (IRIS)
rms phase error = 0.41 rad = ±6.5 percent of 1 bit duration (IRIS)

b. MRIR Channel

The same general comments presented for the IRIS channel apply to the MRIR channel. The PLL characteristics are

Natural frequency: = 230 Hz

Noise bandwidth: = 900 Hz $\epsilon = 1$

3 db bandwidth: = 575 Hz

The peak TDE expected from the MRIR PLL is ±18.3 percent of 1 bit duration.

The MRIR TDE calculations are summarized in Table III-9.

TABLE III-9. MRIR REPEATER PHASE ERROR (BIT RATE = 53.33 kb/s

Flutter Frequency (cps)	Peak Tape Jitter $\lvert\phi_{in}\rvert$ (radians)	$\lvert G(\omega)\rvert = \frac{\lvert\phi_e\rvert}{\lvert\phi_{in}\rvert}$	$\lvert\phi_e(\omega)\rvert$ (radians)
26	9.27	0.013	0.12
110	1.45	0.187	0.271
180	0.89	0.383	0.340
300	0.32	0.63	0.201
600	0.16	0.87	0.139
1800	0.079	0.985	0.078
			1.149 rad.

Peak phase error = 1.149 rad = ±18.3 percent of bit duration (MRIR)

E. SIGNAL CONDITIONER PHASE ERROR

Calculations in the preceding paragraphs were performed early in the program, and were based on the APT recorder breadboard flutter. Later in the program the biphase repeater was deleted from the system, and the tape recorder (EM-2) flutter was used to calculate the net timing error as seen by the Dynatronics signal conditioner without the biphase repeater. The results, given in Table III-10, are very small percentages of a bit, and their effect on the system will be minor.

TABLE III-10. SIGNAL CONDITIONER/EM-2 TAPE RECORDER FLUTTER

Signal Conditioner Bandwidth Setting*	RMS Error (%)		
	-5°C	+25°C	50°C
2.8%	0.95	0.76	1.10
5.0%	0.57	0.45	0.65

* The bandwidth setting is the control panel indication on the Dynatronics decoder; it corresponds to the frequency at which the loop gain passes through 0 db.

F. BIT ERROR RATE AS A FUNCTION OF TAPE DROPOUT

Calculation of the probability of error (P_T) of the IRIS channel is based on the predicted end-of-life signal loss shown on Figure III-27. Figure III-27 is a plot of signal loss in db versus the bit count below the reference level of 12 ma record current. Two additional plots have been added to this figure: one is the expected dropout specification imposed on the tape recorder; the other is a straight line passing through a point whose coordinates are the maximum probability of error the system can accept from the tape recorder and the expected peak-to-peak/rms signal to noise ratio in the equalizer bandwidth.

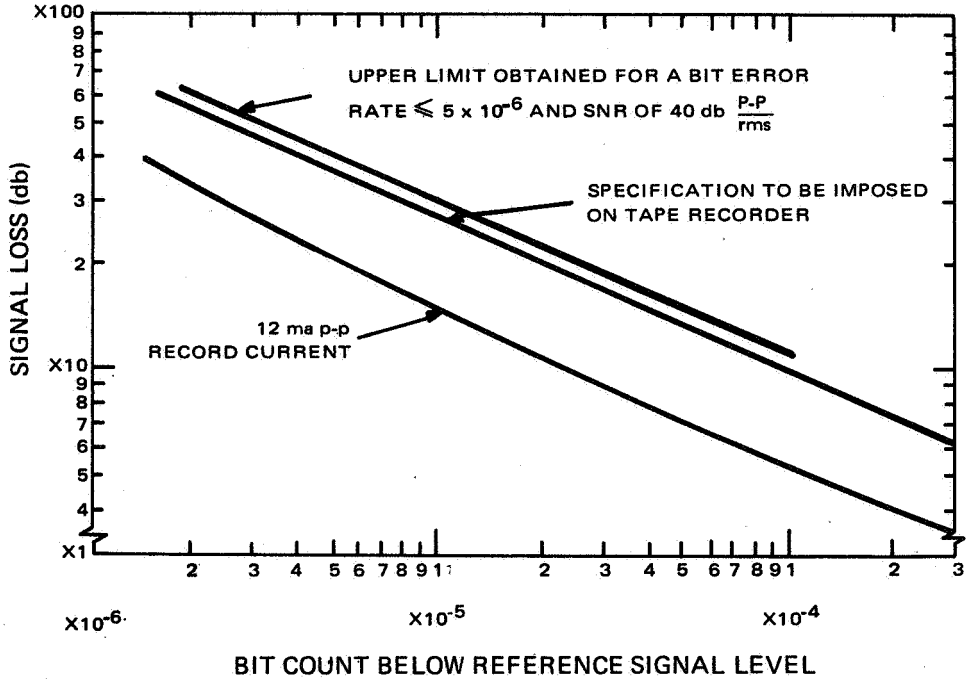

Figure III-27. Predicted End-of-Life Signal Loss for IRIS Channel Operation

The cumulative probability (P_C) that the peak level is equal to or less than any value of x_o is given by:

$$P_C(x_o) = \int_0^{x_o} P_V(x)\, dx$$

where x = the drop-out signal level

$P_V(x)$ = the probability density distribution of x ($P_V(x)$ is not available explicitly.

The probability of making the wrong decision ($P_{be}(x)$ due to Gaussian noise (N_{rms}) is given by:

$$P_{be}(x) = \frac{1}{2} \text{ erfc } \frac{x}{\sqrt{2}\, N_{rms}}$$

where erfc = the complementary error function = $1 - \text{erf}(x) = \frac{2}{\sqrt{\pi}} \int_o^x e^{-y^2}\, dy$

The differential error probability dp_t is $P_{be}(x)$ times the probability that the level drops to x.

$$dP_T = P_{be}(x)\, P_v(x)\, dx$$

$$P_T = \int_o^\infty P_{be}(x)\, P_v(x)\, dx \qquad (1)$$

We have:

$$P_T \leq P_{be}(0) \int_o^{x_o} P_v(x)\, dx + P_{be}(x) \qquad (2)$$

P_T was calculated using the approximation given in equation (2). The results, plotted as P_T versus SNR in the tape recorder equalizer noise bandwidth are shown on Figure III-28.

Examination of the results reveal the following:

- Below 36 db p-p/rms, the probability of error (P_T) increases rapidly for the expected specification of the tape-dropout characteristics.
- P_T is not reduced in a significant manner when the SNR is greatly increased beyond the knee of the curve. Essentially P_T depends only on the tape drop-out characteristics.
- The expected SNR of 40 db will result in a P_T of about 4×10^{-6}. This SNR represents a 4 db margin beyond the knee of the curve.

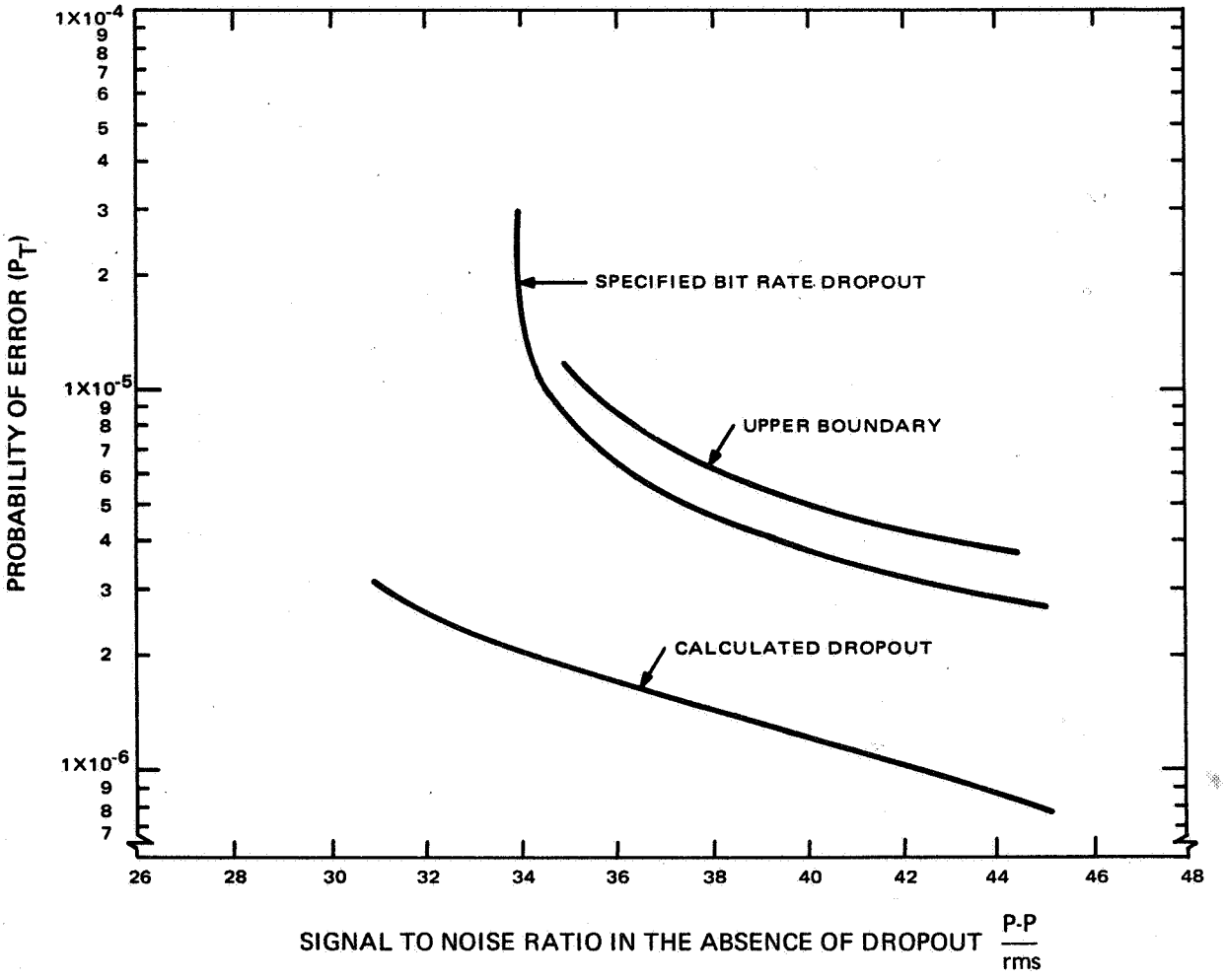

Figure III-28. Probability of Error Due to Tape Drop-Out and Gaussian Noise

G. LIST OF REFERENCES

1. "Evaluation of RCA Modified Biphase Transmission System" (Minuteman) CR-61-419-15, 26 January 1962, RCA-CSD. Surface Communication Division, Figure 2-7.

2. Jim-Twan-Lin and J. O. Scanlon "Group Delay Characteristics of Chebyschev Filters" IEEE Transactions on Circuit Theory, Vol. CT-11, No. 3, pp. 427-530, September 1964.

3. R. W. Lucky, "Analysis Relating Delay Variation and Intersymbol Interference in Data Transmission," B.S.T.J., Vol. 42, pp. 2247-2484, September 1963.

4. H. A. Wheeler, "The Interpretation of Amplitude and Phase Distortion in Terms of Paired Echoes," Proc. IRE, Vol. 27, pp. 359-385, June 1939.

5. A. Papoulis, The Fourier Integral, McGraw Hill, 1962.

6. G. L. Fredendall, "Equalization of Computer Tape Stations," RCA-PTR-1866, April 30, 1965.

7. G. V. Jacoby, "High-Density Digital Magnetic Recording Techniques," RCA-EM-6224, March 1965.

8. L. A. Hoffman "Receiver Design and Phase Lock-Loop," ASTIA No. 459435, Page 86, 15 May 1963.

9. Stanly P. Clurman, HDRSS-IRIS Tape Channel End-of-Life Study, Contract NAS 5-3772, December 2, 1962.

APPENDIX IV
RF LINK AND SNR ANALYSIS

A. INTRODUCTION

This Appendix contains a summary of the analysis of the S-Band link and Multiplexer/Demultiplexer upon which the HDRSS B RF deviation schedule is based. The analysis was performed for nominal values, except where specifically noted otherwise.

The resulting S-Band transmitter deviation schedule and corresponding output signal-to-noise ratios (SNR) are shown in the Table IV-1.

TABLE IV-1. S-BAND TRANSMITTER DEVIATION SCHEDULE PARAMETERS

Channel	Peak Channel RF Deviation		Baseband SNR
1 IRIG	100 kHz		34 db P/rms
2 Timing	75 kHz	Time Code	15.4 db rms/rms
		Flutter	30.2 db rms/rms
3 MRIR	400 kHz		28.2 db P/rms
4 ID	300 kHz		28 db rms/rms
5 HRIR	200 kHz		38 db rms/rms
Peak transmitters RF Deviation	1075 kHz		

B. GOVERNMENT FURNISHED EQUIPMENT

The analyses assume the use of the following RF transmitter and receiver complex:

- A General Electronics Laboratories Type 25A1, 5 watt FM Transmitter.
- A Cutler Hammer Type 2133-H-3 Parametric Amplifier Converter (1710 MHz- to 136 MHz).
- A General Dynamics Model SC-761 Diversity Telemetry Receiver.

By direction, the entire RF transmission link has been assumed to be distortionless. With this assumption, the parametric amplifier noise figure is 2.2 db and the telemetry receiver bandwidth is 3 MHz.

C. SNR REQUIREMENTS

1. IRIS Channel SNR Requirement

The SNR requirement for the IRIS Channel is 29.0 db, peak-to-rms[1] at the input to the biphase decoder (output of the demultiplexer, excluding the loss for intersymbol interference).

2. Time Code Channel SNR Requirement

The limiting SNR consideration for the timing channel is that the subcarrier-to-noise-ratio (SCNR) at the input to the flutter discriminator be 18 db during the valleys of the modulated time code when the valley-to-peak ratio is 0.47 (arithmetic mean of the specification limits of 0.3 and 0.65).

3. MRIR Channel SNR Requirement

SNR: 29.0 db peak-to-rms (See Paragraph C.1).

4. ID Channel SNR Requirement

For the ID channel the objective was to provide performance equivalent to that of the Nimbus A AVCS. The SNR of the AVCS camera-tape recorder system, without link noise or other externally added noise, was specified[2] as 25 db B-W/rms; the peak RF deviation for the 400-530 kHz Nimbus A AVCS channel was 300 kHz. This is enough to keep the subcarrier discriminator above threshold[3] and results in a SNR of 34.4 db, B-W/rms.

For an SSB/FM signal with modular index (B) ≈ 1, the discriminator threshold may be as much as 7 db higher than the equivalent of a DSB/FM signal[2]. This effect has not been included in this analysis. The RF deviation for the IRIS channel, which is developed, is equal to that provided in Nimbus A for this channel.

5. HRIR Channel SNR Requirement

The objective for the HRIR channel was to provide performance equivalent to that of the Nimbus A HRIR; that tape recorder SNR was specified[4] as 30 db p-p/rms.

Since HRIR for Nimbus B fills a higher frequency slot than it did in Nimbus A, the RF deviation assigned to it must be larger than was used for Nimbus A. The limiting requirement for the HRIR channel is that the SCNR $\geq$ 18 db. There is no increase in subcarrier detection threshold for this channel since the HRIR signal is transmitted as a standard DSB FM signal.

D. RF LINK CALCULATIONS

The calculation for the carrier-to-noise-ratio of the RF link is shown in Table IV-2.

TABLE IV-2. CARRIER-TO-NOISE-RATIO CALCULATION FOR THE RF LINK

Parameter	Gain
Transmitter Power (5W)	+7.0 dbw
Spacecraft Cabling, etc.	-0.5 db (assumed)
Spacecraft Antenna Gain	0.0 db (at ±55°) (5)
Propagation	-167.6 db (1840 NM @ 1710 MHz, 5° elevation)
Polarization Loss	0.0 db (assumed)
Ground Station Antenna	+47.7 db (6)
Ground Station Cabling, etc.	-0.2 db (assumed)
Performance Margin	-6.0 db (assumed)
RECEIVER POWER	-119.6 dbw
NOISE POWER	-137.7 dbw (3 MHz BW, Noise Figure: 2.2 db)*
CARRIER TO NOISE RATIO	+18.1 db

*Noise figure measured as 2.2 db; reported verbally by the RCA Service Company at GSFC, 3/1/65.

Particular attention should be drawn to the value given above for the spacecraft antenna gain: 0 db at ±55°. The Nimbus Handbook for Experimenters (Nimbus B), dated October 1965, gives the spacecraft antenna gain as +6.5 db with half power beam width of 90°. It is possible, therefore, that the gain of the antenna is several db higher, at ±55°, than the assumed value of 0 db.

At greater elevation angles each of three factors improve the received CNR:

- shorter path length
- lower ground antenna temperature
- smaller angle (from axis) for spacecraft antenna.

Any evaluation of the possibilities for reduced transmitter power should include these effects.

E. SNR CALCULATIONS

1. IRIS Channel SNR Calculation

The IRIS signal is treated as a baseband signal at the output of the demultiplexer. The SNR for this channel is given by

$$SNR = CNR + 10 \log \frac{3}{2} \frac{(\Delta f_{rf})^2 \, B_{IF}}{(f_u)^3 - (f_\ell)^3}$$

where:

SNR = ratio of rms output signal to rms output noise for a sine wave modulating signal.

CNR = ratio of rms carrier signal (in the IF) to rms noise (in the IF). (18.1 db).

Δf_{rf} = peak deviation of the RF carrier due to the IRIS signal.

B_{IF} = full -3 db bandwidth of the IF filter (3 MHz).

f_u = the upper cutoff frequency of a rectangular post detection filter. f_u = 132 kHz.

f_ℓ = the lower cutoff frequency of a rectangular post detection filter. f_ℓ = 0 kHz.

$$SNR = 18.1 + 10 \log \frac{3}{2} \frac{10^{10} \times 3 \times 10^6}{(1.32)^3 \times 10^{15}}$$

= 31 db (rms/rms).

SNR = 34 db (peak signal/rms noise).

The SNR of the IRIS signal at the output of the demultiplexer, for 100 Hz peak RF deviation, will be 34 db (peak signal/rms noise).

2. Time Code Channel SNR Calculations

a. Subcarrier-to-Noise-Ratio (SCNR) at Demultiplexer Output

The SCNR at the output of the demultiplexer is given by Equation (1) with

f_u = 203 kHz
f_ℓ = 171 kHz
Δf_{rf} = 75 kHz

The resulting SCNR = 26.9 db (rms signal to rms noise for a sinusoidal modulating signal).

During the valleys of the time code modulated signal the SCNR will drop to 20.3 d-c (rms/rms), assuming a valley-to-peak ratio of 0.47. If the valley-to-peak ratio drops to 0.3 (the specification limit), the SCNR will drop to 17.3 db (rms/rms).

b. Id Time Code Detector SNR

With white Gaussian noise at the input, the SNR at the output of an envelope detector is given by:

$$SNR = \left(\frac{m}{m+1}\right)^2 \cdot SCNR \quad \frac{B}{2f_m} \quad \text{for } B \geq 2f_m \qquad (2)$$

$$= \left(\frac{p-v}{2p}\right)^2 \cdot SCNR \quad \frac{B}{2f_m} \qquad (3)$$

where:

SCNR = the ratio of rms value of a sine wave having an amplitude equal to the peak amplitude of the modulated carrier at the envelope detector to the rms noise at the input to the envelope detector.

B = the bandwidth in which SCNR is measured.

f_m = the cutoff frequency of a low-pass rectangular post detection filter (Assume $f_m = B/2$).

m = modulation index.

v = the peak-to-peak value of the modulated input signal at the valley of the input wave form.

p = the peak-to-peak value of the modulated signal at the peak of the input wave form.

The nominal value for the valley-to-peak ratio of the received timing signal has been taken to be 0.47. From paragraph E.2.a., SCNR is 26.9 db; using these values in equation (3) the resulting SNR at the output of the envelope detector is 15.4 db (rms/rms).

c. ID F&W Discriminator SNR

The worst case subcarrier to-noise-ratio at the input to the F&W discriminator is given, in Paragraph E.2.a., as 17.3 db during the modulation valleys; thus the discriminator is always at a minimum of 5.3 db above threshold.

The SNR at the output of the F&W discriminator is given by:

$$SNR = CNR \frac{3}{4} \frac{(\Delta f_{rf})^2 \ (\Delta f_{SC})^2 \ B_{IF}}{(f_m)^3 \ (f_{SC})^2 \ 1 + \left[(3/5) \ (f_m/f_{SC})^2\right]} \qquad (4)$$

where:

SNR = ratio of rms signal to rms noise, for sinusoidal modulation, at the output of the low-pass signal post detection filter.

f_m = the cutoff frequency of the low-pass post detection filter.

CNR = the ratio of rms signal to rms noise at the input to the RF discriminator.

B_{IF} = the bandwidth in which CNR is measured.

f_{SC} = the nominal center frequency of the subcarrier.

Δf_{SC} = the peak frequency deviation of the subcarrier.

Δf_{rf} = the peak frequency deviation of the RF carrier which is apportioned to this subcarrier.

The following values apply to the F&W channel:

$\Delta f_{rf} = 7.5 \times 10^4$

$\Delta f_{SC} = 0.8 \times 10^3$

$f_m = 1 \times 10^3$

$f_{SC} = 1.87 \times 10^5$

$B_{IF} = 3 \times 10^6$

CNR = 18.1 db

Using these values in Equation (4), the resultant SNR is a 41.7 db rms signal-to-rms noise. During the time code modulation valleys this number could be reduced by 11.5 db (for worst case v/p ratio = 0.3) resulting in 30.2 db rms signal-to-rms-noise.

3. MRIR Channel SNR Calculation

The peak RF deviation for the MRIR channel was chosen as 400 kHz. With $f_u = 3.65 \times 10^5$, $f_\ell = 2.35 \times 10^5$, the SCNR at the input to the envelope detector is given by Equation (1) as 31.2 db rms signal-to-rms-noise. Assuming a nominal loss of 6 db through the envelope detector (the penalty for transmission of the MRIR local oscillator), the SNR at the output of the envelope detector will be 25.2 db rms-to-rms or 28.2 db peak-signal-to-rms-noise.

4. ID Channel SNR Calculation

The peak RF deviation for the ID channel was chosen as 300 kHz to provide a SCNR = 18 db (rms/rms). With this value of Δf_{rf} and $f_{SC} = 4.65 \times 10^5$, with $f_m = 6 \times 10^4$, $\Delta f_{SC} = 4.8 \times 10^4$, the SNR at the output of the ID demodulator is given by Equation (4) as 28 db rms signal to rms noise. This corresponds to 34.4 db black-to-white signal rms noise.

5. HRIR Channel SNR Calculation

The peak RF deviation for the HRIR channel was chosen as 200 kHz to provide a SCNR at the output of the demultiplexer of 18 db. With this value of r_{rf}, with $f_{SC} = 6.3 \times 10^5$, $f_{SC} = 2.75 \times 10^4$, and $f_m = 1.15 \times 10^4$, the SNR at the output of an HRIR demodulator before the MINCOM tape recorder would be given (by Equation (4) as 38 db rms signal-to-rms-noise. This corresponds to 47 db black-to-white signal/rms noise. The fifth order Bessel demodulation filter, down -1 db at 1.15×10^4 Hz allows excess noise to pass, reducing this to about 38 db B-W/rms.

F. TOTAL RF DEVIATION

It is of interest to note that if the multiplexed 700 kHz baseband were assumed to be replaced by a single sinusoidal modulating tone at 700 kHz, an estimate of the maximum allowable peak deviation may be obtained using Carson's rule:

$$f_d \leq BIF/2 - f_m$$

$$f_d \leq 1.5 \times 10^6 - 0.7 \times 10^6$$

$$f_d \leq 900 \text{ kHz}$$

It is estimated[7] taht this value of 800 kHz peak deviation will be exceeded approximately 1.5 percent of the time in the Nimbus B HDRSS system. A similar analysis for Nimbus A indicates that the " Carson deviation" was exceeded the greater percentage of time as shown in Table IV-3.

TABLE IV-3. NIMBUS RF LINK PARAMETERS

Nimbus A		% of time $\Delta f_{rf} > \Delta f$ Carson	% RF Energy within 3.4 MHz BW
HRIR & AVCS	ON	5	.99934
(3) AVCS	ON	2.5	
(2) HRIR	ON		
Nimbus B			
IDCS & HRIR	ON	1.5	.99963
IDCS	ON	0	
HRIR	ON	0	

Carson's rule, $B_{if} = 2(f_m + f_d)$, is a rule of thumb which includes all sidebands having energy .01 or greater relative to the unmodulated carrier. This results in a distortion-to-signal-ratio of -25 db (.003) for sinusoidal modulation and 45 db (3×10^{-5}) for noise-like modulation[8].

The second listed parameter, in-band energy, was obtained by representing the FDM data as the sum of five (four for Nimbus A) sinusoids; each sinusoid was located in the center of a channel. The complex baseband then frequency modulated the RF carrier, the Bessel functions were tabulated, and the total energy was summed over the interval from the carrier frequency to ±1.7 MHz. The results were listed in Table IV-3.

G. LIST OF REFERENCES

1. Radio Corporation of America, Performance Specification, Biphase Decoder, PS 1759290, November 24, 1965 and Addendum.

2. Radio Corporation of America, Test Log and Calibration Curve for AVCS Satellite Equipment, Prototype P1, Contract NAS 5-877, AED-1567, October 8, 1962.

3. Glorioso and Brazeal, "Experiments in SSB FM" IEEE Transactions on Communication Technology, March 1965.

4. Radio Corporation of America, Test Log and Calibration Curve for HRIR Satellite Equipment, Prototype P1, Contract NAS 5-877, AED-1466, June 21, 1963.

5. Stampfl, "The Nimbus Spacecraft and its Communication System as of September 1961," NASA Technical Note, D-1422, January 1963.

6. Paul A. Lantz, Handbook of NASA/GSFC Tracking, Data Acquisition, and Communication Antennas, Goddard Space Flight Center, Green Belt, Maryland, October 1964.

7. Margaret Slac, "The Probability Distributions of Sinusoidal Oscillations Combined in Random Phase," Proc. IEE, London, September 1945.

8. S. Plotkin, "FM Bandwidth as a Function of Distortion and Modulation Index," IEEE Transactions on Communication Technology, June 1967.